P1 1177312

THE UNITED STATES OF AMERICA

TO ALL TO WHOM THESE PRESENTS SHALL COME:

UNITED STATES DEPARTMENT OF COMMERCE
United States Patent and Trademark Office

June 01, 2004

THIS IS TO CERTIFY THAT ANNEXED HERETO IS A TRUE COPY FROM THE RECORDS OF THE UNITED STATES PATENT AND TRADEMARK OFFICE OF THOSE PAPERS OF THE BELOW IDENTIFIED PATENT APPLICATION THAT MET THE REQUIREMENTS TO BE GRANTED A FILING DATE.

APPLICATION NUMBER: *60/458,856*
FILING DATE: *March 28, 2003*
RELATED PCT APPLICATION NUMBER: *PCT/US04/09610*

By Authority of the
COMMISSIONER OF PATENTS AND TRADEMARKS

L. Edelen

L. EDELEN
Certifying Officer

PRIORITY DOCUMENT
SUBMITTED OR TRANSMITTED IN
COMPLIANCE WITH
RULE 17.1(a) OR (b)

03-31-03 60458856.032803

Patent and Trademark Office; U.S. DEPARTMENT OF COMMERCE

PROVISIONAL APPLICATION COVER SHEET

This is a request for filing a PROVISIONAL APPLICATION under 37 CFR 1.53(c).

DOCKET NUMBER: B01075.70042
Express Mail Label No. EV 208 517 825 US
Date of Deposit: March 28, 2003

03/28/03 JC962 U.S. PTO

B101 U.S. PTO 60/458856 03/28/03

INVENTOR(S)/APPLICANT(S)

LAST NAME	FIRST NAME	MIDDLE INITIAL	RESIDENCE (CITY AND EITHER STATE OR FOREIGN COUNTRY)
Stevens-Wright	Debbie		North Andover, MA

[ ] ***Additional inventors are being named on the separately numbered sheets attached hereto.***

TITLE OF THE INVENTION (280 characters max)

CATHETER TIP/ELECTRODE JUNCTION DESIGN FOR ELECTROPHYSIOLOGY CATHETERS

CORRESPONDENCE ADDRESS

CUSTOMER NUMBER: 23628

ENCLOSED APPLICATION PARTS *(check all that apply)*

[X]Specification - Number of Pages = 84

[ ]Drawing(s) - Number of Sheets

[ ]Application Data Sheet, See 37 CFR 1.76

[X]Return receipt postcard

The invention was made by an agency of the United States Government or under a contract with an agency of the United States Government.
[X]No
[ ] Yes, the name of the U.S., Government Agency and the Government Contract Number are:

_____

[ ] Other: _____

METHOD OF PAYMENT *(check all that apply)*

[X] A check is enclosed to cover the Provisional Filing Fees.

[ ] The Commissioner is hereby authorized to charge any additional fees or credit overpayment to Deposit Account 23/2825. A duplicate of this sheet is enclosed.

[ ]Small Entity Status is claimed.

PROVISIONAL FILING FEE AMOUNT $ 160.00

Respectfully submitted,

March 28, 2003
Date

James H. Morris, Reg. No. 34,681
Telephone No.: 617-720-3500

U.S. Patent No. 5,257,635 (attached) illustrates a conventional electrode to tip junction design.

US005257635A

United States Patent [19]

Langberg

[11] Patent Number: 5,257,635

[45] Date of Patent: Nov. 2, 1993

[54] ELECTRICAL HEATING CATHETER

[75] Inventor: Edwin Langberg, Mount Laurel, N.J.

[73] Assignee: Sensor Electronics, Inc., Mt. Laurel, N.J.

[21] Appl. No.: 736,253

[22] Filed: Jul. 26, 1991

Related U.S. Application Data

[60] Division of Ser. No. 563,562, Aug. 3, 1990, which is a continuation-in-part of Ser. No. 435,361, Nov. 17, 1989, which is a continuation-in-part of Ser. No. 276,294, Nov. 25, 1988, Pat. No. 4,945,912.

[51] Int. Cl.[5] A61N 1/05

[52] U.S. Cl. 607/122; 606/41

[58] Field of Search ..... 128/784–786, 128/419 P, 804; 606/33, 41, 49

[56] References Cited

U.S. PATENT DOCUMENTS

4,352,360 10/1982 King 128/786

4,896,671 1/1990 Cunningham et al. ..... 128/786 X

FOREIGN PATENT DOCUMENTS

2822829 11/1979 Fed. Rep. of Germany 128/786

2122092 1/1984 United Kingdom 128/804

Primary Examiner—Lee S. Cohen

Attorney, Agent, or Firm—Ryan, Kees & Hohenfeldt

[57] ABSTRACT

The invention provides a thermal design of a catheter where the active electrode is partially covered by a heat conducting and electrically insulating heat-sink layer for localizing and controlling an electrical heating of tissue and cooling of the active electrode by convective blood flow. The invention further comprises a current equalizing coating for gradual transition of electrical properties at a boundary of a metallic active electrode and an insulating catheter tube. The current equalizing coating controls current density and the distribution of tissue heating.

13 Claims, 5 Drawing Sheets

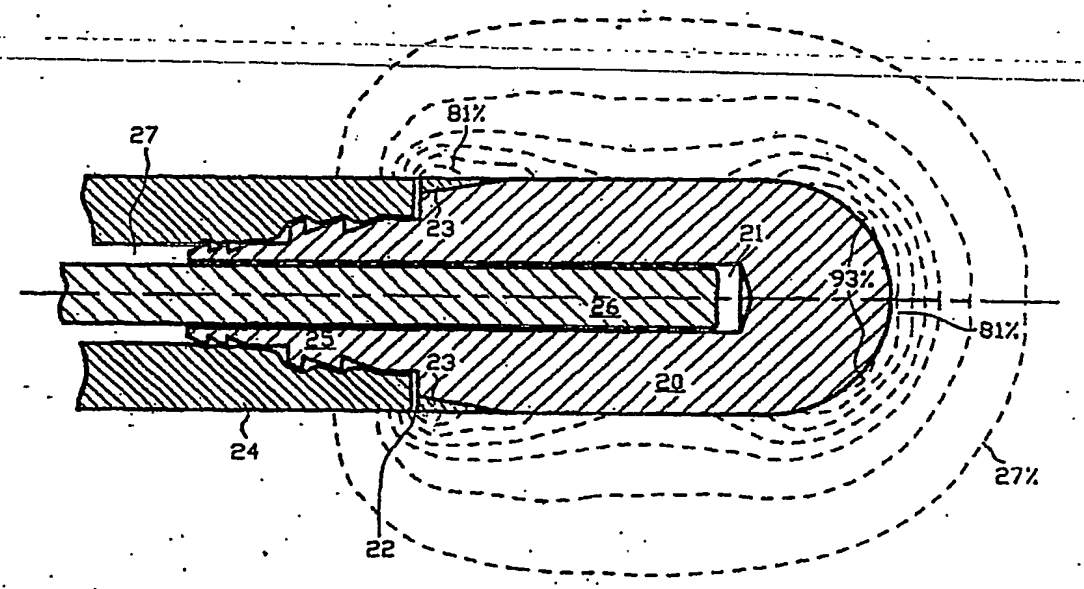

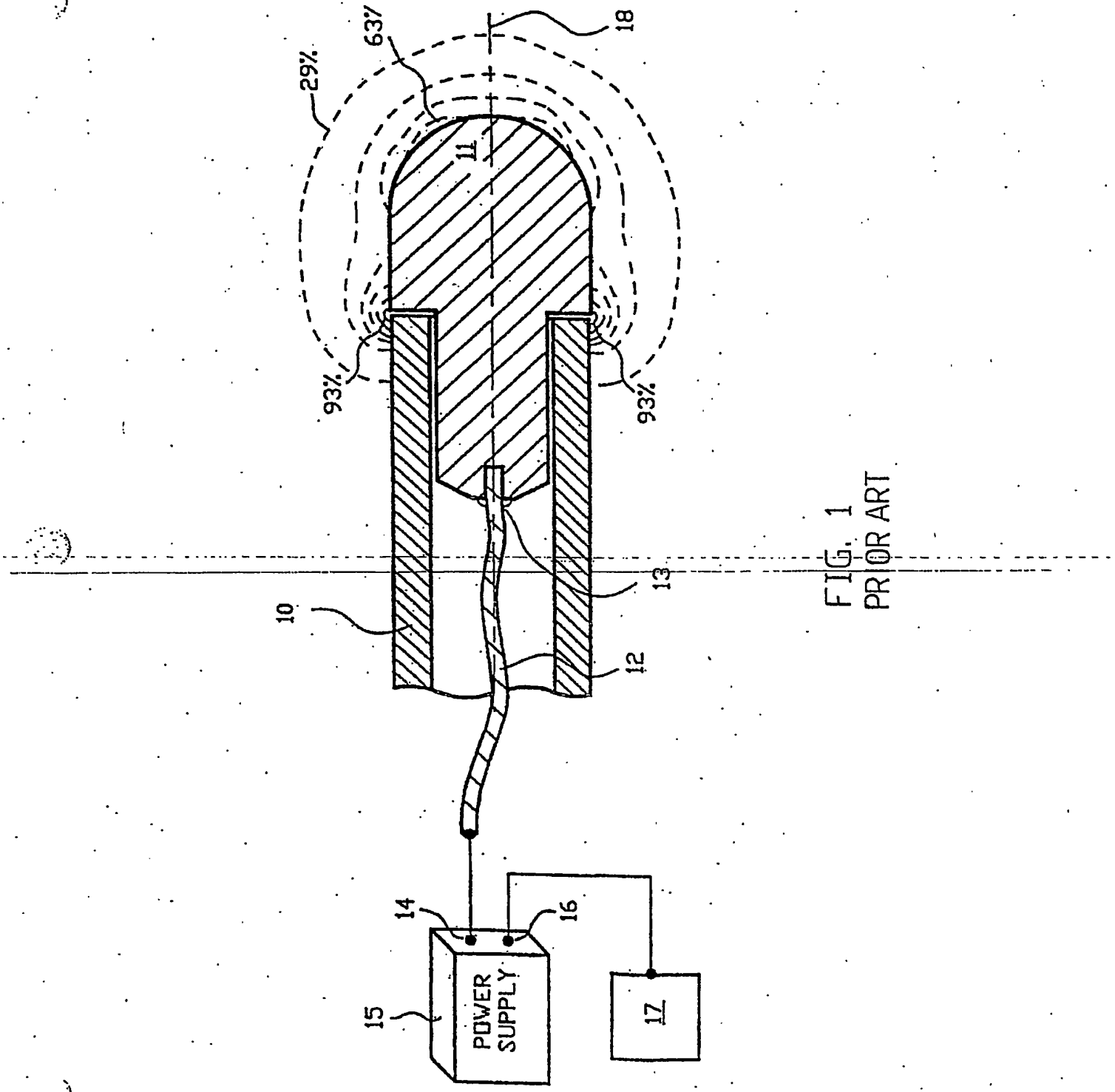

FIG. 1
PRIOR ART

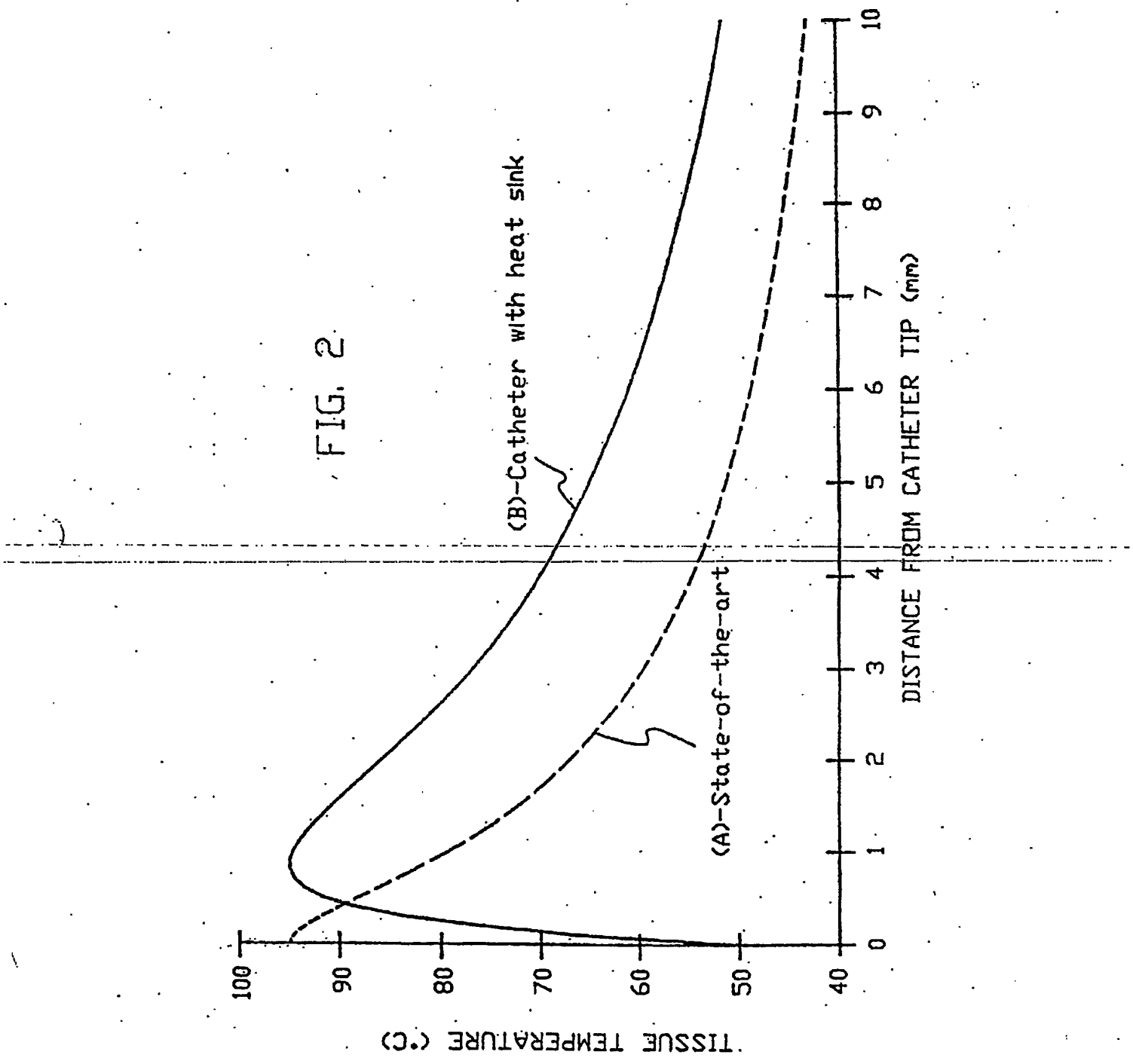
(B)-Catheter with heat sink
(A)-State-of-the-art
DISTANCE FROM CATHETER TIP (mm)
0
1
2
3
4
5
6
7
8
9
10
TISSUE TEMPERATURE (°C)
100
90
80
70
60
50
40

FIG. 2

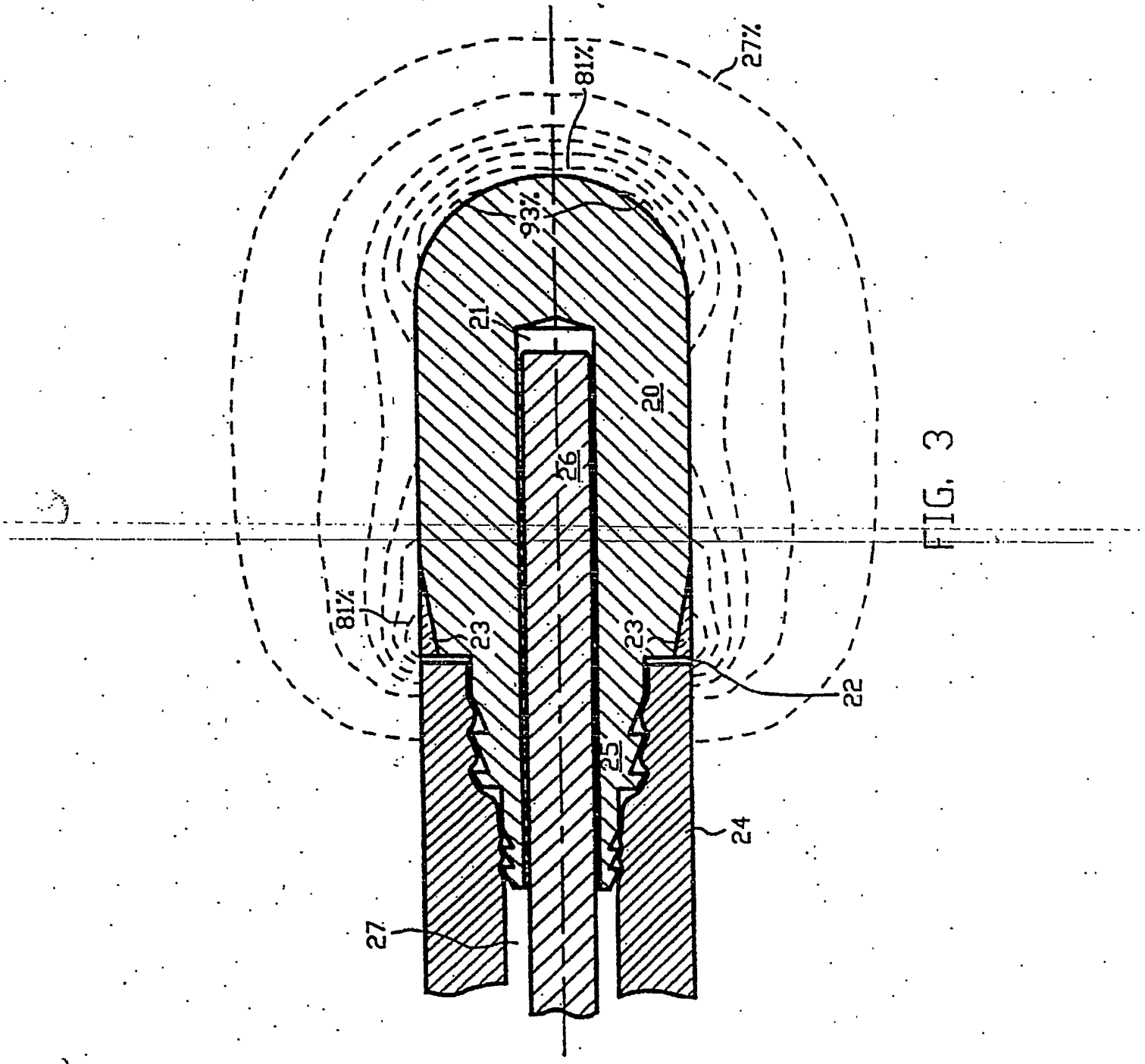

FIG. 3

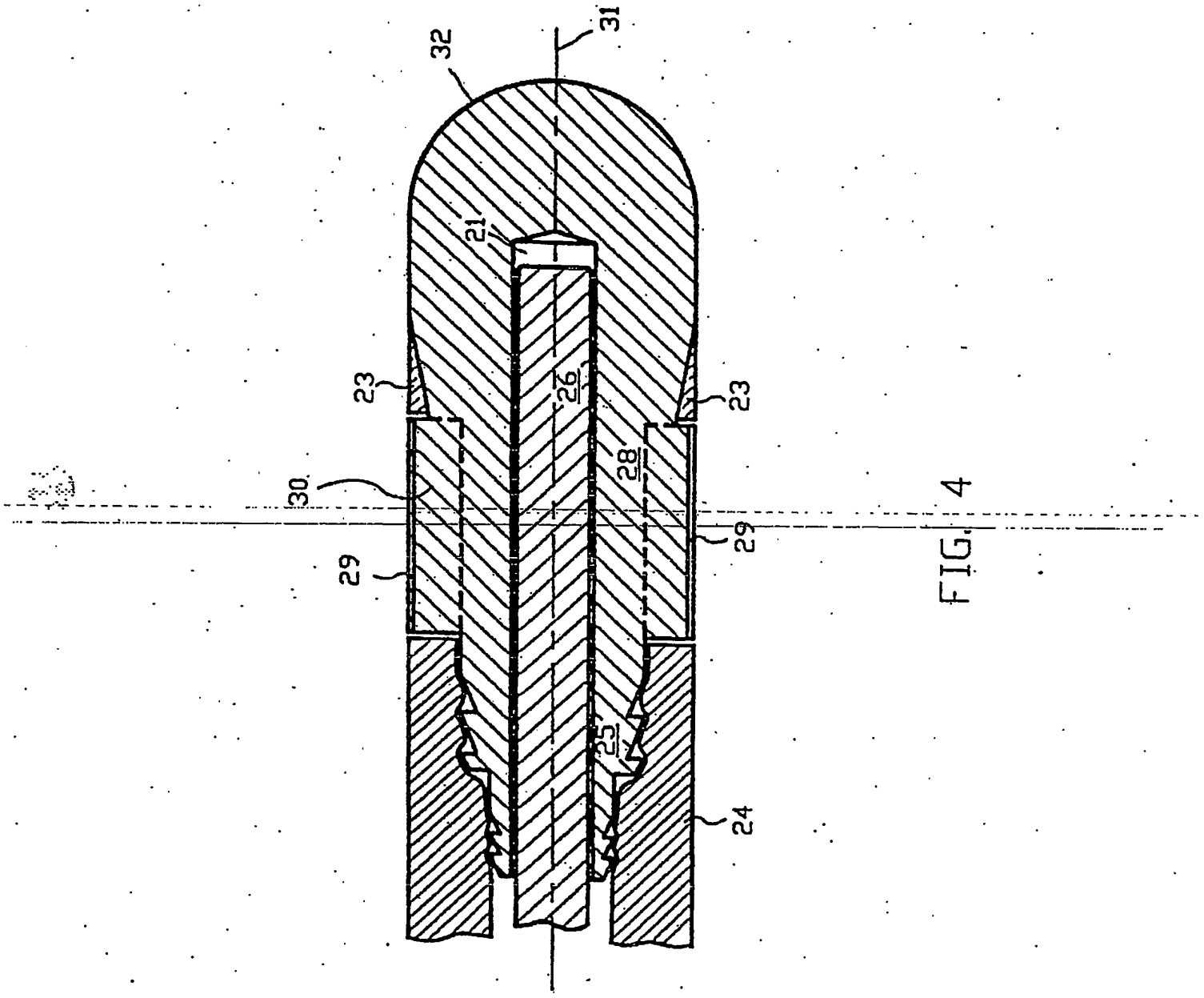

FIG. 4

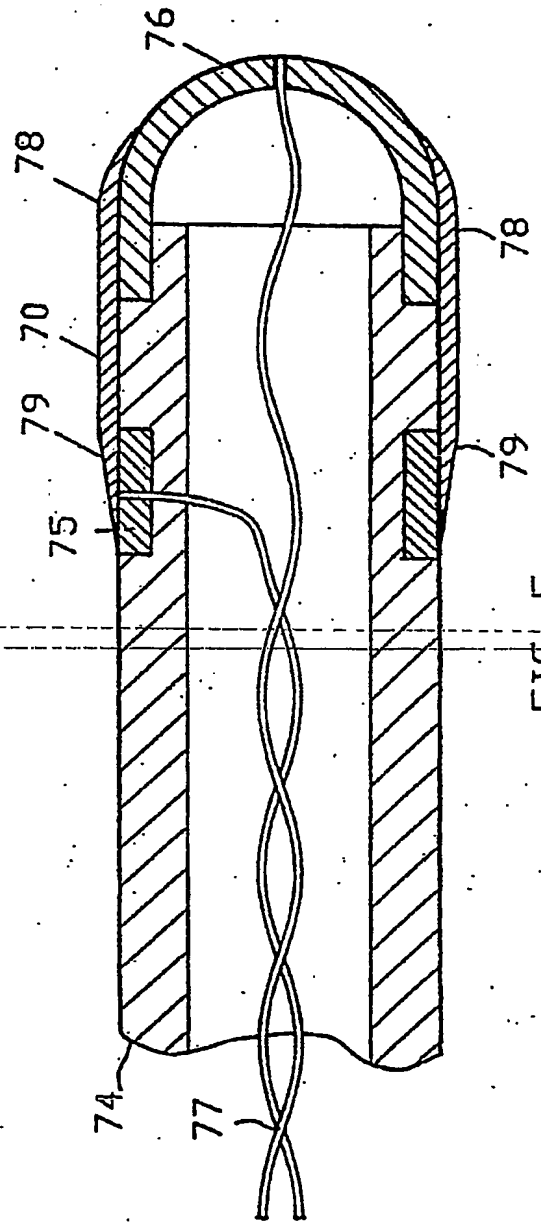

FIG. 5

ELECTRICAL HEATING CATHETER

This application is a division, of application Ser. No. 07/563,562 filed, Aug. 3, 1990, which is a continuation-in-part of application Ser. No. 07/435,361, filed Nov. 17, 1989. which is a continuation-in-part of application Ser. No. 276,294 filed Nov. 25, 1988, now U.S. Pat. No. 4,945,912.

BACKGROUND

An electrical heating catheter is a tube typically between 1 and 10 millimeters in diameter used for insertion into biological structure and equipped at the distal end with one or more electrodes and at the proximal end with electrical connectors for application of electric power. Electrical heating catheters are useful in many medical applications, e.g., for hyperthermia treatment of cancer or for cardiac ablation of arithmogenic tissue in the endocardium. In such medical applications it is desirable to maintain a fairly uniform generation of heat in a controlled volume of tissue adjoining the catheter.

A radiofrequency (RF) cardiac ablation catheter is presented here as a preferred embodiment. Catheter ablation is a non-surgical method of destroying an arrhythmogenic focus tissue in the endocardium. Typically, an ablation catheter is introduced percutaneously and advanced under fluoroscopic guidance into the left heart ventricle. It is manipulated until the site of the earliest activation is found, indicating the location of problem tissue. RF power is then applied to the distal catheter electrode. The heat in the vicinity of the electrode destroys the cardiac tissue responsible for the arrhythmia.

The temperature boundary between viable and non-viable tissue is approximately 48° Centigrade. Tissue heated to a temperature above 48° C. is non viable and defines the ablation volume. For therapeutic effectiveness the ablation volume must extend a few millimeters into the endocardium and must have a surface cross-section of at least a few millimeters square. The objective is to elevate the basal tissue temperature, generally at 37° C., fairly uniformly to the ablation temperature above 48° C., keeping however the hottest tissue temperature below 100° C. At approximately 100° C. charring and desiccation take place which seriously modifies the electrical conductivity of blood and tissue, and causes an increase in the overall electrical impedance of the electrical heating circuit and a drop in the power delivery to the tissue. Charring is particularly troublesome at the surface of the catheter electrode, since the catheter must be removed and cleaned before the procedure can continue.

In cardiac ablation catheters, the operative electrode is typically metallic and is located on a distal-tip end of the device. This electrode which serves as the heating applicator is referred to as an active electrode. Such an active electrode is the source of electrical or electromagnetic field, which causes heating of neighboring tissue. Even though no significant amount of heat is generated in the electrode itself, adjacently heated endocardial tissue heats the electrode via heat conduction through the tissue.

The field generated by the active electrode also heats the rapid blood flow in the heart chamber, which however very effectively carries away this generated heat so that the flowing blood temperature, except for the boundary layer, stays close to the basal temperature. Some cooling of the catheter tip takes place due to forced convective cooling caused by fast flowing blood in the heart chamber. The active electrode temperature is the result of the balance between such conductive heating and convective cooling.

In one preferred embodiment, the heating and cooling of the active electrode, for the purpose of tip temperature regulation and improved tissue temperature control, is carried out by covering the active electrode with thermally conductive and electrically insulating material. It is therefore appropriate to review the use of dielectric coatings in catheter art and to point out the fundamental difference between the preferred embodiments and the catheter microwave radiator art.

Frequencies for powering heating catheters range from dc to microwaves. It is customary to divide the spectrum of operating frequencies into conductive and radiative regions because of fundamental differences of implementation in these two regions. The dividing frequency between the two regions depends on the characteristic admittance of the tissue surrounding the active electrode. The conductive region is defined by operating frequencies where the conductivity term dominates. Alternatively, in the radiative region the dielectric term dominates. For blood and muscle, the dividing frequency is approximately at 400 MHz. The conductive region corresponds to dc to 400 MHz; the radiative region corresponds to microwave frequencies above 400 MHz.

Implementation of catheter heating applicators for the radiative and the conductive region is quite different. In the radiative region, the heating applicator acts as an antenna causing electromagnetic wave propagation into the tissue. The art of radiative catheter heating applicators, relying on wave propagation, is quite rich, e.g., dipole antennas, helical radiators, and resonators.

An example of a radiative catheter heating applicator, using a resonator, is described in the UK Patent Application GB 2 122 092 A by J. R. James, R. H. Johnson, A. Henderson, and M. H. Ponting. James matches a wave impedance of a resonant radiator, in a mode corresponding to multiples of a quarter wavelength, to a wave impedance of surrounding tissue, by appropriate selection of (1) an electrode coating size, (2) a coating dielectric constant, and (3) a coating magnetic permeability. Neither thermal nor electrical conductivity of the coating is a part of James's design. It should also be noted that the coating in James has both uniform thickness and uniform dielectric properties.

In the conductive region, there is no electromagnetic wave propagation and so techniques relying on wavelength resonance and matching of wave impedance are not applicable. Also in the conductive region, especially in the lower frequencies below 1 MHz, the capacitive impedance of a typical dielectric coating is so high, in comparison with the tissue impedance, that a dielectric coating, in effect, prevents a current flow into the tissue.

Typical state of the art catheter heating applicators for the conductive region, such as the United States Catheter Industries (USCI) catheter shown in FIG. 1, and described in detail later, has an active electrode at the end of the catheter tube and possibly ring electrode or electrodes around the diameter of the tube. Electrodes are connected to the proximal end with a thin, flexible wire.

One undesirable feature associated with such a state-of-the art catheter is a formation of hot spots along the

circular junction of the active electrode with the insulating catheter tube due to a sudden transition of electrical properties at the boundary. For example, an article "Catheter ablation without fulguration: Design and performance of a new system", A. J. Ahsan, D. Cunningham, E. Rowland, and A. F. Rickards. *PACE*. Vol. 12, Part II, January: 001–005, 1989 ("Ahsan") shows such formation of hot spots along the circular junction of the active electrode with the insulating catheter tube. To remedy this problem, Ahsan suggests a cylindrical electrode with hemispherical termination at both ends. The problem with Ahsan's solution is that the electrical connection to such an electrode breaks the smoothness of the surface and so generates a hot spot at the junction of the wire with the hemisphere.

The other undesirable feature of the state-of-the art catheter heating applicators is that there is no provision for cooling of the active electrode and as a result, maximum temperature is reached at the electrode and the resultant charring frequently fouls the electrode during a procedure. The temperature profile taken along the axis of the catheter as it extends into the tissue, similar to that shown by the dashed line in Graph (A) in FIG. 2, has been studied by D. E. Haines and D. D. Watson. (PACE Vol. 12, June: 962–976, 1989) and is described in some detail later. It will suffice here to observe that state-of-the-art catheters exhibit the highest temperature at the active electrode and therefore worst charring occurs at the active electrode-tissue boundary.

SUMMARY OF THE INVENTION

The invention provides a thermal design of a catheter where the active electrode is partially covered by a heat conducting and electrically insulating heat-sink layer for localizing and controlling an electrical heating of tissue and cooling of the active electrode by convective blood flow. This design moves peak temperature away from the active electrode surface thus preventing fouling of the active electrode. The cooling provided by the heat-sink layer also increase the depth and volume of an ablation region.

Without the heat-sink layer, as the size of the active electrode increases, the cooling area expands. Simultaneously, the area of current flow increases, thereby increasing the overall heating volume, decreasing the precision of localization of electrical heating; and leading to an undesirable increase in the overall heating power required for ablation.

Additional cooling of the active electrode can be provided by increasing the diameter of an electrical power supply wire, to a cable size so that the cable can carry a significant amount of heat away from the active electrode and dissipates it along the catheter shaft.

The invention further comprises a current equalizing coating for gradual transition of electrical properties at a boundary of a metallic active electrode and an insulating catheter tube. The current equalizing coating controls current density and the distribution of tissue heating. Absence of an abrupt transition in the electrical properties at the catheter tissue boundary, smoothes heat generation and reduces hot spots in tissue.

BRIEF DESCRIPTION OF THE DRAWINGS

FIG. 1 schematically shows a state-of-the-art catheter system and, in detail, a catheter electrode with the resulting tissue heating power density pattern adjacent to the electrode, indicating formation of a hot spot at the base of the electrode.

FIG. 2 shows a temperature profile along the extension of the catheter axis into the tissue, produced by (A) the state-of-the-art catheter, and by (B) a catheter with heat sink.

FIG. 3 shows an active electrode with a conductive skirt around the base of the active electrode and shows the resulting equalization of heating power density distribution. FIG. 3 also shows a wire implementation of the heat sink.

FIG. 4 shows a heat sink in the form of an electrically insulating and thermally conductive film on an active electrode.

FIG. 5 shows a bipolar catheter with a current equalizing coating.

DESCRIPTION OF THE PREFERRED EMBODIMENTS

Materials used for the design of the catheter can be conveniently divided into three ranges of electrical resistivity. Metals or metallic materials have resistivity of the order 10^{-6} Ω-cm to 10^{-3} Ω-cm. The term "conductive" material is used here to describe intermediate materials in the range of resistivity between 10^{-3} Ω-cm and 10^{5} Ω-cm. Materials with resistivity larger than 10^{5} Ω-cm are referred to as dielectrics or insulators.

FIG. 1 shows a state-of-the-art electrical catheter with an active electrode similar to the standard (USCI) catheter quoted in Ahsan, and referred to in the Background section. The active electrode serves as a heat applicator in distinction to other electrodes which may also be placed on the catheter. A plastic catheter tube 10 connects at a distal end to an active electrode 11, typically made of Platinum. Wire 12 is electrically connected between the active electrode 11 at junction 13 and, at the proximal end of the catheter, to an electrical power source 15, at terminal 14. To maintain flexibility, wire 12 is thin; typical size is 28 gage copper wire with a 0.4 millimeter diameter.

The connection at the proximal end of the catheter to the electrical power source 15 can be between two electrodes on the catheter (bipolar connection, seen later in FIG. 5), or between one active electrode and a large neutral external skin electrode (unipolar connection). A unipolar power supply connection is completed in FIG. 1 by connecting an external skin electrode 17 to a neutral power supply terminal 16. The frequency of operation of the power supply is 450 kHz.

A pattern of dashed lines and associated numbers with a "%" symbol, on the outside of tube 10 and active electrode 11 represent contours of equal heating power density. The percentages associated with pattern lines indicate the relative magnitude of electrical power dissipation in the tissue, with the relative scale adjusted, so that 100% represents maximum dissipation, and 0% represents dissipation at a distant neutral boundary. It should be noted in FIG. 1 that the maximum dissipation ranging from 100% to 93% is in the immediate vicinity of the junction between the metallic active electrode 11 and insulating catheter tube 10. Tissue adjacent to the tip of the active electrode 11 is only in the 63% heating density region. The hot spot at the junction of active electrode 11 and tube 10 acts as an undesirable focus for charring. The temperature of tissue along extension 18 of the catheter axis beyond the tip of active electrode 11 is discussed in connection with FIG. 2.

Graph (A) in FIG. 2, shown as a dashed line, is a temperature distribution along extension 18 of the catheter axis produced by the state-of-the-art catheter heat-

ing pattern shown in FIG. 1. The temperature is highest directly at the surface of the active electrode (distance=0). In operation, power is typically increased in order to increase the ablation volume until impedance change in noticed due to onset of charring. Since the tissue temperature is highest at the active electrode surface the charring is most likely to take place there. Charring frequently necessitates the removal of the catheter for cleaning.

The objective of the thermal design of a heating catheter is to heat a controlled volume of tissue to a temperature which causes ablation while at the same time assuring that the peak temperature is away from the electrode surface so that charring does not foul the active electrode surface. Graph (B) in FIG. 2 shows such a temperature profile. Graph (B) is described later in conjunction with a heat sink catheter design shown in FIG. 3 and FIG. 4.

FIG. 3 shows a catheter with improved electrical and thermal design. Axial blind hole 21, in active electrode 20, houses a metallic cable 26. Comparing FIG. 3 with the state-of-the-art catheter in FIG. 1, cable 26 provides an electrical connection to the active electrode 20, as did wire 12 in FIG. 1. Unlike the wire 12, the cross section of cable 26 is much greater, and is typically at least 20% of the cross-section of active electrode 20. Flexibility of cable 26 is maintained by stranded or laminated construction from multiple metallic conductors. Cable 26 provides a much greater heat conduction away from active electrode 20 and into catheter tube 24, thereby reducing a temperature rise of active electrode 20 during operation. Cable 26 also provides a range of possibilities for movable support of active electrode 20. Catheter tube 24 is firmly seated on a undercut protruding proximal end 25 of active electrode 20.

Active electrode 20 is tapered at its base 22 with a tapered angle of 10 degrees. Conductive epoxy fills this tapered region and forms a conductive skirt 23. The contours of equal heating power density, are shown in FIG. 3 for conductive epoxy with resistivity of 150 Ω-cm. The power density percentages, are scaled the same way as in FIG. 1. It can be seen that the uniformity of heating density at the junction of active electrode 20 and tube 24 is much improved when compared with the state-of-the-art catheter in FIG. 1 due to a graduated impedance, presented to the surface current flow, provided by the wedge-shaped cross section of conductive skirt 23.

Such a gradual transition between metallic and insulating surface properties for heating equalization can be accomplished by alternate means to those described above. In one example, conductive skirt 23 is made of uniform thickness but of graduated electrical properties. In another example the transition is implemented by graduated surface capacitance, rather than graduated surface resistance above. A skirt in the form of a tapered deposit of metal oxide on electrode 20 can accomplish such graduated capacitive implementation, e.g., through the formation of a tantalum oxide film, discussed in some detail later.

The impedance graduation need not be accomplished by a surface layer but can if fact extend into the body of the electrode: In yet another implementation, the active electrode is built from axially layered regions of different electrical properties. The direction of current flow can be selectively controlled in individual layers. If radial flow is desired the layer is separated from its neighbors by an insulator and is connected in the center to cable 26. If axial flow is desired the layer is insulted from the cable 26 and electrically joined to its neighbors.

The flow of heat from the electrode 20 is aided by the large cross section of cable 26. The heat flow path in the cable heat sink implementation, shown in FIG. 3, is completed by modification of the catheter tube 24 to increase thermal conductivity from cable 26 to the outside tissue. The heat conductivity of a plastic elastomer material for tube 24 is reduced by embedding heat conductive particles in the material. The region between the cable 26 and the tube 24 is filled with heat conductive paste 27. The technology of improved heat conductivity plastics, and the technology of heat conductive pastes are well established in conjunction with heat sink techniques for solid state devices. In the cable heat sink implementation above, heat dissipated in the tissue, heats active electrode 20. Active electrode 20 in turn, is cooled by heat outflow along cable 26, through the conductive paste 27 and a wall of catheter tube 24 to the blood and tissue surrounding tube 24.

FIG. 4 shows an alternative heat sink design. The mounting of cable 26 and tube 24 to active electrode 28 and the function of conductive skirt 23 is substantially the same as described in conjunction with FIG. 3. Active electrode 28 in FIG. 4, preferably made from silver, which is the best heat conductor, has a different shape from active electrode 20 in FIG. 3: Active electrode 28 is longer and is shaped to seat a cylindrical film heat sink 29. The heat sink film 29 is electrically insulating and thermally conductive.

The distal end of active electrode 28 provides a bare metal interface to tissue, generating a heating pattern just as active electrode 20 in FIG. 3. When compared with FIG. 3, the interface between cylindrical film heat sink 29 and the external blood flow provides an added cooling element. The amount of heating and cooling is independently controlled by the ratio of the electrically interacting bare electrode area to the heat sink area.

The overall effectiveness of the heat sink is determined by the thermal conductivity of film 29 and by the heat transfer coefficient. The heat transfer coefficient associated with the thermal boundary layer in forced convection of heat between the catheter surface and the adjacent blood flow, is determined by thermal and hydrodynamic properties of blood. As long as the thermal conductivity of film 29 is significantly smaller than the heat transfer coefficient of the heat convection of the blood flow, the heat sink is close to optimum design. Implementation of heat sink film 29 by a 0.025 mm plastic tube meets this requirement.

The design in FIG. 4 provides very effective forced convective cooling by the flow of blood, while at the same time, allows full control over the size of the area which generates the electrical current flow. It will be noted that the active electrode in FIG. 4 can also comprise the impedance skirt 23 which prevents the formation of a hot spot at the juncture where active electrode 28 and electrically insulating film heat sink 29 meet. The capacitive impedance skirt implementation can be implemented using the same material as heat sink film 29. Cable 26, attached to active electrode 28 provides additional cooling of active electrode 27 by allowing the heat flow into the catheter tube, as previously discussed in conjunction with FIG. 3.

An attractive heat sink/impedance skirt implementation involves a tantalum tube 30 (shown dashed in FIG. 4) which is pressed onto active electrode 28 and so

maintains a good thermal and electrical contact with active electrode 28. This tantalum tube is covered by a 0.5 μm thick film of tantalum oxide on its external surface and is graduated to 0 thickness in the skirt area.

It is well known from the technology of tantalum capacitors that a tantalum film only 0.5 μm thick is adequate to provide an electrical insulation with a breakdown voltage in excess of 350 volts. The relative dielectric constant of the tantalum oxide film is 27.6 and so 0.5 μm thick layer 29 produces a capacitance of 8.85 pF to the tissue. At an operating frequency of 300 kHz, this film represents a capacitive reactance of 60 kΩ. When compared with the resistance of the active electrode metal-tissue interface, which is of the order of 100 Ω, the capacitive current through oxide film 29 is insignificant, and film 29 in effect blocks the current flow between the oxide covered tantalum tube 30 and the surrounding tissue and so eliminates electrical heat generation in the tissue surrounding the tantalum oxide heat exchanger.

The same tantalum oxide film 29 has a thermal conductivity of 0.3 watts/(meter C°). For the specified film thickness of 0.5 μm and film area of 12.6 mm^2, oxide film 29 represents a large thermal conductance of 75.6 watts/C°, which is very adequate for an efficient heat sink.

Graph (B) in FIG. 2 shows the temperature distribution along projection 31 of the axis beyond the distal end of the catheter for an optimized heat sink design in FIG. 4. Comparison of Graph (A) and Graph (B) in FIG. 2 indicates the superior features of the heat sink catheter: The peak temperature is no longer at the catheter surface. The ablation temperature is reached some distance from the catheter surface. Also the ablation region where the tissue temperature is above 48° C. is much larger.

The shape of Graph (B) in FIG. 2 can be adjusted by modification of the ratio of the electrically interacting bare metal active electrode area 32, to the heat sink area 29, and so can be optimized for the requirements of the specific medical procedure.

FIG. 5 shows a proximal ring electrode 75 and a distal tip electrode 76, mounted or plated on a catheter tube 74 and shaped very similarly to the currently used pacing catheters. An electrical connection in maintained by a twisted pair transmission line 77. Unlike currently u&M catheters where the electrodes are made from plain metal, proximal ring electrode 75 and distal tip electrode 76 have their notallic surfaces coated with control coatings 79 and 78 respectively. Optionally, the gap between proximal ring electrode 75 and distal tip electrode 76 can be filled with gap coating 70. (Thickness of coatings is exaggerated in FIG. 5 for the sake of clarity.)

Control coatings 78 and 79 vary in thickness as a function of the axial distance from the inter-electrode gap, being thickest along the edges of the inter-electrode gap and thinning away from the gap. The electrical properties of the uniform thickness coating 70 can be constant or can vary in the axial direction. Without the coatings, the strongest E_Z field in adjacent to the inter-electrode gap. The coatings, by changing the surface impedance, equalize the external electric field and improve radial penetration of the field.

Coatings 78, 79, and 70 can be made from a resistive material or from a dielectric. A resistive coating introduces the highest resistance close to the inter-electrode gap. As a result, the external field adjacent to the inter-electrode gap is reduced, the external field intensity is equalized and the radial penetration is improved. A capacitive coating, made from a dielectric, exhibits a smallest capacitive impedance near the inter-electrode gap and accomplishes field equalization similar to the resistive coating. There is, however, significantly less heat dissipation in the capacitive coating than in the resistive coating.

While certain specific embodiments of improved electrical catheters and systems have been disclosed in the forgoing description it will be understood that various modifications within the scope of the invention may occur to those skilled in the art. Therefore, it is intended that adaptations and modifications should and are intended to be comprehended within the meaning and range of equivalents of the disclosed embodiments:

What is claimed is:

1. An electrical heating catheter comprising:
an electrical cable housed in an electrically insulating catheter tube;
the electrical cable adapted to be connected at a proximal end to a source of electrical power;
an active electrode including a metallic material;
the electrical cable connected at a distal end to said active electrode;
a graduated electrical impedance coating on the active electrode for providing a smooth transition of surface current density between said metallic material of the active electrode and a material of the electrically insulating catheter tube.

2. An electrical heating catheter in claim 1 wherein said coating comprises a material with substantially uniform electrical properties and a varying thickness.

3. An electrical heating catheter in claim 2 wherein said material of said coating is conductive epoxy.

4. An electrical heating catheter in claim 2 wherein said material of said coating is a cermet.

5. An electrical heating catheter in claim 2 wherein said material of said coating is a plastic.

6. An electrical heating catheter in claim 2 wherein said material of said coating is a metal oxide.

7. An electrical heating catheter in claim 2 wherein said coating with said varying thickness comprises a conductive skirt surrounding a base of said active electrode, the skirt characterized by a wedge-shaped cross section with a wide face of the wedge against a junction with said electrically insulating catheter tube and a pointy end of the wedge against said metallic material of said active electrode.

8. An electrical heating catheter in claim 1 wherein said graduated electrical impedance coating comprises an electrical material of a substantially uniform thickness and a spatially varying electrical impedance.

9. An electrical heating catheter in claim 1 wherein said graduated electrical impedance coating comprises axially stratified layers, each layer of a substantially constant impedance, and an impedance value graduated from layer to layer.

10. In a catheter for electrical heating, comprising an active electrode formed of metallic material and a catheter transmission line having a proximal end and a distal end, said line being adapted to be connected at its proximal end to a source of electrical power and being connected at its distal end to said active electrode, said electrode in operation being immersed in a lossy medium, said catheter characterized by:
a graduated impedance coating deposited on a surface of the said active electrode for shaping an

electric field in the lossy medium outside of said electrode and coating being heat conducting and electrically insulating, said coating controlling an electrical heating of tissue and cooling of said active electrode by convective blood flow.

11. A catheter for electrical heating in accordance with claim 10, wherein said graduated impedance coating comprises a resistive coating of a varying thickness deposited on the metallic material of said electrode.

12. A catheter for electrical heating in accordance with claim 10, wherein said graduated impedance heat sink coating comprises a dielectric coating of a varying thickness deposited on said metallic material.

13. A catheter for electrical heating in accordance with claim 10, further comprising a graduated electrical impedance coating located in a gap and electrically interacting with said active electrode.

* * * * *

TITLE Catheter - Electrode to Tip Junction Design:

Page

From Page No.

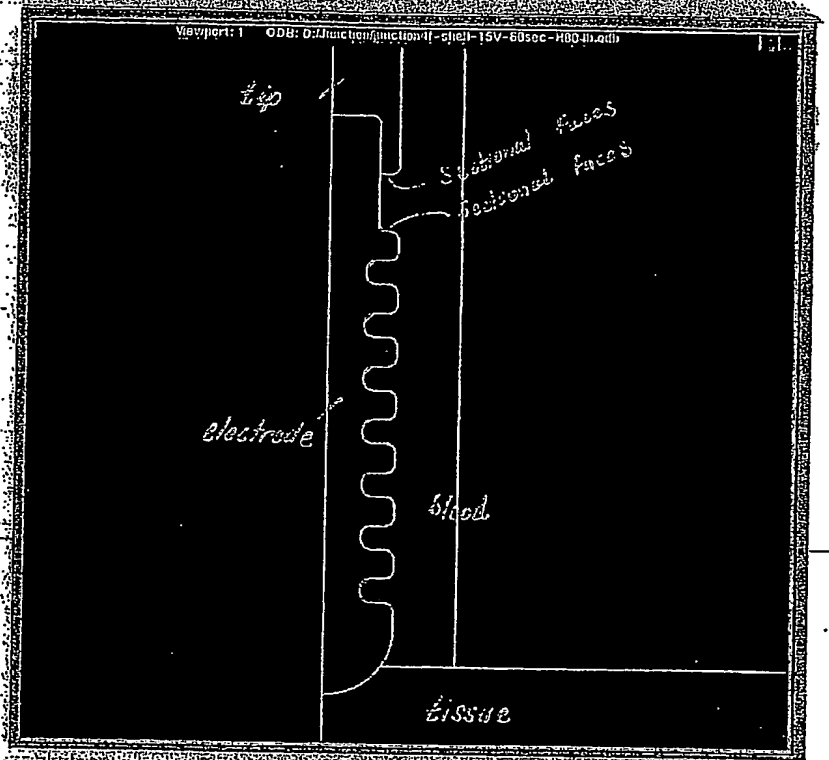

Previous electrode to tip junction designs incorporate a third material that provides a gradual transition of the electrical properties at a boundary between the ablation electrode and an insulating catheter tube. In the above design, no secondary material is introduced at this boundary or junction. A gap is maintained between the sectional faces of the electrode and the tip in the above design. The blood flows in this recessed area and assists in

To Page No. 2

TITLE Catheter Electrode-Tip Junction Design

From Page No.

to the control of the current density. The sectional faces are normal to the tip surface of the catheter tip and electrode. The junction between the electrode tip and the catheter tip surface that is exposed to the blood is recessed and lies at the base of one of the sectional faces. These characteristics control the current density at the junction and therefore minimize the formation of coagulum.

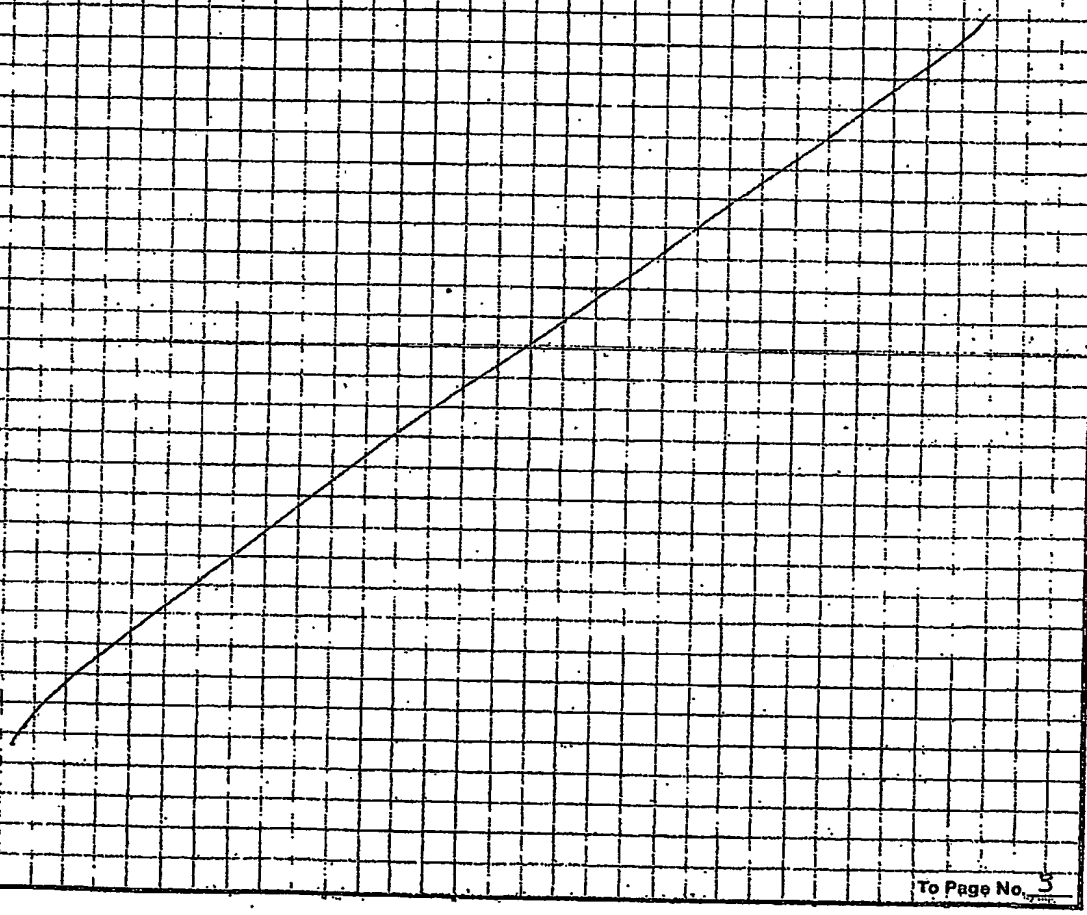

To Page No. 3

TITLE Catheter E

From Page No.

electrode

Junction Design

TITLE Catheter Electrode-Tip Junction Design

...ce normal to the ...
...tween the electrode
...ad is accessed
...se characteristics
... minimize the

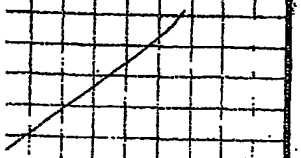

To Page No. 5

From Page No.

Tip

The body of the electrode surface may assume
various shapes. The junction shown to the
left shows the same characteristics with
a smoothed electrode body.

blood recess area

electrode

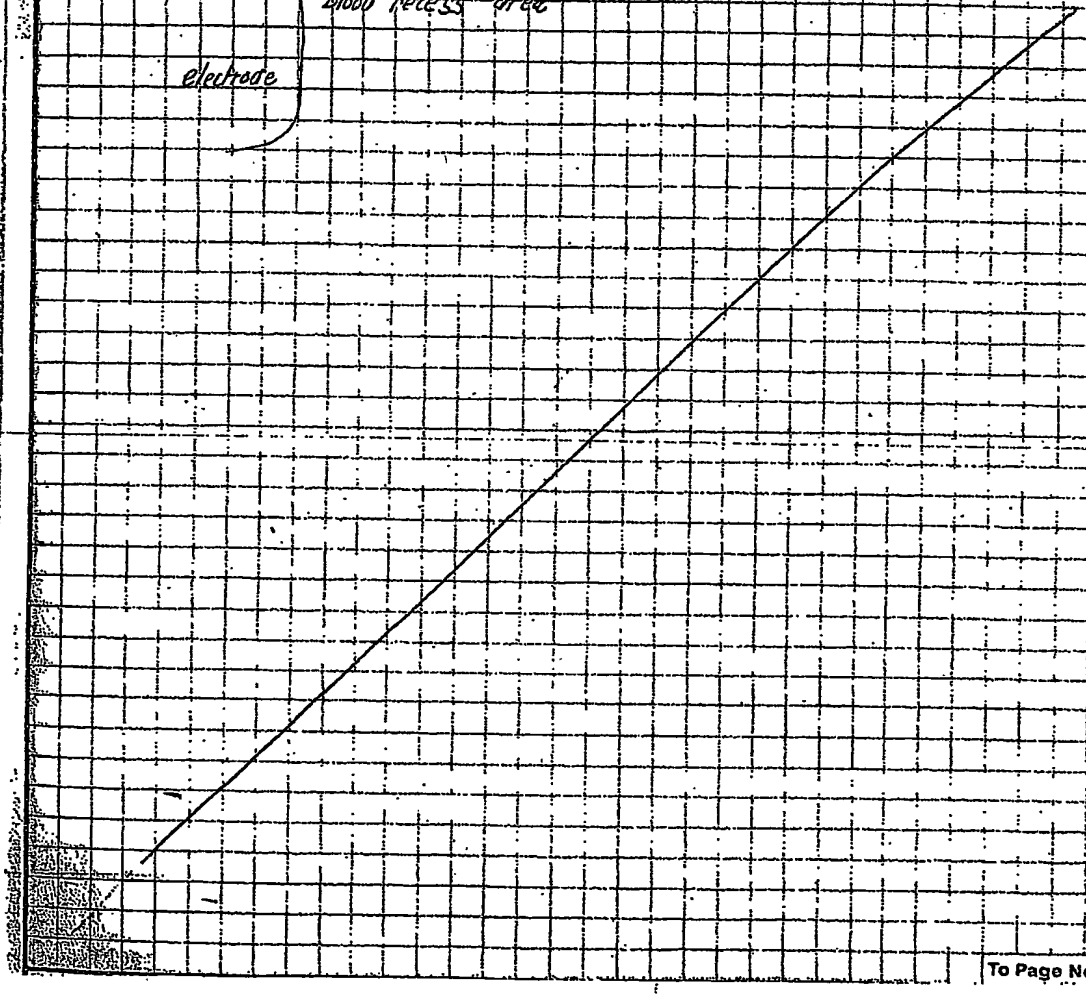

To Page No.

Bard electrophysiology

Re: Radiator Electrode – Concept Analysis

Background:

The catheter R&D department has done preliminary evaluations of a radiator electrode throughout the year. The radiator electrode concept employs a grooved surface. This grooved surface increases the electrode surface area. This increase in surface area may allow greater convective cooling that could in turn allow the radiator type electrode to maintain lower temperatures at higher power settings. It is thought that this cooling effect could potentially lead to the generation of larger and deeper lesions.

~~Through the use of Pro/E,~~ I modified the design to include a larger number of grooves that were deeper. This electrode design is shown in the attached Drawing: RAD-MOD10. This geometry increased the surface area by 41% relative to a standard 8mm electrode. The previous design evaluated increased the surface area by 5%.

Objective:

The objective of this study was to evaluate the effects of the increased surface area of the radiator electrode on electrode temperature and lesion depth. In addition, the effect of electrode mass on lesion development and electrode temperature was also evaluated. The electrode concept was evaluated at varying power settings and varying convective flow conditions. Control runs were made of five other electrode configurations:

1) 8mm electrode with the same mass as the radiator electrode (Matched Mass)
2) 8mm electrode – solid
3) 8 mm electrode – shell
4) 4 mm electrode – solid
5) 4 mm electrode - shell

These configurations are shown in Table (1). The results of radiator electrode analysis were compared to the analysis results obtained with these configurations.

Drawing: RAD-MOD10

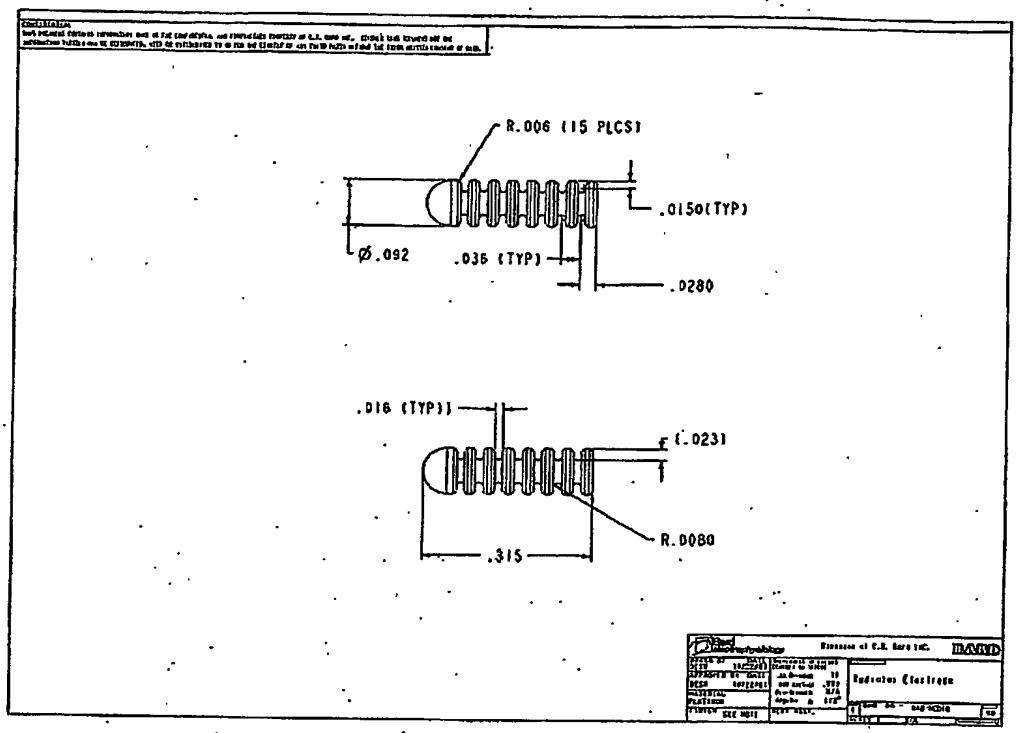

Table 1. Electrode Configurations

Electrode Type	Surface Area (in^2)	Volume (in^3)
 8mm Radiator Electrode *(41% More Surface Than Standard 8mm Electrode)*	.1285 (Solid) .1285 (Shell)	.00143 (Solid) .00051 (Shell) *(.0039" Thick)*
 8mm Electrode *(Same Mass as Radiator Electrode)*	.0910	.00143
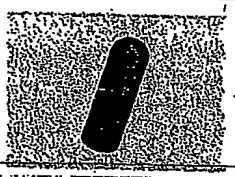 8mm Electrode – Solid	.0910	.00199
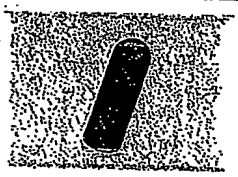 8mm Electrode – Shell *(Wall Thickness - .0061")*	.0910	.00053
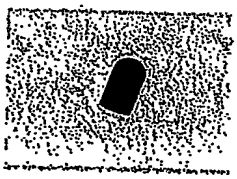 4mm Electrode – Solid	.0455	.00095
 4mm – Shell *(Wall Thickness - .0061")*	.0455	.00026

Model Description

The ablation model consisted of an electrode, plastic tip, tissue block, and blood field. Figure (1) depicts this simplified model. The material properties used in the model are listed in Table (2). Due to the symmetry of the geometry, an axisymmetric model was used. The following boundary conditions were used in the model:

Dirichlet boundary conditions set at the surfaces:

Outer surface – 0 volts
Outer surface – 37°C
Electrode surface – 5 volts to 75 volts

Convective boundary condition set along electrode-blood interface, tip-blood interface, and tissue-blood interface:

H=. 002 to .125

The initial temperature of the model was set to 37°C.

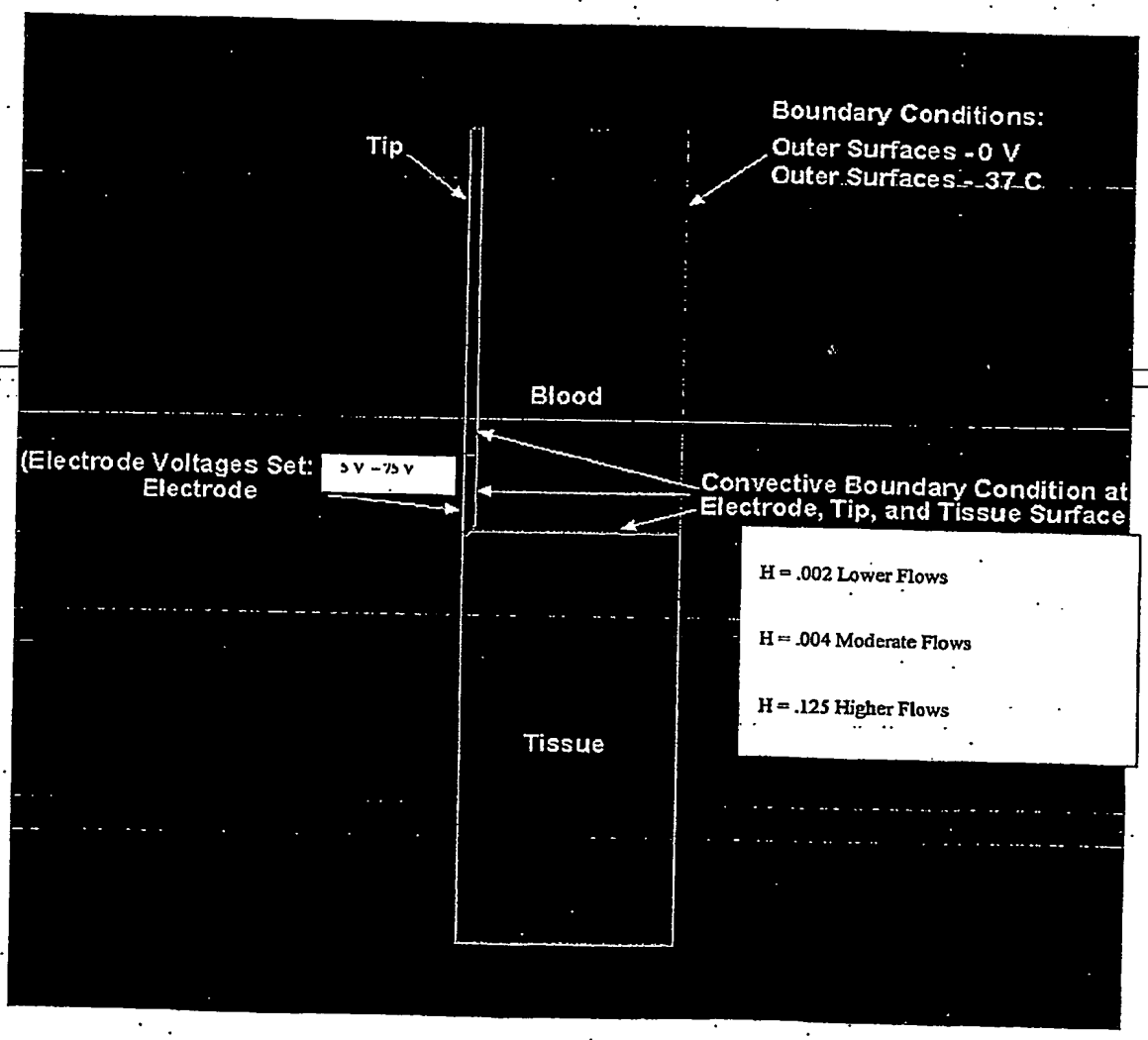

Figure 1. Model

60458856.032803

Table 2. Material Properties Used in Radiator Study

Part	Material	Specific Heat*Density J/mm3*K	Density g/mm^3	Specific Heat J/g*K	Thermal Conductivity W/mm*K	Electrical Conductivity S/mm	Thermal Diffusivity mm^2/s
Blood	Blood	0.004180	0.0010	4.180	0.000543	6.670E-04	0.13
Tip	80% Pebax 6333/ 20% Barium Sulfate, Panton	0.005500	0.0010	5.500	0.000290	1.072E-17	0.05
Electrode	Platinum	0.002838	0.0215	0.132	0.071000	4.000E+03	25.02
Tissue	Cardiac Muscle	0.003864	0.0012	3.220	(37^{0}C) 0.00053670	2.220E-04	1.39
					(50^{0}C) 0.00055225		
					(63^{0}C) 0.00057779		
					(76^{0}C) 0.00058332		
					(89^{0}C) 0.00059886		
					(102^{0}C) 0.00061390		

Model Description (continued)

The following bio-heat equations were solved through the analysis. Equation (2) is the Laplace equation for voltage potential. This equation was solved to determine the potential field established by each electrode configuration. For each electrode-geometry, the potential field at a constant power setting is depicted in Figure (2). The potential field results were used to solve the heat equation in which joule heating, conduction, and convection are considered.

$$\rho c \frac{dT}{dt} = k\nabla^2 T + JE - h_{bl}(T - T_{bl}) \qquad (1)$$

$$\sigma \nabla^2 V = 0 \qquad (2)$$

$$J = \sigma E = -\sigma \nabla V \qquad (3)$$

ρ *(density – kg/m^3)*
c (specific heat- J/kgAK)
k (thermal conductivity-W/mAK)
J (current density- A/m^2)
E (electric field density-V/m)
h_{bl} *(convective heat transfer coefficient)*
T(°C)
T_{bl} *(temperature of blood-37°C)*
V(potential distribution)
σ *(electrical conductivity-S/m)*

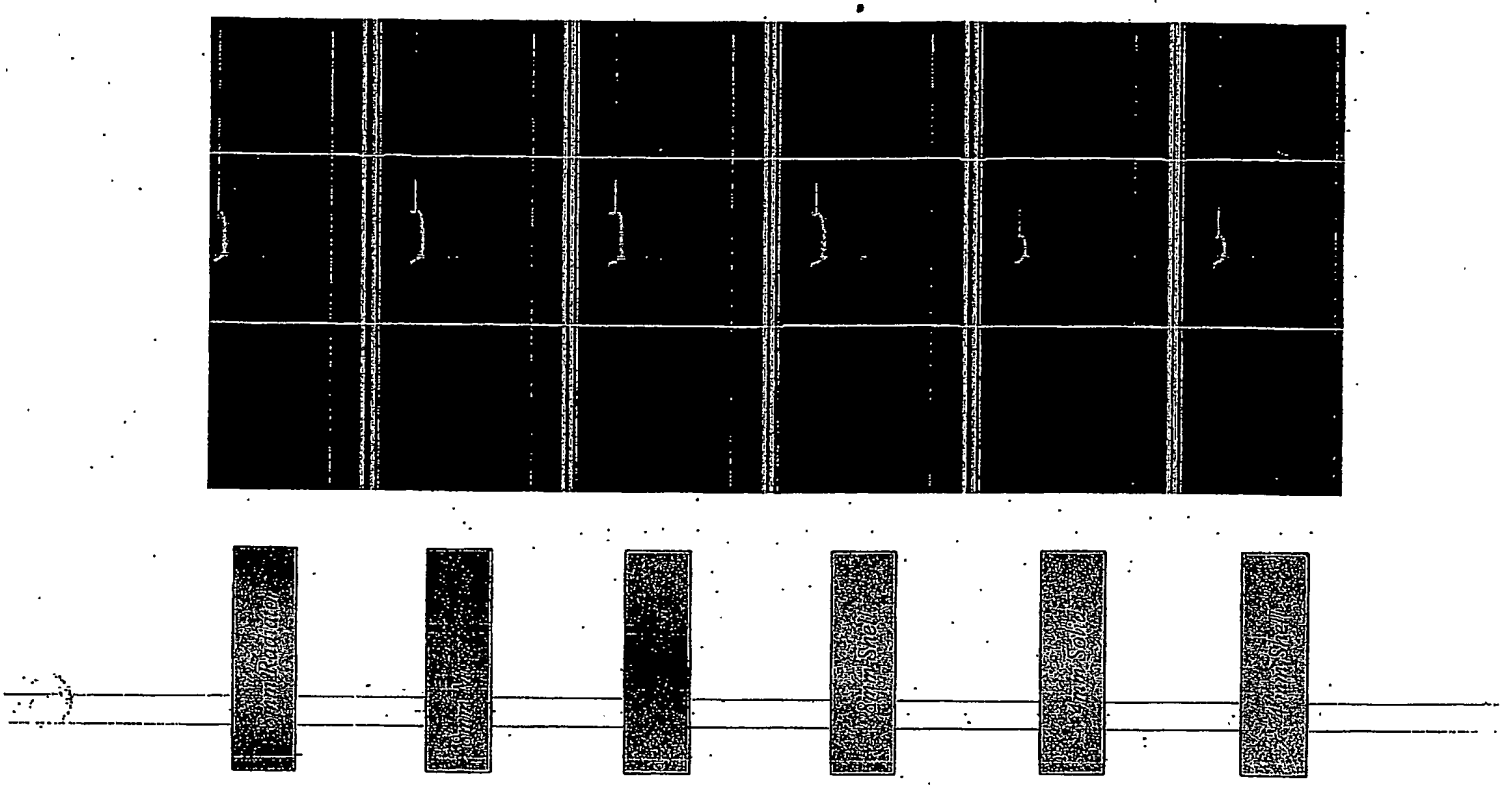

Figure 2. Potential Fields for Varying Electrodes

Protocol and Rationale for Analysis Runs

Voltage values ranging between 25V and 75V have been observed in clinical settings. Therefore this range was explored. Values below 25 volts were explored to understand the minimum power requirements for lesion generation for the varying electrode geometries. For each electrode-geometry, twenty-four analysis runs were performed at the settings depicted in Table (3). Each run simulated an ablation of duration of 120 seconds.

Table 3. Voltage and Flow Setting for Analysis Runs

Run	Flow Condition	Voltage
1	H=.125	5
2	H=.125	15
3	H=.125	25
4	H=.125	35
5	H=.125	45
6	H=.125	55
7	H=.125	65
8	H=.125	75
9	H=.004	5
10	H=.004	15
11	H=.004	25
12	H=.004	35
13	H=.004	45
14	H=.004	55
15	H=.004	65
16	H=.004	75
17	H=.004	5
18	H=.004	15
19	H=.004	25
20	H=.004	35
21	H=.004	45
22	H=.004	55
23	H=.004	65
24	H=.004	75

The following field results were obtained for each electrode-geometry at the above run conditions:

- *Potential Field*
- *Temperature Field*
- *Current Density Field*

Through analysis of the temperature fields at the end of a 60-second period, the following values were tabulated:

- *Maximum Tissue Temperature*
- *Maximum Electrode Temperature*
- *Minimum Electrode Temperature*
- *Lesion Depth*

An evaluation of the time history of the joule heat dissipation *(JE)* allowed the calculation of power, current, and impedance values. The equations used for these calculations is shown below:

Model Analysis Calculations

$$\text{Power} = \frac{JE}{\text{Time Interval}}$$

$$\text{Impedance} = \frac{V^2}{\text{Power}}$$

Analysis Description

A transient analysis was run using a full Newton method. The time increments for each analysis were determined automatically. The step size for sixty-second ablation simulations ranged from .0012 to 2 seconds. The average mesh size for the runs was about .3 mm. Figure 3 shows an example mesh.

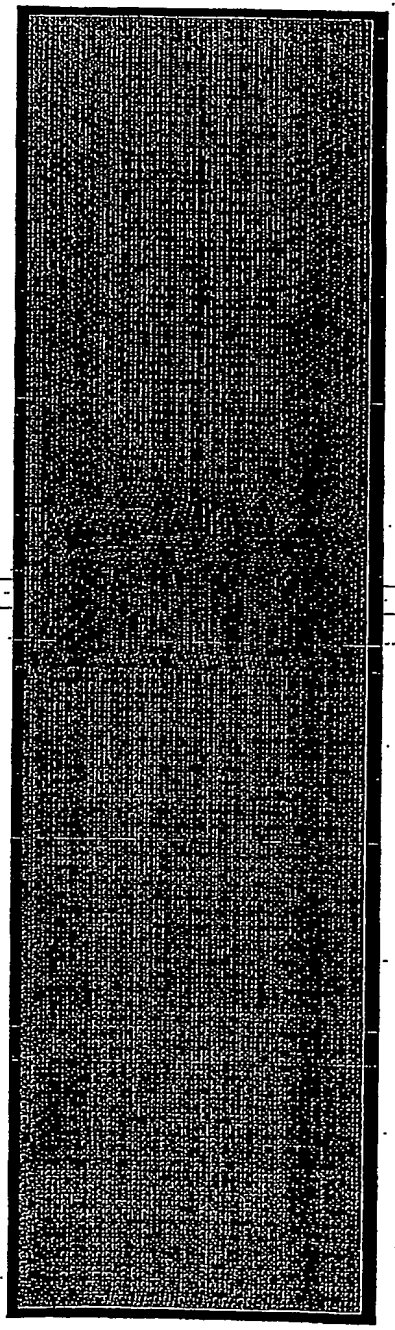

Results and Discussion

Operation Parameters

The power, voltage, maximum electrode temperature, and minimum electrode temperature were determined for maximum tissue temperatures ranging between 55°C and 95°C. These values are shown in Table (4). This table was developed to understand the appropriate temperature ranges and power ranges for data comparison. Comparisons of the lesion formation and cooling effects for the various electrode geometries were evaluated within these ranges. Table (4a) and Table (4b) show the operating parameters at H values of .002 and .125 repsectively.

Table (4). Operating Parameters for Various Electrode Configurations (H=. 004)

Maximum Tissue Temperature	55°C	65°C	75°C	85°C	95°C
Power (W)	5.10	8.00	10.90	13.86	13.90
Voltage (V)	21.40	27.00	31.60	35.60	39.30
Max Electrode Temperature(°C)	50.15	57.60	65.20	72.90	80.65
Min Electrode Temperature (°C)	48.30	54.75	61.20	67.80	74.55
Lesion Depth (mm)	1.34	2.54	3.41	4.09	4.61
Power (W)	5.30	8.30	11.35	14.40	14.40
Voltage (V)	21.60	27.10	31.70	36.00	39.45
Max Electrode Temperature(°C)	51.50	59.75	68.10	76.60	85.20
Min Electrode Temperature (°C)	47.65	53.75	59.90	66.05	72.40
Lesion Depth	1.38	2.55	3.42	4.12	4.63
Power (W)	9.85	15.50	21.20	27.03	27.05
Voltage (V)	24.00	30.00	35.40	39.70	44.00
Max Electrode Temperature(°C)	50.20	57.80	65.50	77.00	81.20
Min Electrode Temperature (°C)	45.00	49.60	54.25	59.00	63.75
Lesion Depth	1.47	2.79	3.87	4.57	5.11
Power (W)	10.05	16.00	21.90	27.86	27.90
Voltage (V)	24.40	30.40	35.90	40.30	44.70
Max Electrode Temperature(°C)	53.40	63.00	72.55	82.40	92.00
Min Electrode Temperature (°C)	43.50	47.20	51.00	54.80	58.65
Lesion Depth	1.45	2.85	3.97	4.69	5.24
Power (W)	9.65	15.20	20.80	26.45	26.45
Voltage (V)	23.40	29.20	34.20	38.60	42.65
Max Electrode Temperature(°C)	51.60	60.00	68.45	73.40	85.70
Min Electrode Temperature (°C)	47.30	53.10	59.10	65.10	71.20
Lesion Depth	1.46	2.73	3.81	4.51	5.01
Power (W)	9.85	15.45	21.10	26.90	26.95
Voltage (V)	23.40	29.20	34.70	39.60	42.70
Max Electrode Temperature(°C)	53.60	63.10	72.65	82.20	92.20
Min Electrode Temperature (°C)	46.35	51.90	57.60	62.90	68.20
Lesion Depth	1.48	2.77	3.85	4.55	5.08
Power (W)	9.80	15.40	21.00	26.75	26.80
Voltage (V)	23.20	29.00	34.10	38.60	43.05
Max Electrode Temperature(°C)	52.10	60.80	69.60	78.50	87.50
Min Electrode Temperature (°C)	47.00	52.65	58.40	64.30	70.20
Lesion Depth	1.48	2.73	3.77	4.48	5.03

Table (4A). Operating Parameters for Various Electrode Configurations (H=.002)

Maximum Tissue Temperature	55°C	65°C	75°C	85°C	95°C
[redacted]					
Power (W)	3.45	5.65	7.80	9.90	12.00
Voltage (V)	17.50	22.40	26.45	29.70	32.90
Max Electrode Temperature(°C)	53.70	63.10	72.50	82.10	91.70
Min Electrode Temperature (°C)	52.20	60.80	69.40	78.10	86.90
Lesion Depth (mm)	.71	2.13	3.05	3.65	4.12
[redacted]					
Power (W)	3.65	6.00	8.20	10.20	12.60
Voltage (V)	18.10	23.00	27.00	30.30	33.60
Max Electrode Temperature(°C)	55.30	65.50	76.00	86.40	96.90
Min Electrode Temperature (°C)	51.90	60.10	68.60	77.10	85.50
Lesion Depth	.80	2.22	3.11	3.73	4.22
[redacted]					
Power (W)	7.55	12.10	16.55	21.05	25.55
Voltage (V)	20.80	26.60	30.95	35.20	38.60
Max Electrode Temperature(°C)	55.10	65.40	75.80	86.30	96.90
Min Electrode Temperature (°C)	49.20	56.40	63.50	70.60	77.95
Lesion Depth	1.39	2.66	3.54	4.24	4.77
[redacted]					
Power (W)	8.20	12.90	17.55	22.30	27.15
Voltage (V)	21.50	27.30	31.95	36.20	39.80
Max Electrode Temperature(°C)	59.70	72.60	85.70	99.50	112.4
Min Electrode Temperature (°C)	47.20	53.30	59.30	65.40	71.10
Lesion Depth	1.49	2.72	3.60	4.30	4.86
[redacted]					
Power (W)	7.15	11.10	15.25	19.35	23.45
Voltage (V)	19.50	25.20	29.00	32.80	36.20
Max Electrode Temperature(°C)	55.60	66.10	76.70	87.30	98.00
Min Electrode Temperature (°C)	51.70	60.00	68.40	76.75	85.20
Lesion Depth	1.13	2.47	3.33	3.94	4.46
[redacted]					
Power (W)	7.30	11.75	16.05	20.30	24.60
Voltage (V)	20.10	25.80	29.80	33.90	37.30
Max Electrode Temperature(°C)	58.70	71.00	83.40	95.80	108.40
Min Electrode Temperature (°C)	50.90	58.70	66.60	74.75	82.55
Lesion Depth	1.23	2.53	3.37	4.04	4.58
[redacted]					
Power (W)	7.10	11.00	15.20	19.35	23.50
Voltage (V)	19.50	25.20	29.00	32.80	36.20
Max Electrode Temperature(°C)	56.00	66.70	77.60	88.50	99.50
Min Electrode Temperature (°C)	51.25	59.30	67.40	75.50	83.70
Lesion Depth	1.11	2.44	3.26	3.88	4.43

[redacted]

Table (4B). Operating Parameters for Various Electrode Configurations (H=.125)

Maximum Tissue Temperature	55°C	65°C	75°C	85°C	95°C
[illegible]					
Power (W)	7.850	12.40	16.95	21.60	26.35
Voltage (V)	26.50	33.40	39.10	44.30	48.85
Max Electrode Temperature(°C)	38.05	38.65	39.25	39.85	40.48
Min Electrode Temperature (°C)	37.45	37.70	37.97	38.25	38.50
Lesion Depth (mm)	.40	2.95	4.12	4.7	5.25
[illegible]					
Power (W)	7.95	12.50	17.10	21.75	26.55
Voltage (V)	26.50	33.50	39.10	44.30	48.85
Max Electrode Temperature(°C)	38.55	39.45	40.70	41.25	42.20
Min Electrode Temperature (°C)	37.43	37.65	37.90	38.15	38.78
Lesion Depth	.4	2.95	4.12	4.70	5.24
[illegible]					
Power (W)	13.30	20.95	28.70	36.60	44.60
Voltage (V)	28.10	35.20	41.20	46.50	51.35
Max Electrode Temperature(°C)	38.50	39.36	40.50	41.15	42.05
Min Electrode Temperature (°C)	37.20	37.30	37.40	37.51	37.62
Lesion Depth	.80	3.29	4.33	5.04	5.66
[illegible]					
Power (W)	13.20	20.70	28.50	36.25	44.20
Voltage (V)	27.60	35.00	40.70	46.20	50.90
Max Electrode Temperature(°C)	39.50	40.95	42.45	43.96	45.50
Min Electrode Temperature (°C)	37.10	37.15	37.20	37.25	37.31
Lesion Depth	.75	3.25	4.28	4.98	5.60
[illegible]					
Power (W)	14.10	22.15	30.40	38.75	47.20
Voltage (V)	27.90	35.30	41.15	46.6	51.45
Max Electrode Temperature(°C)	38.30	39.05	39.83	40.60	41.40
Min Electrode Temperature (°C)	37.38	37.60	37.83	38.06	38.29
Lesion Depth	.83	3.38	4.42	5.14	5.73
[illegible]					
Power (W)	13.9	21.8	29.90	38.10	46.50
Voltage (V)	27.8	35.2	41.0	46.5	51.20
Max Electrode Temperature(°C)	38.32	39.07	39.89	40.68	41.45
Min Electrode Temperature (°C)	37.35	37.55	37.75	37.95	38.15
Lesion Depth	.81	3.35	4.41	5.11	5.70
[illegible]					
Power (W)	14.10	22.15	30.40	38.75	47.20
Voltage (V)	27.90	35.30	41.15	46.60	51.45
Max Electrode Temperature(°C)	38.30	39.05	39.83	40.60	41.40
Min Electrode Temperature (°C)	37.38	37.57	37.81	38.04	38.27
Lesion Depth	.83	3.38	4.40	5.11	5.74

Results and Discussion (continued)

Electrode Cooling Effect

Figures (5), (6), and (7), are graphs of the minimum electrode temperature vs. power curves for each electrode-geometry. The convective heat transfer coefficients are H=.004, H=.125, and H=.002 for Figures (5), (6) and (7) respectively. The radiator shell electrode design has a lower minimum electrode temperature over the power range for all convection-coefficient values. This is due to the combined effects of increased surface area and lower electrode mass. The minimum electrode temperature occurs in the portion of the electrode adjacent to the tissue. Therefore, the graphs show that with the radiator shell design, maximum cooling is achieved over this area for a given power input. The solid radiator design is second most effective in achieving cooling over this area for a given power input. The cooling of the 8mm electrode geometries is less effective over this area due to the decreased surface area. The 8mm-electrode shell design was more effective than the larger mass 8mm electrode designs in the area adjacent to the tissue. The 4mm electrode designs were less effective in achieving cooling for a given power input. The same pattern of behavior was observed for each convective heat transfer coefficient setting.

Figures (8), (9), and (10), are graphs of the maximum electrode temperature vs. power curves for each electrode-geometry. The maximum electrode temperature for the various configurations was located at or near the junction where the tip and the electrode meet. This hot spot is due to the abrupt change in material properties and interface geometry. The figure below shows the relative and approximate positioning of the maximum and minimum electrode temperature for a radiator electrode as an example. The temperature profiles for all configurations are shown in Figure (22). In Table (5), the effective cooling of each configuration is rated in regard to maximum electrode temperature. The Table shows that no consistent pattern is observed over the range of flow settings when evaluating the maximum electrode temperature. However, for convection-coefficient settings of H=.004 and H=.002, the solid radiator design performed better in regards to junction area. This suggests that the heating in this area is effected by the mass of the radiator design. The cooling achieved by the increased surface area seems to compete with the spot heating that occurs at the tip junction. This data suggests that the most effective radiator design should minimize this effect in order to achieve the greatest advantage.

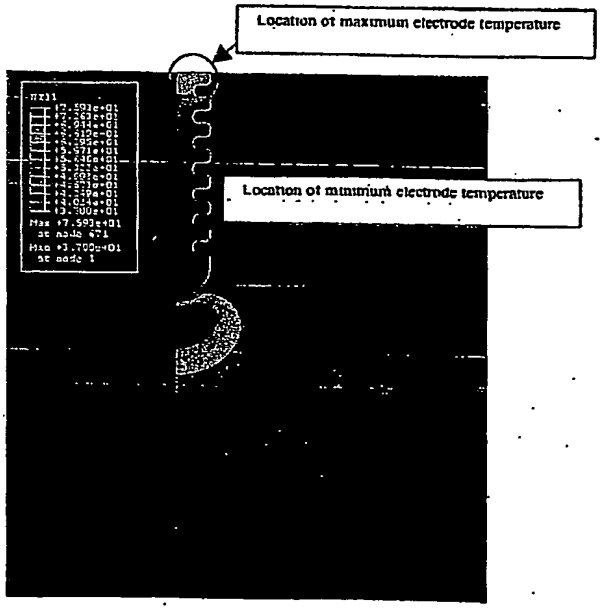

Figure 4. Approximate Locations of Maximum and Minimum Temperatures

Table 5. Cooling Effectiveness per Evaluation of Maximum Electrode Temperature

Effectiveness Rank	*H=.002*	*H.004*	*H=.125*
1 (Most effective)	8mm Radiator Solid	8mm Radiator Solid	8mm Solid 8mm Matched
2	8mm Solid	8mm Solid	
3	8mm Matched	8mm Radiator Shell	8mm Shell
4	8mm Radiator Shell	8mm Shell	8mm Radiator Solid
5	8mm Shell	8mm Matched	4mm Solid
6	4mm Solid	4mm Solid	8mm Radiator Shell
7 (Least effective)	4mm Shell	4mm Shell	4mm Shell

Figure 5. Cooling Effect of Radiator Type Electrode (H = .004)

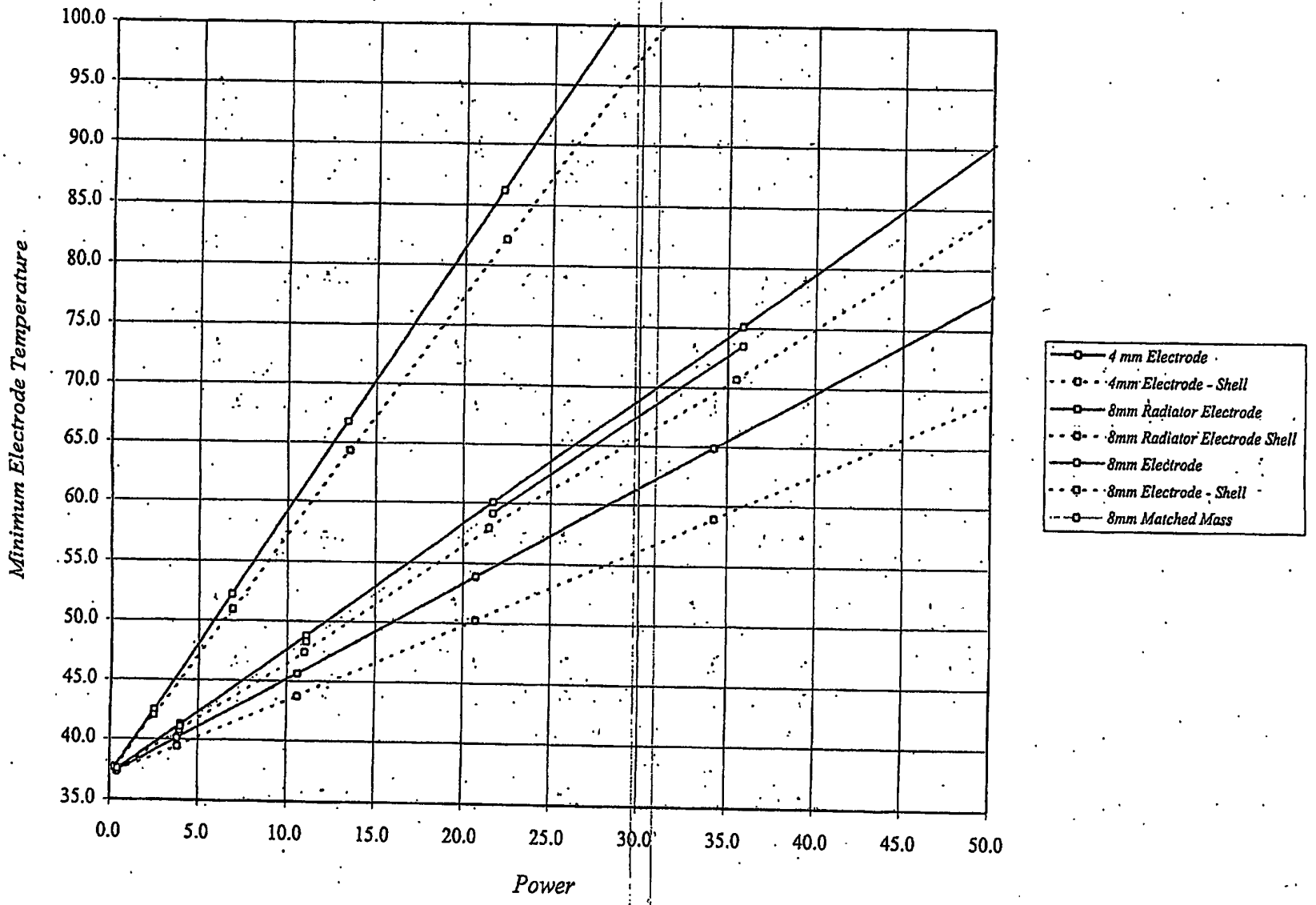

Figure 6 Cooling Effect of Radiator Type Electrode (H = .125)

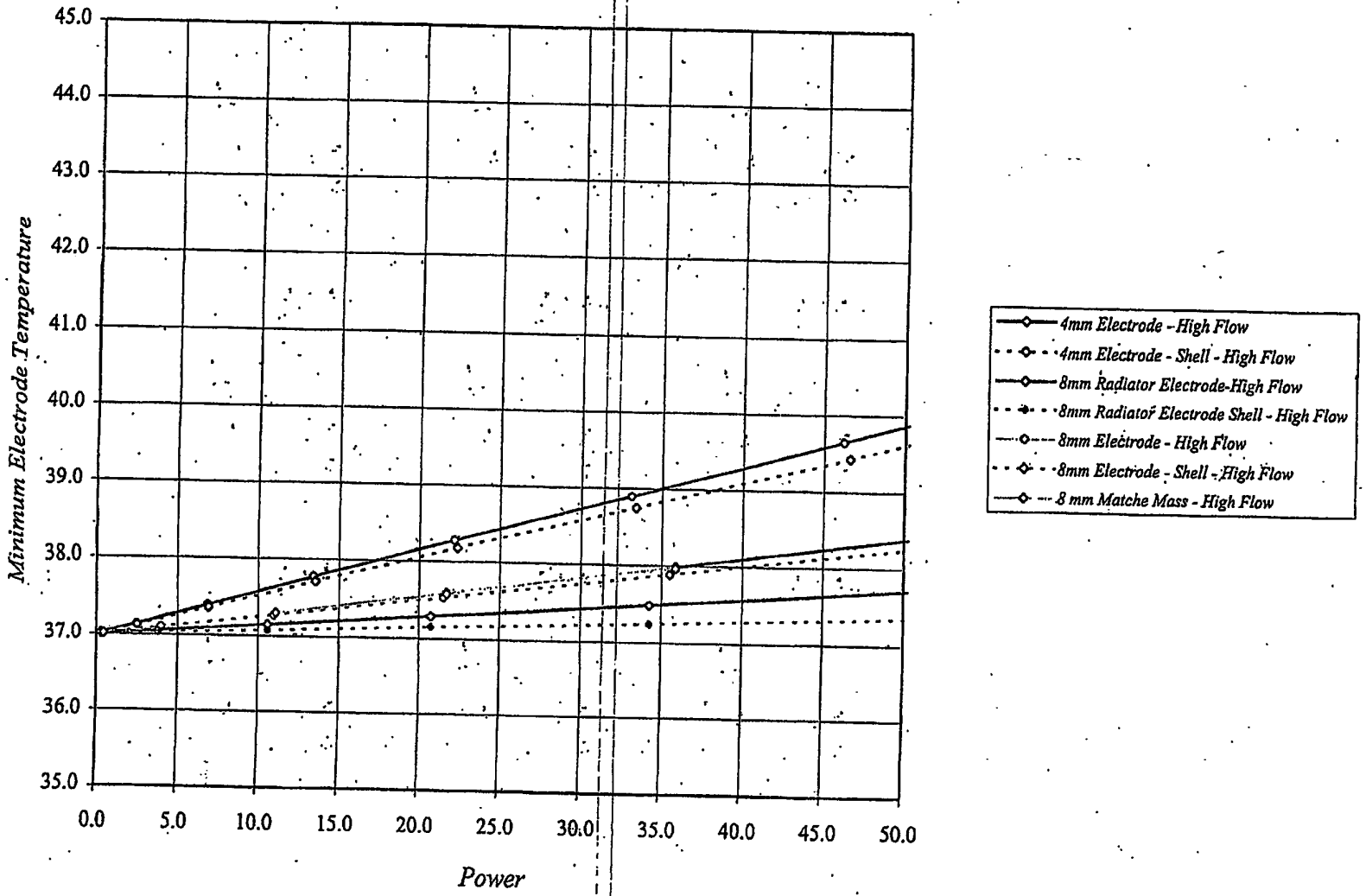

Figure7. Cooling Effect of Radiator Type Electrode (H = .002)

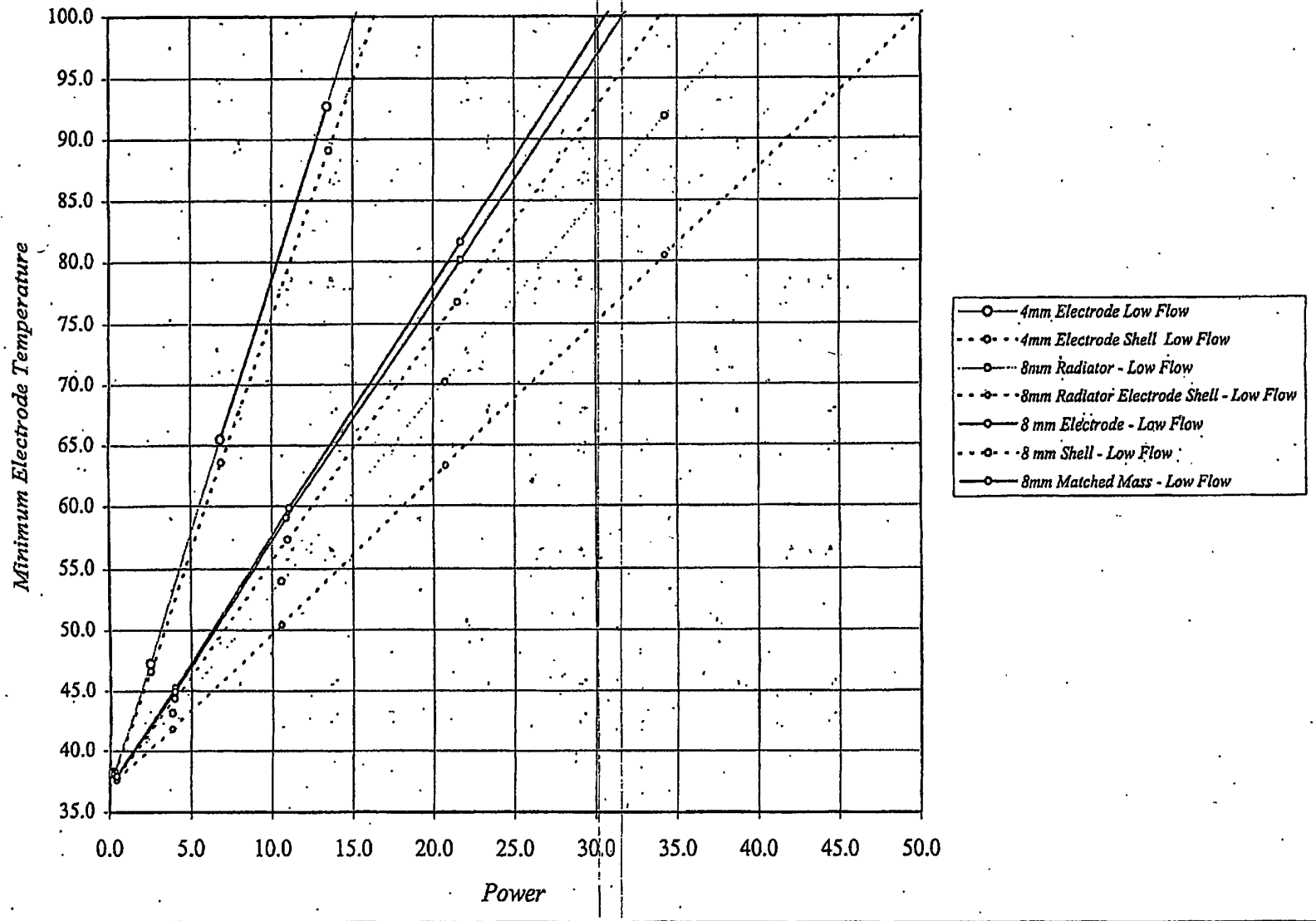

Figure8. Cooling Effect of Radiator Type Electrode (H=.004)

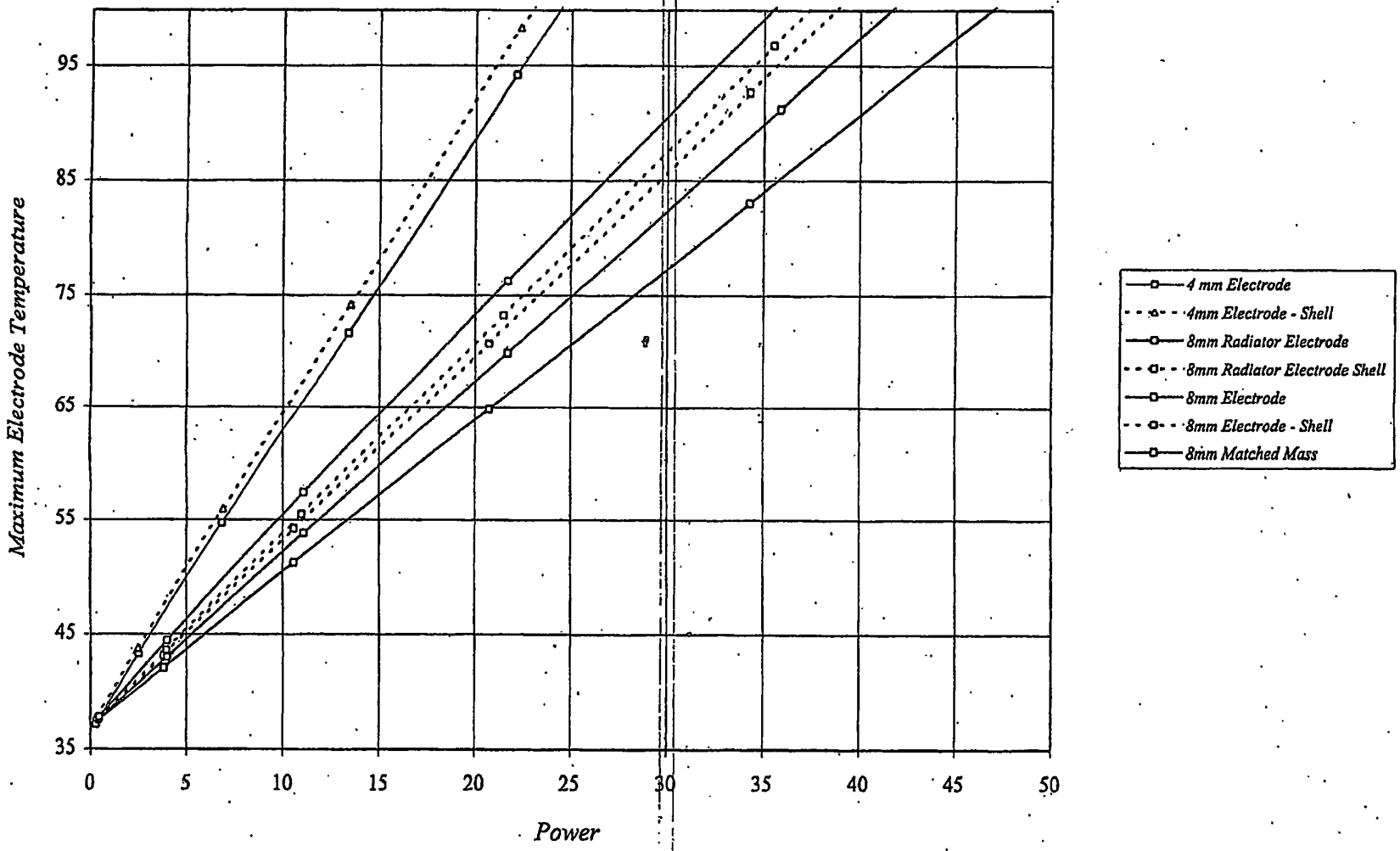

Figure 9. Cooling Effect of Radiator Type Electrode (H=.125)

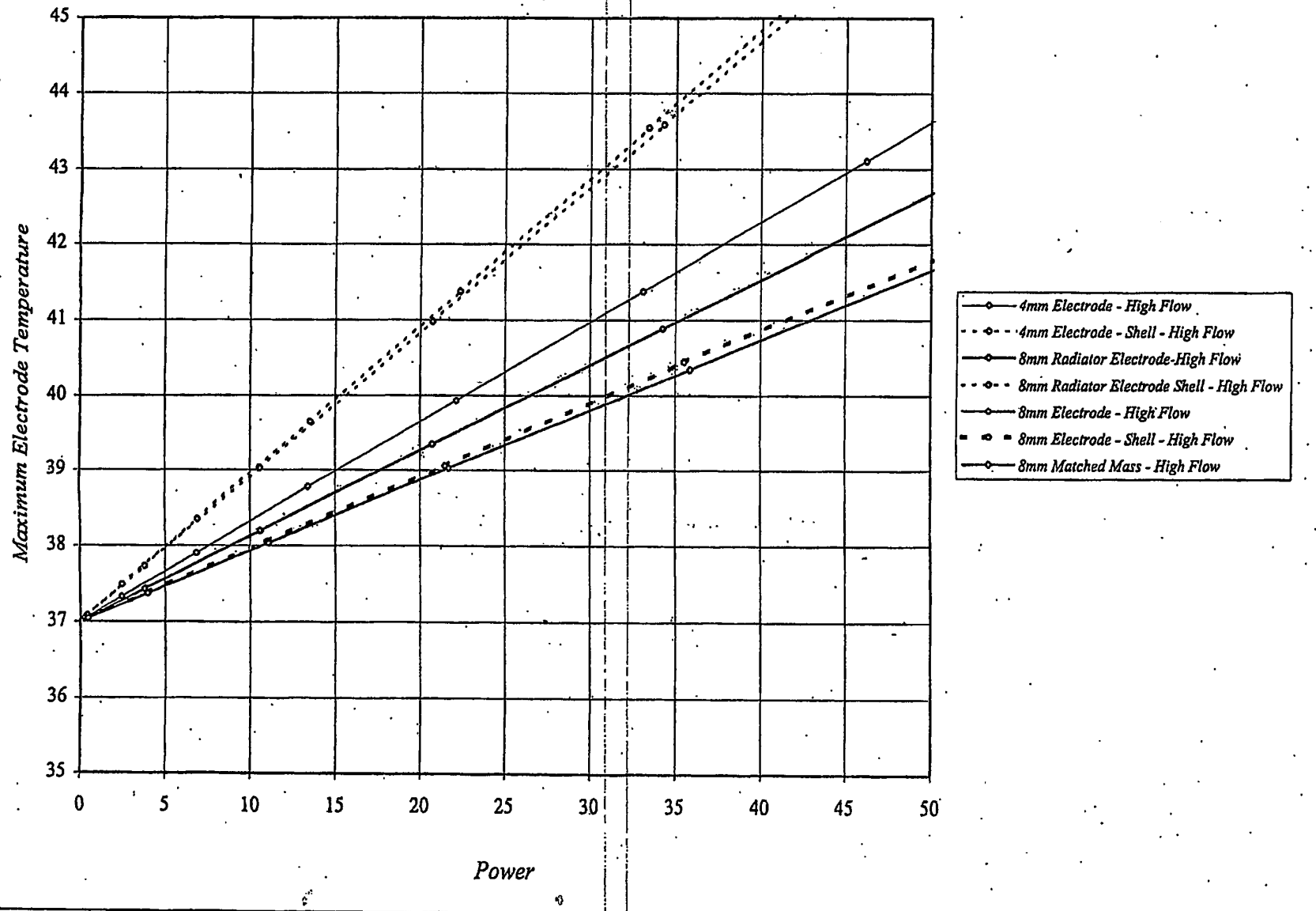

Figure10. Cooling Effect of Radiator Type Electrode (H=.002)

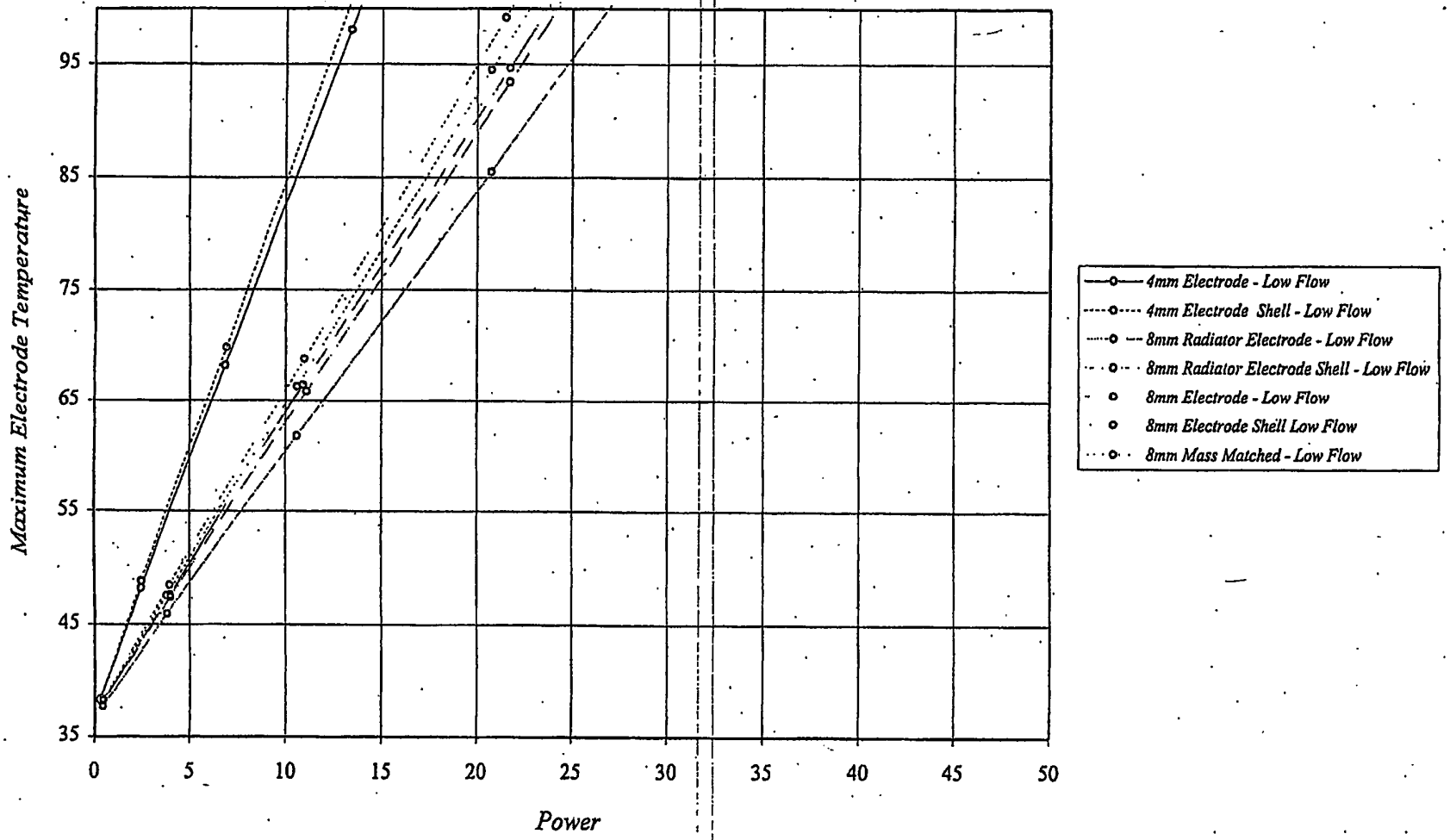

Results and Discussion (continued)

Lesion Development

Figures (11), (12), and (13), are graphs of lesion depths vs. minimum electrode temperature for each electrode-geometry. The convective heat transfer coefficients are H=.004, H=.125, and H=.002 for the Figures (11), (12) and (13) respectively. These graphs show that the radiator designs will produce a deeper lesion for a given minimum electrode temperature. Therefore, in the region adjacent to the tissue, the radiator design electrode will remain cooler than the 8mm and 4mm electrode configurations when creating the same depth lesion. Table (6) shows the radiator shell offers the best improvement to lesion depth for a given electrode temperature within this region. At a convection-coefficient of H=.002, the radiator shell design offers improvements of 12.6%, 20.87%, and 33.9% to the solid radiator design, 8mm solid design, and 4mm solid design respectively. At higher flows (H=.004), the improvements increase to 41.9%, and 66.7% for the 8mm solid design, and 4mm solid design respectively. The improvements over the solid radiator do not change a lot with increasing flows since both radiator configurations have the same amount of surface area. Table (6) and Figure (12) also show that at high flows (H=.125), for a given electrode temperature within this region, the radiator configurations are able to create lesions when the other configurations have not begun to generate a lesion at all.

Figures (14), (15), and (16), are graphs of lesion depths vs. maximum electrode temperature for each electrode-geometry. The convection heat transfer coefficients are H=.004, H=.125, and H=.002 for the Figures (14), (15) and (16) respectively. These graphs show that the radiator solid designs will produce a deeper lesion for a given maximum electrode temperature for H=.002 and H=.004. Therefore, in the region where the electrode and the catheter tip meet (junction region), the solid radiator design electrode will remain cooler than the radiator shell, 8mm and 4mm electrode configurations when creating the same depth lesion. At higher flow rates (H=.125) the solid radiator design does not offer much benefit. Table (7) shows that at a convection-coefficient of H=.002, the solid radiator design offers improvements of 13.7%, 7.7%, and 9.7% over the shell radiator design, 8mm solid design, and 4mm solid design respectively. At higher flows (H=.004), the improvements are 11.1%, 6.5%, 10.4% for the shell radiator design, 8mm solid design, and 4mm solid design respectively. These improvements to lesion depths are much lower than the improvements observed when evaluating lesion depths relative to minimum electrode temperature. In addition, these improvements are not improved by increasing flow, except in the case of the radiator shell at H=.125. For the radiator design, we would expect convective flow rates to influence the improvement in lesion depth for a given maximum temperature, this does not seem to be the case. Again this seems to be reflective of the competing contributions of convective cooling and junctional heating in this region.

Figures (17), (18), (19), are graphs of lesion depth vs. maximum tissue temperature. These graphs in combination with Table (4), Table (4a) and Table (4b) were used to establish the appropriate ranges for the above graphs. In addition, these graphs and tables were used to establish the temperature maximum and minimum electrode values used in the development of Tables (6) and (7).

Table 6. Comparison of Lesions Depths to Best Performance of Radiator Shell in Minimum Electrode Temperature Region and Various Flows

F	F=.002 (72 C)		F=.004 (68 C)		F=.125 (37.3 C)	
	[redacted]					
8mm Solid Radiator	4.35	12.64	4.6	14.13	3.4	64.71
8mm Shell Radiator	4.90	N/A	5.25	N/A	5.6	N/A
8mm Solid	3.60	20.83	3.7	41.89	No Lesion	Infinite Improvement
8mm Shell	3.85	12.99	4.05	29.63	0.3	1766.67
8mm Matched	3.63	19.83	3.85	36.36	No Lesion	Infinite Improvement
4mm Solid	3.25	33.85	3.15	66.67	No Lesion	Infinite Improvement
4mm Shell	3.40	27.94	3.35	56.72	No Lesion	Infinite Improvement

**Minimum Electrode Temperature of Radiator Shell Electrode at Maximum Tissue Temperture = 95°C*

Table 7. Comparison of Lesions Depths to Best Performance of Solid Radiator in Maximum Electrode Temperature Region and Various Flows

**Maximum Electrode Temperature of Radiator Solid Electrode at Maximum Tissue Temperature = 95°C*

	H=.002 (97.0 C)		H=.004 (81.2 C)		H=.125 (42.0 C)	
	[redacted]					
8mm Solid Radiator	4.77	N/A	5.11	N/A	5.66	N/A
8mm Shell Radiator	4.20	13.57	4.60	11.09	4.05	39.75
8mm Solid	4.43	7.67	4.80	6.46	6.10	-7.21
8mm Shell	4.10	16.34	4.50	13.56	6.05	-6.45
8mm Matched	4.30	10.93	4.65	9.89	6.10	-7.21
4mm Solid	4.35	9.66	4.63	10.37	6.20	-8.71
4mm Shell	4.20	13.57	4.40	16.14	5.15	9.90

6045B856 .032803

Figure11. Lesion Depth vs. Minimum Electrode Temperature (H=.004)

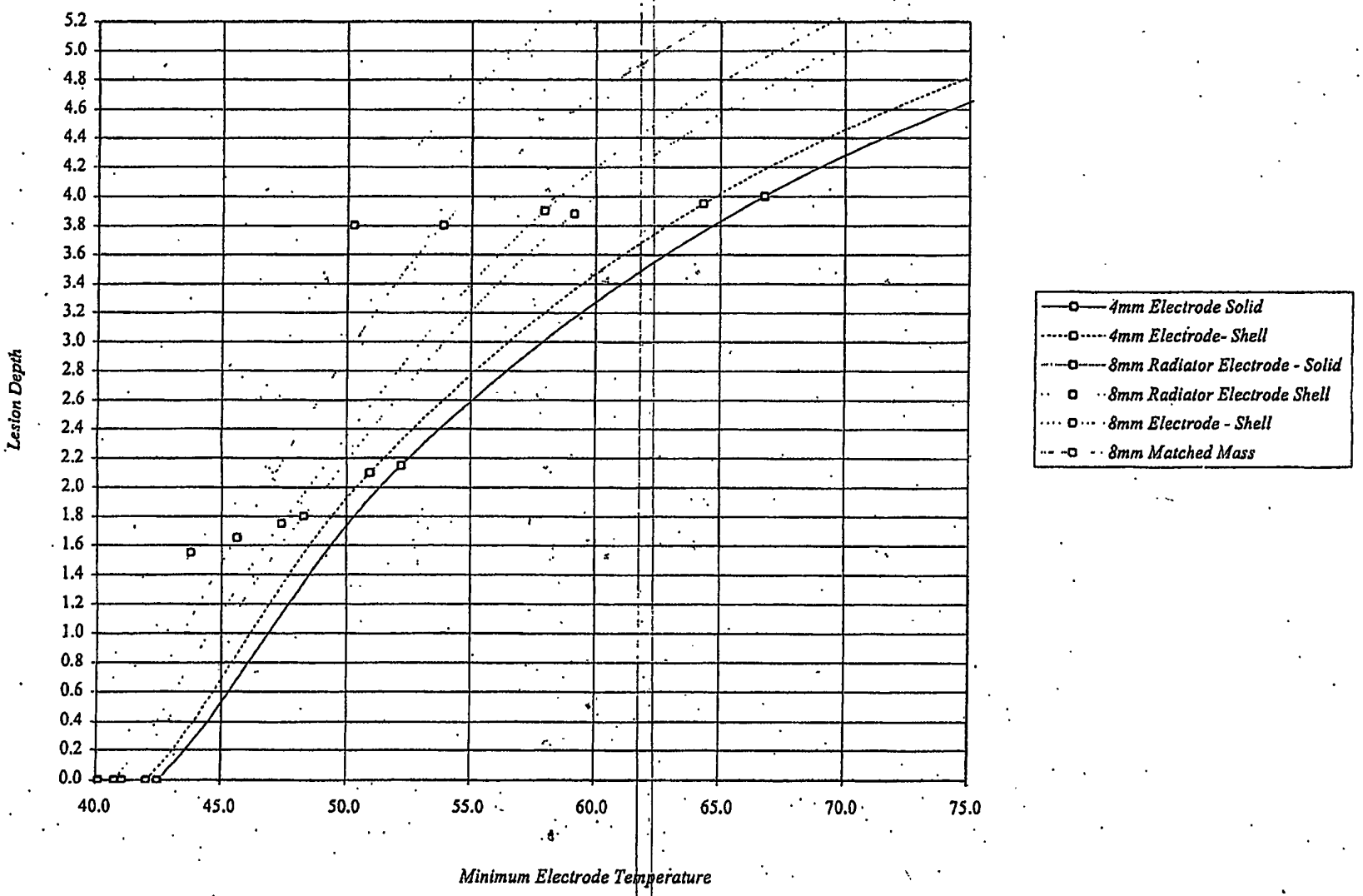

Figure 12: Lesion Depth vs Minimum Electrode Temperature (n = 125)

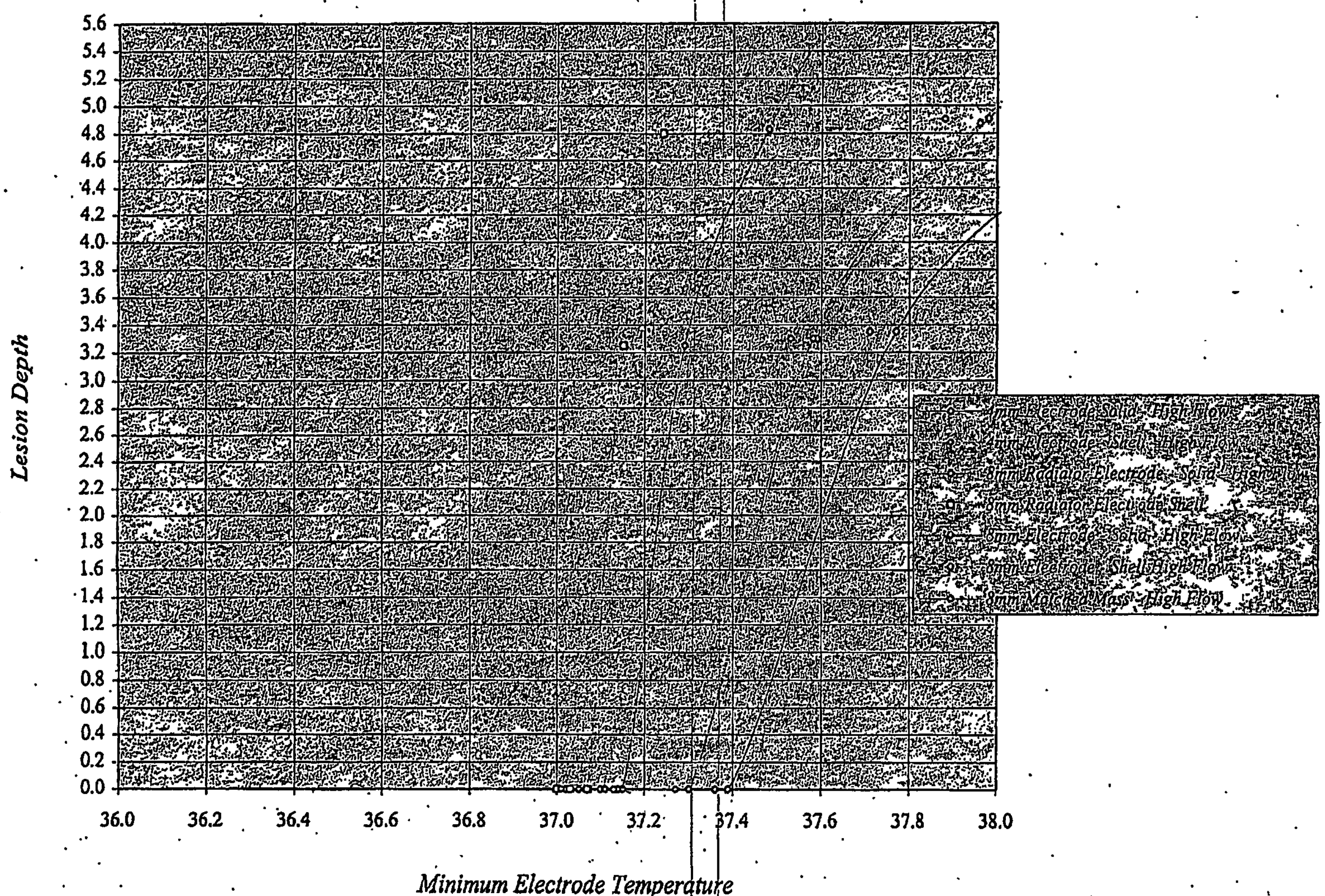

Figure 13: Lesion Depth vs. Minimum Electrode Temperature (H = 0.02)

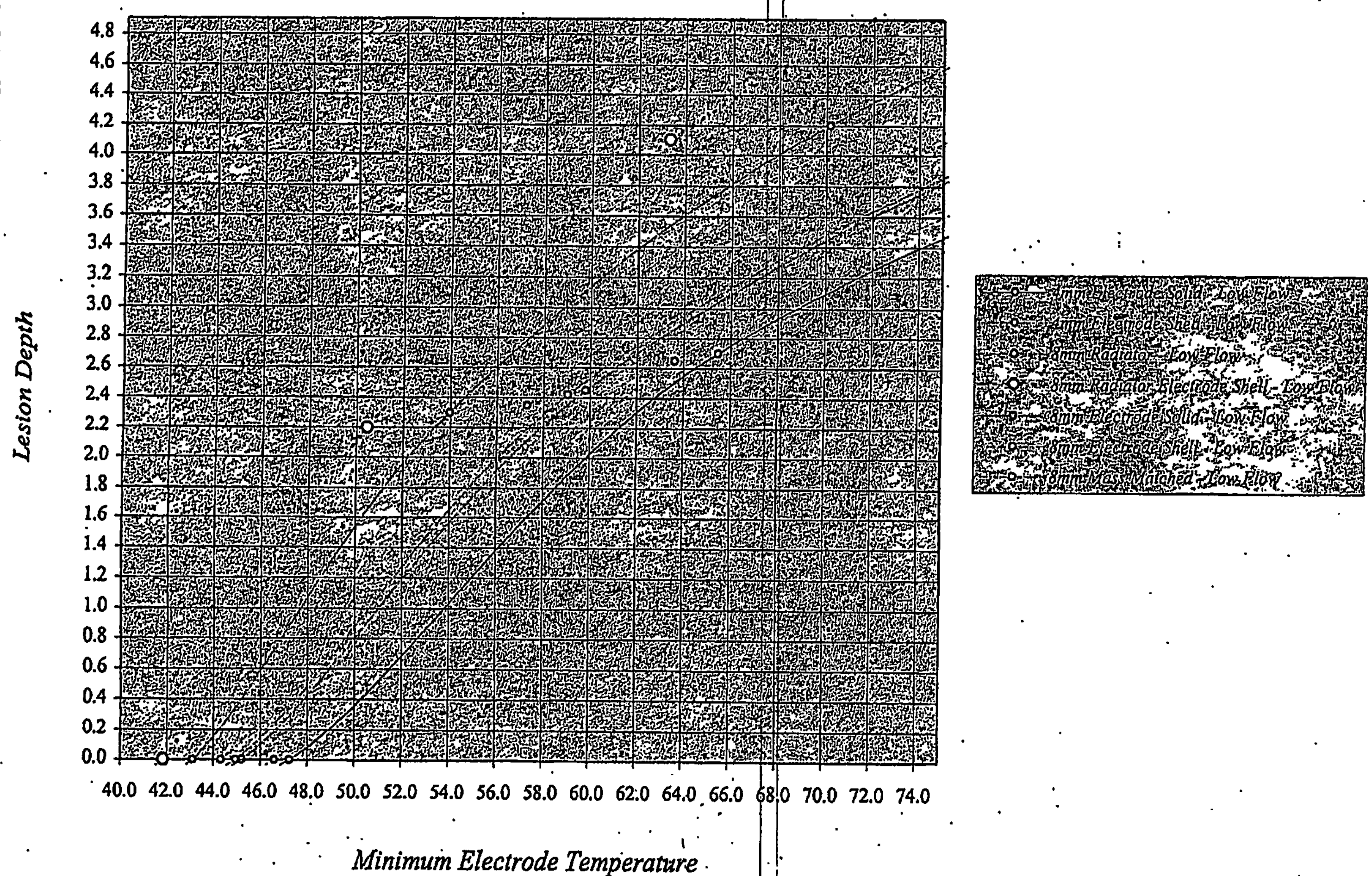

Figure 14: Lesion Depth vs. Maximum Electrode Temperature (H = 004)

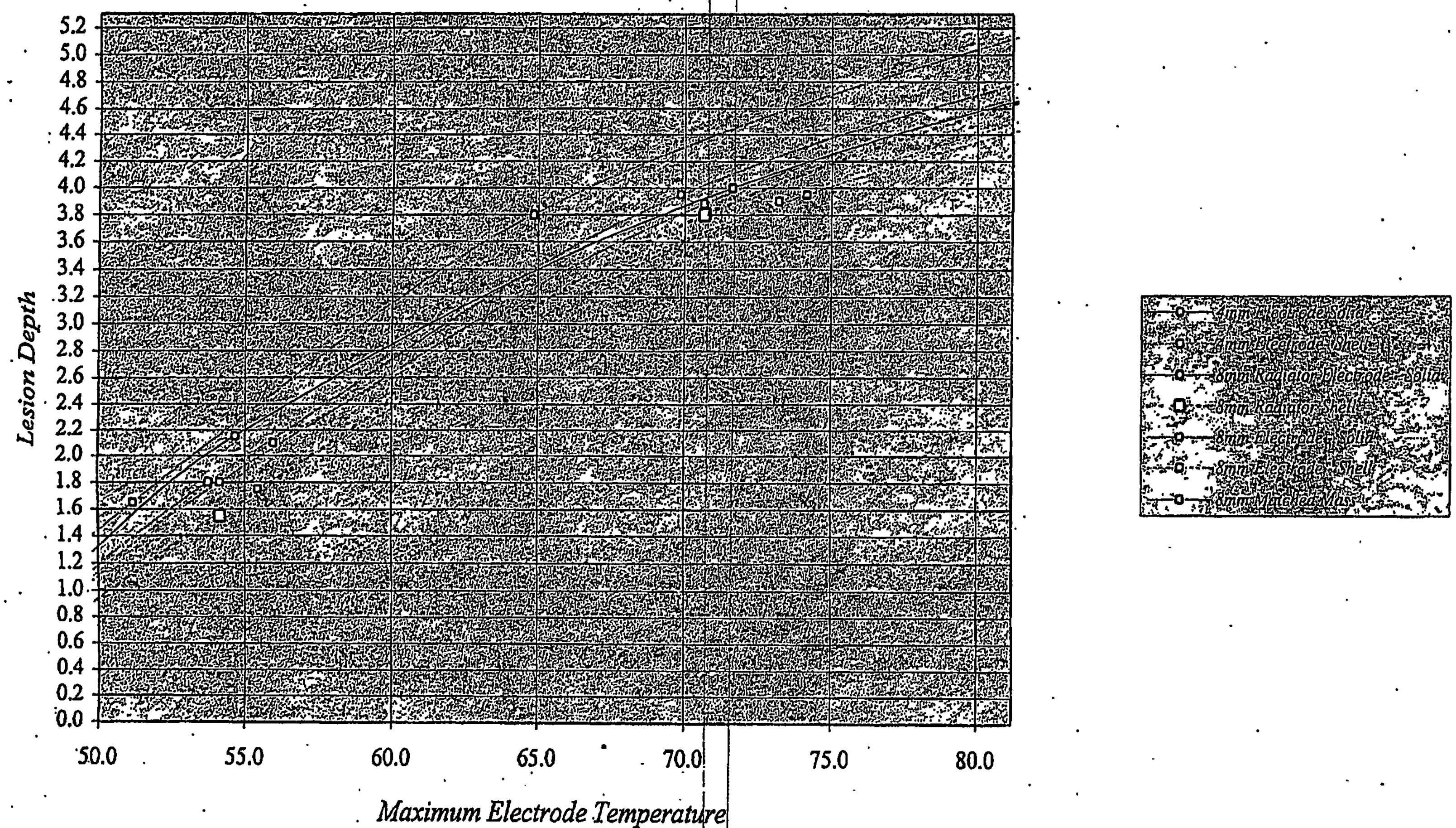

Figure 15. Lesion Depth vs. Maximum Electrode Temperature (H=.125)

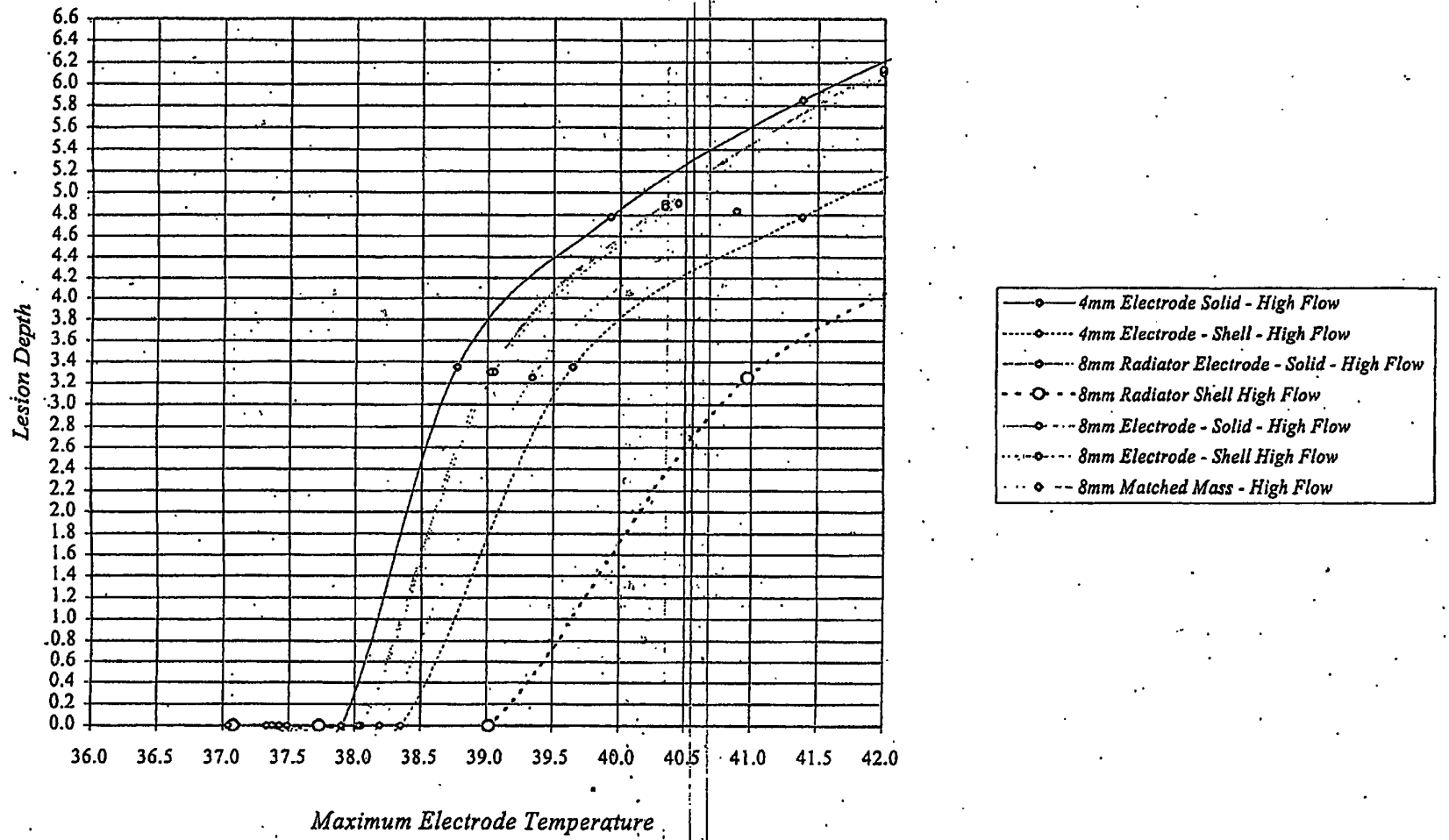

Figure 16. Lesion Depth vs. Maximum Electrode Temperature (H=.002)

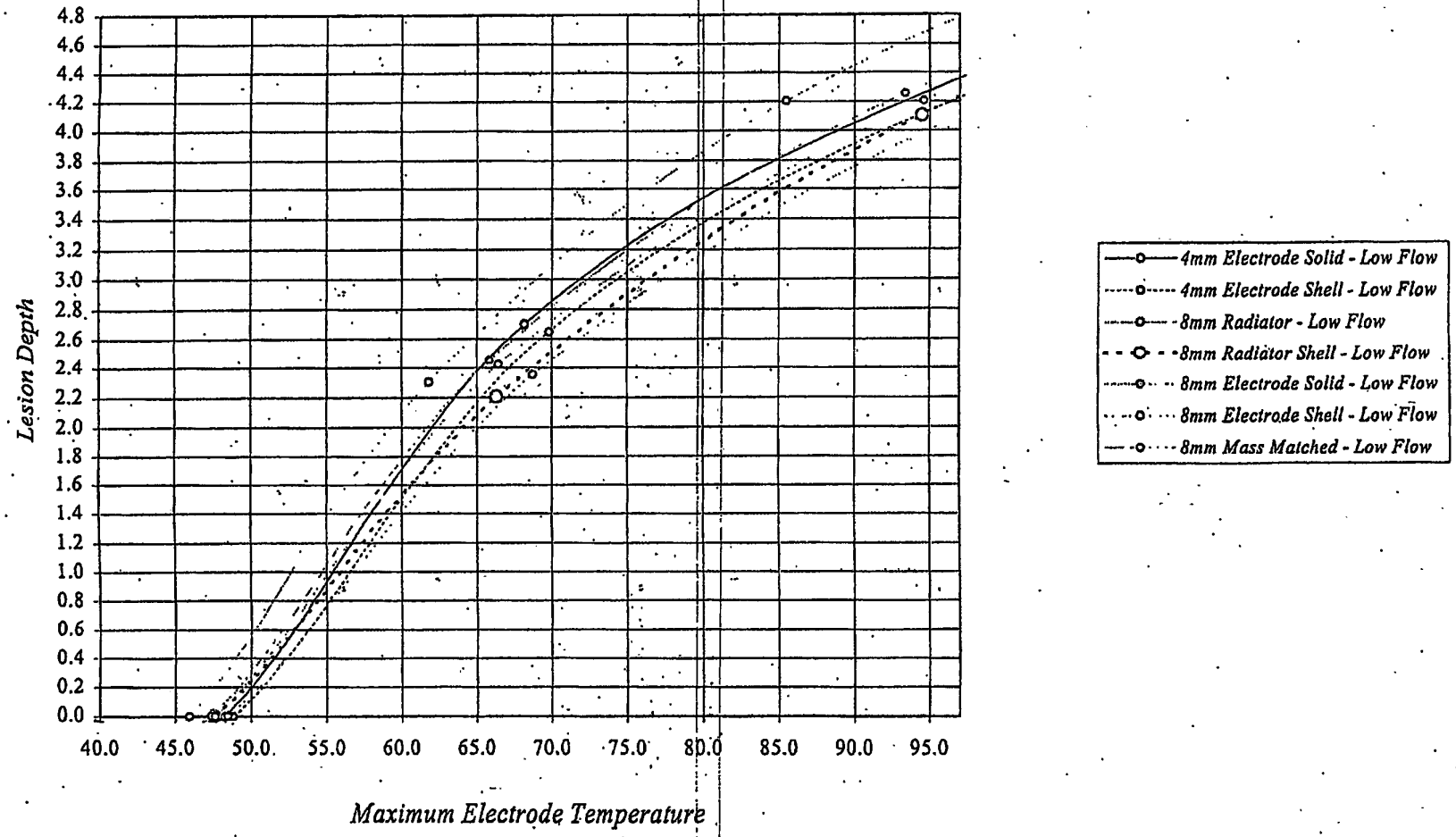

Figure 17. Lesion Depth vs. Maximum Tissue Temperature (H=.004)

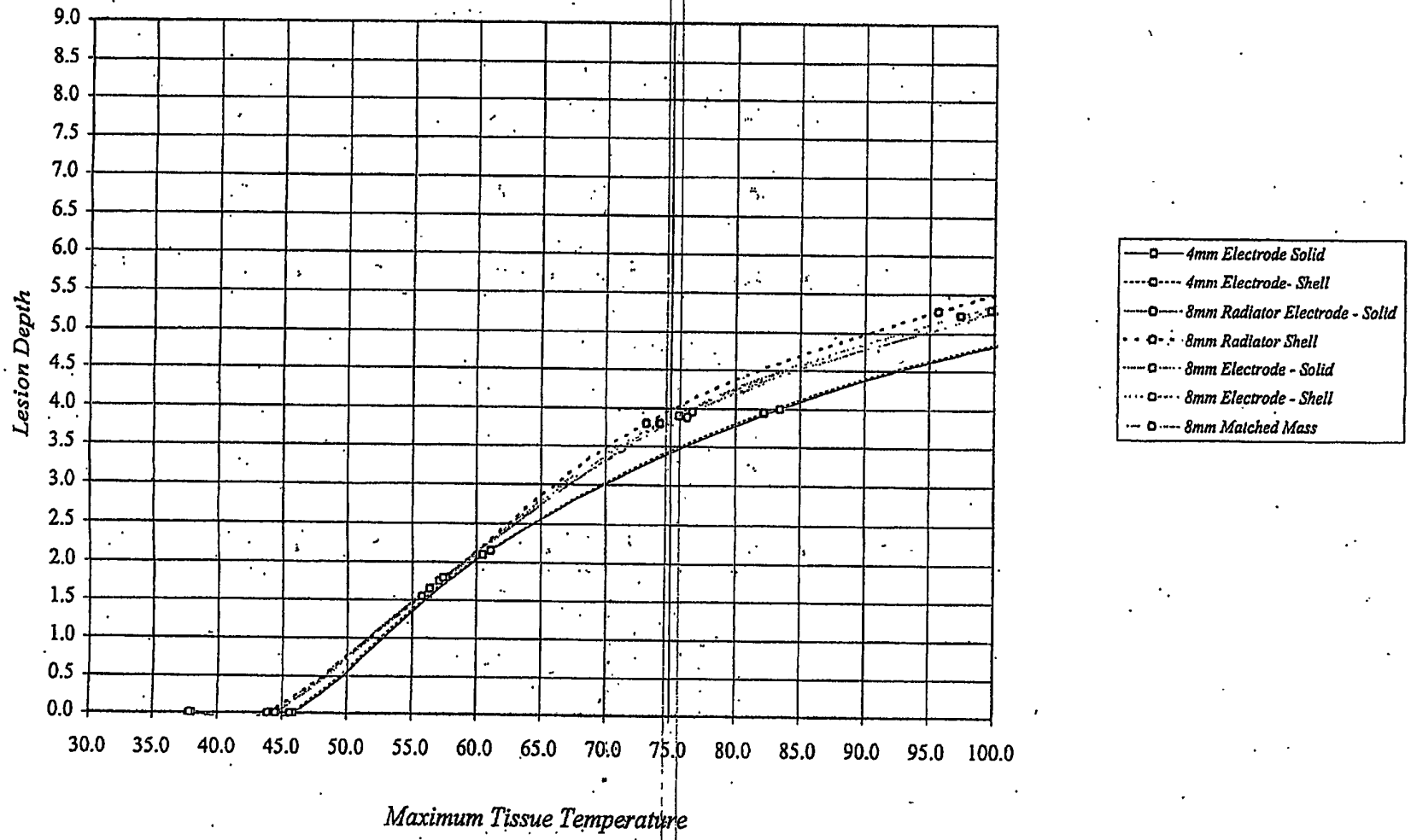

Figure 18. Lesion Depth vs. Maximum Tissue Temperature (H=.125)

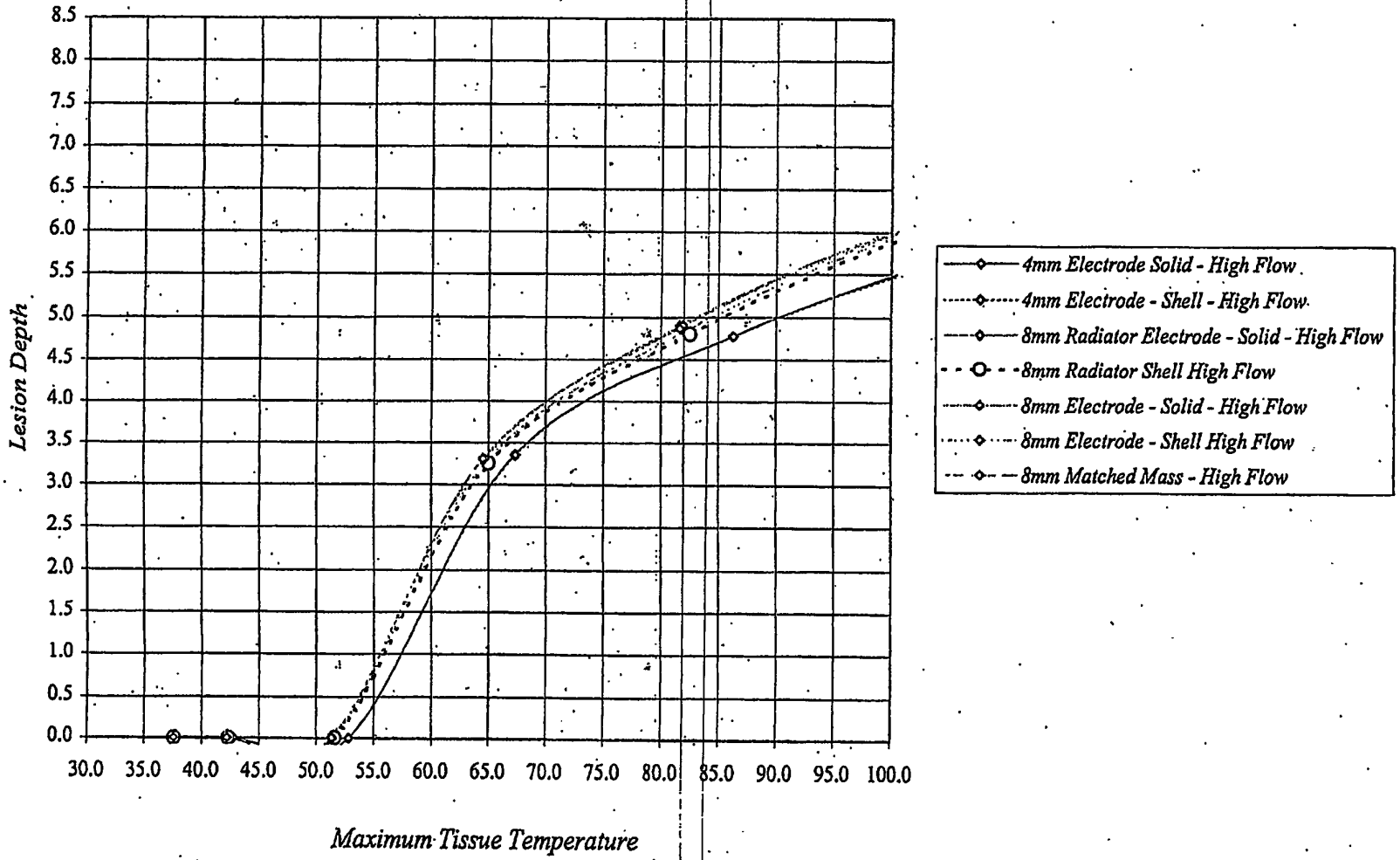

Figure 19: Lesion Depth vs. Maximum Tissue Temperature (h = 0.02)

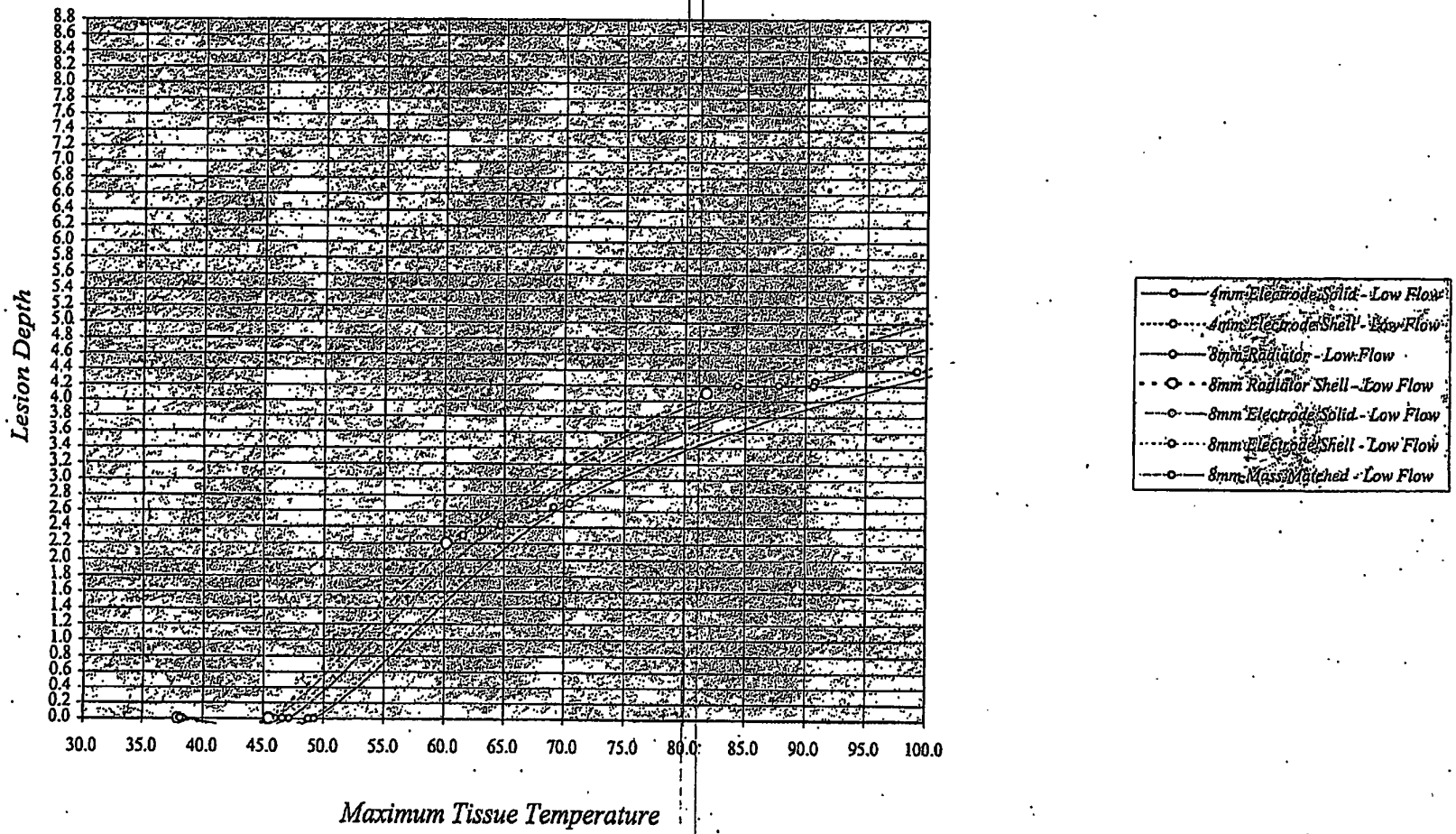

Results and Discussion (continued)

Electrode Temperature Histories

Figure (20) is a graph of the minimum electrode temperature during a 120-second ablation period for all the electrode-configurations. The maximum tissue temperature during the ablation for each configuration is 65°C. The graph shows that the shell radiator electrode maintains the lowest minimum electrode temperature over the ablation period. Therefore, the electrode region adjacent to the electrode-tissue interface remains the coolest over the ablation period for the shell radiator electrode. Within this region, the solid radiator design remains the second coolest. The 8mm electrode designs have higher minimum electrode temperatures than the radiator designs. The 4mm electrodes have the highest minimum electrode temperatures of all the configurations during the first eighty seconds of the cycle. At about eighty seconds the minimum temperatures of the 8mm solid design and 4 mm shell design have similar values. After the first ten seconds of the ablation period, the minimum electrode temperature for all configurations remained somewhat stable.

Figure (21) is a graph of the maximum electrode temperature during a 120-second ablation period for all the electrode-configurations. As in Figure (21), the maximum tissue temperature during the ablation for each configuration is 65°C. The graph shows that the solid radiator electrode maintains the lowest maximum electrode temperature during the first sixty seconds of the ablation cycle. Therefore, the junction region remains the coolest during the first sixty seconds for the solid radiator electrode. However, the 4mm electrode is slightly cooler during the second half of the ablation cycle. The rate of maximum electrode temperature increase is slightly higher for the 8mm electrode configurations than for the increase for the 4mm electrode configurations. These differing rates of temperature increase account for the changes seen over the ablation cycle. The solid versions of each configuration (radiator, 8mm, 4mm) have a consistently lower maximum electrode temperature over the ablation cycle. This again implies that in the junction region the presence of more mass helps counter the heating due to material mismatches and interface geometry.

Figure 20. Electrode Minimum Temperature Histories

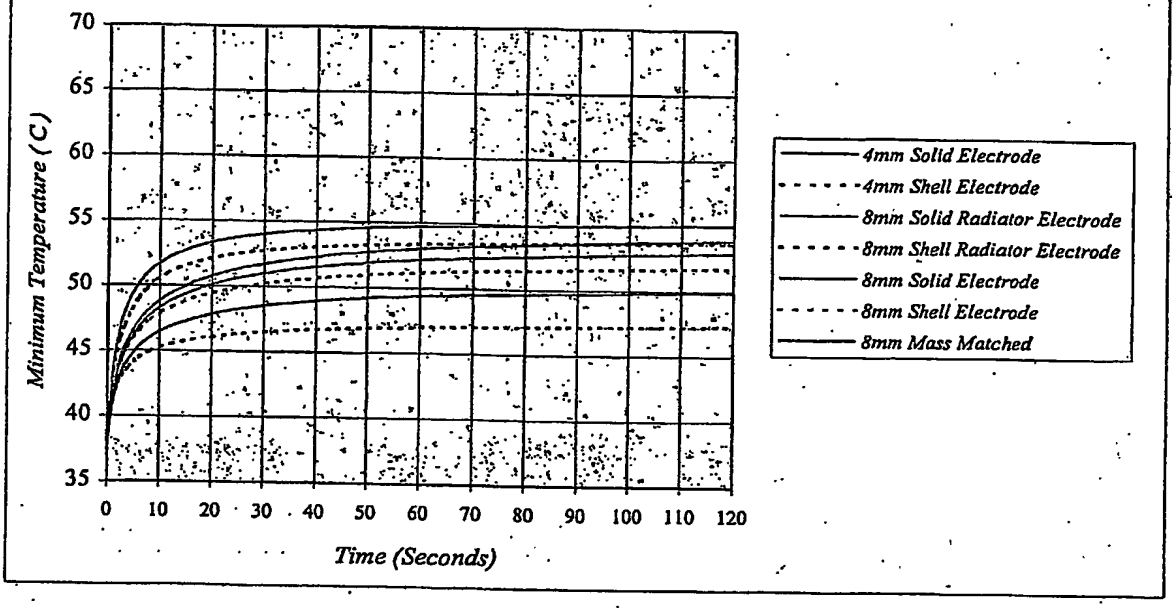

Figure 21. Electrode Maximum Temperature Histories

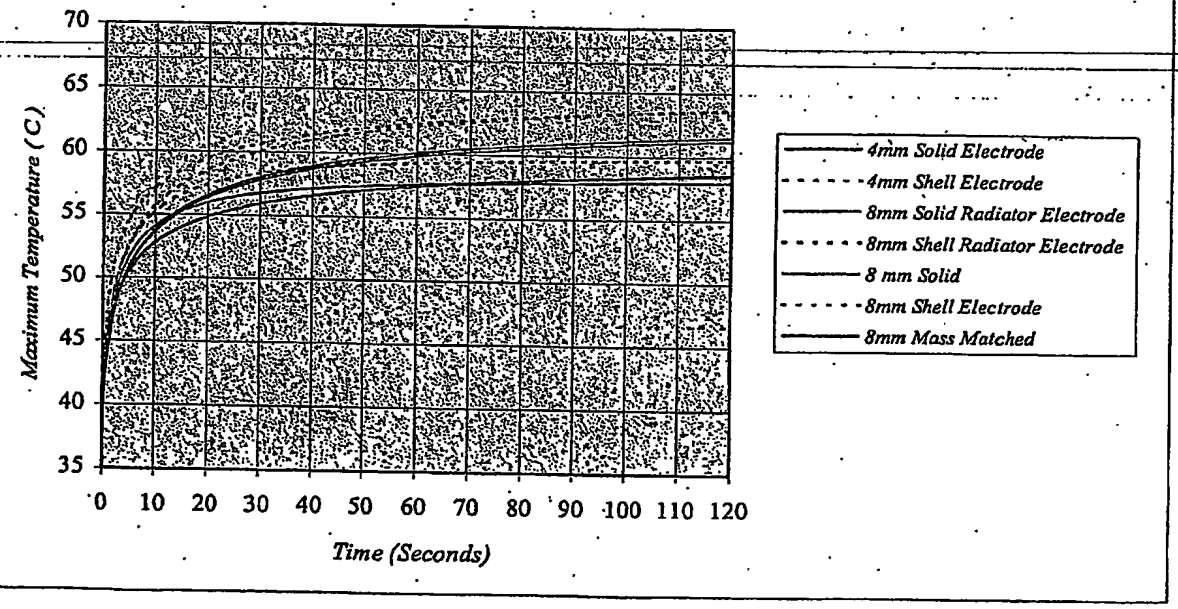

Results and Discussion (continued)

Field Results

Figures (22), (23) and (24) depict the temperature fields, potential fields, and the potential gradient fields respectively for each electrode configuration. All fields are shown at a maximum tissue temperature of 65°C. As previously mentioned, the temperature fields show the minimum electrode temperature regions adjacent to the tissue-electrode interface. The regions with the maximum electrode temperatures are located at the junction of the electrode and the catheter tip material. The potential fields for the 8mm electrode configurations are of similar size. This indicates that the area of current flow and the heating volume will be similar for the 8mm configurations (*radiator as well as standard*). This accounts for the similar impedance values found in Table (4). This also accounts for the fact that at equal power settings the 8mm configurations create lesions of equivalent depths as shown in Figure (25). The 4mm potential fields are much smaller than the 8mm potential fields. Therefore the area of current flow and the heating volume are much smaller when compared to the 8mm electrode configurations. This accounts for the higher impedance values shown in Table (4). At equal power settings the 4mm electrode will create deeper lesions when compared to the 8mm electrode configurations. However, as shown in Table (4), for a 4mm electrode, the operating range is 5W to 14W (H=.004) whereas for the 8mm configurations, the operating range is10W to 28W (H=.004). The operating range is defined as the voltage range and power range required to create maximum tissue temperatures ranging between 55°C and 95°C during an ablation cycle (60 seconds). The maximum lesion depth ranges between 4.61 to 4.63 for 4mm configurations at H=.004 in the previously mentioned power range. The maximum lesion depth ranges between 5.01 to 5.24 for 8mm configurations at H=.004 in the previously mentioned power range. Therefore even though the 4mm configurations create deeper lesions for a given power setting, the 8mm configurations create deeper lesions for comparable operating ranges defined with respect to maximum tissue temperature. As indicated in equation (3) the current density is proportional to the gradient of potential field. Thus, Figure (24), shows areas of high current density occurring at the electrode tissue interface junction and at the electrode-tip junction.

Conclusion

The minimum electrode temperature evaluations are more reflective of the cooling effects of the radiator design. The minimum electrode temperature evaluations show that the radiator design can provide a deeper lesion for a given minimum electrode temperature. This improvement in lesion depth for a given minimum temperature is enhanced at higher flow rates. Clinically, this would be very beneficial, given that currently it is more difficult to make deep lesions in high flow areas. However, spot heating at the electrode-tip junction compromises the effectiveness of the design. I would recommend that this matter be resolved in any proposed design.

Further Analysis Work

This analysis work assumes a convective heat boundary condition. With the current tools we are not able to evaluate the details of the fluid field and its effects. The ability to perform such analysis will help us to better define potential coagulation hazards.

Figure 22. Temperature Fields for Varying Electrode Configurations (Maximum Tissue Temperature = 65°C)

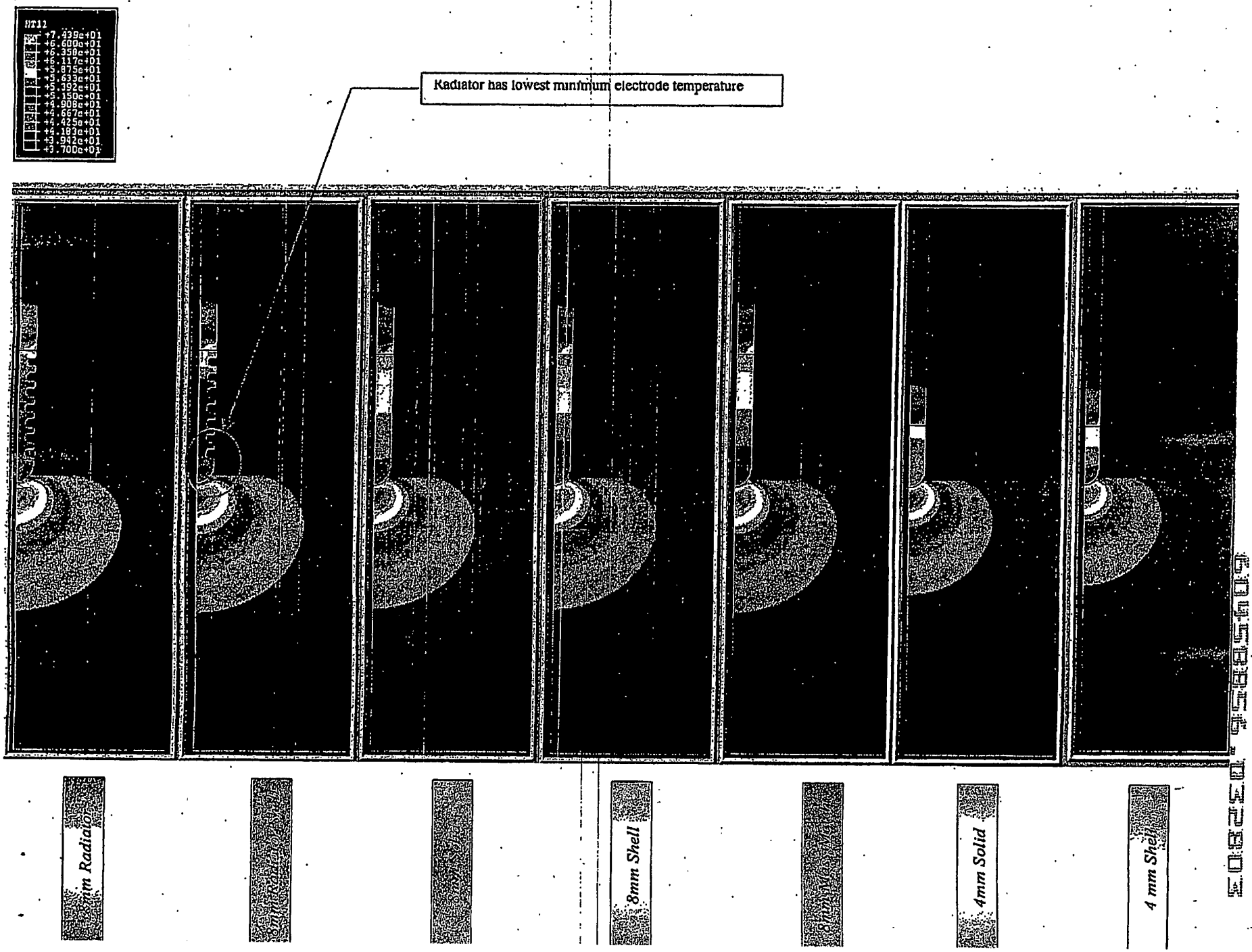

Figure 23. Potential Fields for Varying Electrode Configurations (Maximum Tissue Temperature = 65^{0}C)

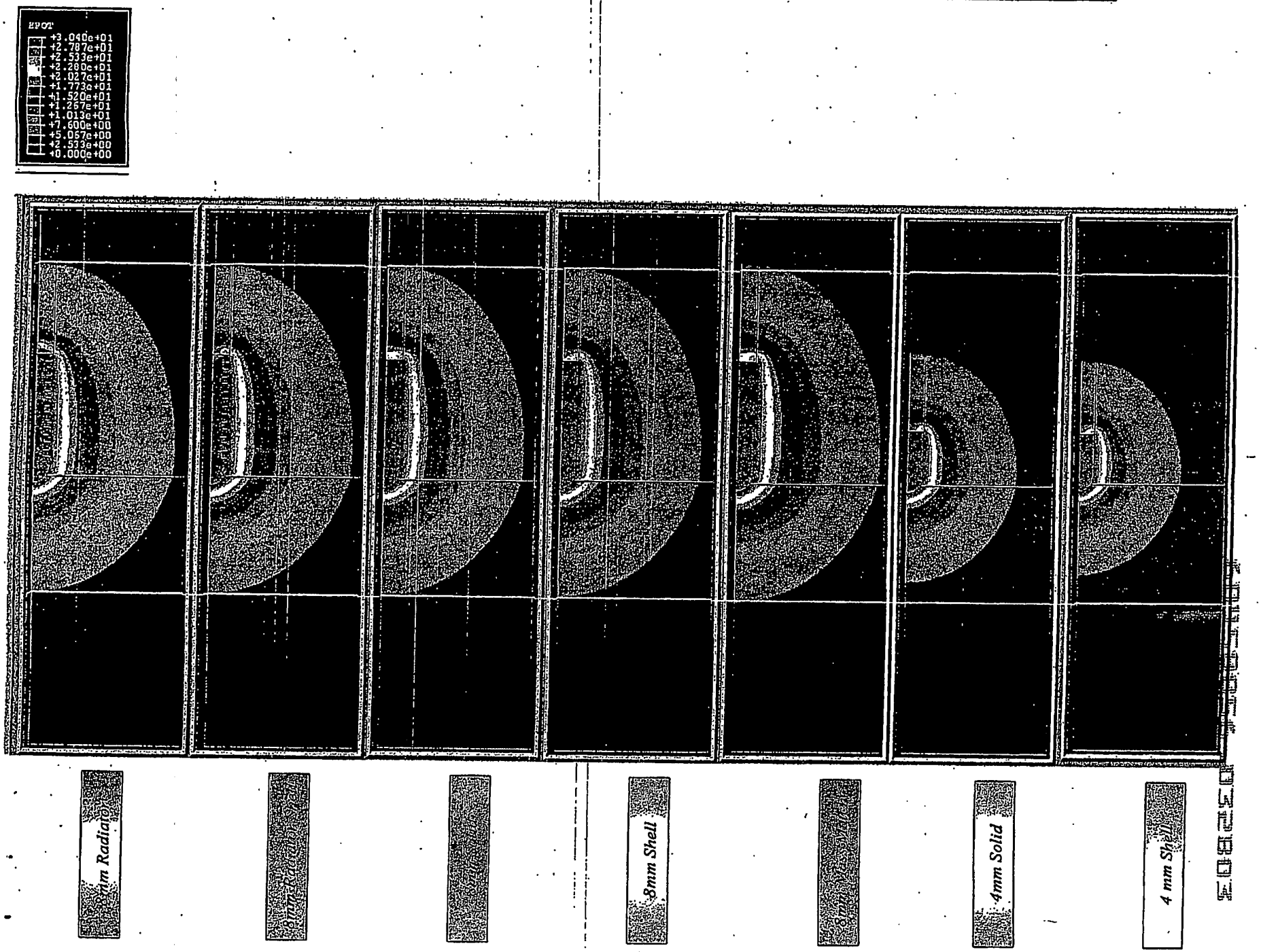

Figure 24. Potential Gradient Fields for Varying Electrode Configurations (Maximum Tissue Temperature = 65°C)

Lesion Depth
9.0
8.0
7.0
6.0
5.0
4.0
3.0
2.0
1.0
0.0
0.0
20.0
40.0
60.0
80.0
100.0
120.0
Power

APPENDIX-1

Table A1-1. Analysis Data - 60 Second Ablation Runs

Electrode Type	Power	Voltage	Impedance	Energy	Time	Current	Min Temp (Electrode)	Max Temp (Electrode)	Max Temp (Tissue)	Temperature Difference Electrode/Tissue	Lesion Depth	Energy/mm	ODB File
[redacted]													
8 mm Radiator	0.42	5.00	59.11	25.57	60.48	0.08	37.27	37.68	37.78	0.49	0.00	N/A	radr1-shell-05v-120sec-H004
(Shell)	3.81	15.00	59.10	234.24	61.53	0.25	39.43	43.19	43.85	4.42	0.00	N/A	radr1-shell-15v-120sec-H004
	10.57	25.00	59.11	640.68	60.61	0.42	43.78	54.15	55.76	12.01	1.55	413.47	radr1-shell-25v-120sec-H004
	20.72	35.00	59.11	1282.04	61.88	0.59	50.24	70.67	73.10	22.86	2.80	337.38	radr1-shell-35v-120sec-H004
Radius on Tip	34.28	45.00	59.11	2117.88	61.82	0.76	58.89	92.66	95.06	36.77	5.28	401.11	radr1-shell-45v-120sec-H004
Interface	51.18	55.00	59.11	3188.78	61.88	0.93	69.70	120.20	123.20	53.50	6.35	497.92	radr1-shell-55v-120sec-H004
	71.48	65.00	59.10	4421.06	61.68	1.10	82.85	151.20	156.60	73.95	7.20	609.08	radr1-shell-65v-120sec-H004
	85.17	75.00	59.10	5894.94	61.84	1.27	97.77	191.70	193.70	97.93	8.02	735.03	radr1-shell-75v-120sec-H004
8 mm Radiator	0.42	5.00	59.11	25.57	60.46	0.08	37.00	37.08	37.59	0.59	0.00	N/A	radr1-shell-05v-120sec-H125
(Shell)	3.81	15.00	59.10	234.24	61.53	0.25	37.03	37.73	42.30	5.27	0.00	N/A	radr1-shell-15v-120sec-H125
	10.57	25.00	59.10	647.37	61.22	0.42	37.07	39.02	51.58	14.51	0.00	N/A	radr1-shell-25v-120sec-H125
	20.72	35.00	59.11	1252.30	60.43	0.59	37.16	40.97	65.00	27.83	3.25	385.32	radr1-shell-35v-120sec-H125
High Flow	34.28	45.00	59.10	2078.29	60.68	0.76	37.24	43.58	82.51	45.27	4.80	432.98	radr1-shell-45v-120sec-H125
	51.18	55.00	59.11	3155.13	61.65	0.93	37.36	46.83	103.80	56.44	6.06	520.63	radr1-shell-55v-120sec-H125
	71.48	65.00	59.10	4420.63	61.84	1.10	37.50	50.75	129.00	91.50	7.06	628.15	radr1-shell-65v-120sec-H125
	85.17	75.00	59.10	5856.76	61.54	1.27	37.67	55.30	158.40	120.73	7.75	755.71	radr1-shell-75v-120sec-H125
8 mm Radiator	0.42	5.00	59.11	25.57	60.48	0.08	37.54	38.17	37.94	0.40	0.00	N/A	radr1-shell-05v-120sec-H002
(Shell)	3.81	15.00	59.10	234.24	61.53	0.25	41.63	47.54	45.49	3.63	0.00	N/A	radr1-shell-15v-120sec-H002
	10.57	25.00	59.11	652.21	61.68	0.42	50.43	68.28	60.17	9.74	2.20	296.46	radr1-shell-25v-120sec-H002
	20.72	35.00	59.11	1256.31	60.57	0.59	63.33	94.47	81.73	18.40	4.10	306.17	radr1-shell-35v-120sec-H002
Low Flow	34.28	45.00	59.10	2111.52	61.83	0.76	80.45	131.80	109.60	29.16	5.50	383.91	radr1-shell-45v-120sec-H002
	51.18	55.00	59.10	3076.96	60.12	0.93	101.70	178.40	144.20	42.80	6.60	473.38	radr1-shell-55v-120sec-H002
	71.48	65.00	59.11	4330.82	61.29	1.10	127.50	234.90	186.70	59.20	7.41	591.20	radr1-shell-65v-120sec-H002
	85.17	75.00	59.11	5553.82	61.51	1.27	157.50	300.60	236.10	78.60	8.15	718.25	radr1-shell-75v-120sec-H002

604588856 .032803

Table A1 - Analysis Data - 60 Second Ablation Runs

Electrode Type	Power	Voltage	Impedance	Energy	Time	Current	Min Temp (Electrode)	Max Temp (Electrode)	Max Temp (Tissue)	Temperature Difference Electrode/Tissue	Lesion Depth	Energy/mm	ODB File
8 mm Solid	0.44	5.00	96.48	26.76	60.46	0.09	37.17	37.67	37.84	0.37	0.00	N/A	8mm-05V-120sec-H004
	3.96	15.00	88.47	245.18	61.53	0.27	41.24	43.03	44.51	3.27	0.00	N/A	8mm-15V-120sec-H004
	11.07	25.00	88.47	684.44	61.84	0.44	48.78	53.76	57.61	8.83	1.50	380.25	8mm-25V-120sec-H004
	21.59	35.00	88.47	1337.75	61.87	0.62	60.07	69.65	78.05	16.58	3.60	338.87	8mm-35V-120sec-H004
	35.58	45.00	88.47	2185.23	61.02	0.80	75.08	91.24	101.40	26.31	5.31	412.10	8mm-45V-120sec-H004
	53.57	55.00	88.47	3310.22	61.79	0.97	93.85	116.10	132.10	38.15	6.50	509.26	8mm-55V-120sec-H004
	74.82	65.00	88.47	4560.43	60.95	1.15	116.40	150.20	159.00	52.60	7.40	616.27	8mm-65V-120sec-H004
	99.80	75.00	88.47	6093.66	61.18	1.33	142.50	187.50	212.50	69.70	8.10	752.30	
6mm Solid	0.44	5.00	96.47	26.77	60.46	0.09	37.01	37.04	37.58	0.57	0.00	N/A	6mm-05V-120sec-H125
	3.96	15.00	88.47	245.18	61.53	0.27	37.11	37.37	42.20	5.09	0.00	N/A	6mm-15V-120sec-H125
	11.07	25.00	88.47	684.44	61.84	0.44	37.30	38.03	51.30	14.00	0.00	N/A	6mm-25V-120sec-H125
	21.59	35.00	88.47	1328.69	61.16	0.62	37.59	39.01	64.49	26.90	3.30	402.63	6mm-35V-120sec-H125
High Flow	35.85	45.00	88.47	2183.96	60.90	0.80	37.88	40.34	81.83	43.85	4.90	445.71	6mm-45V-120sec-H125
	53.57	55.00	88.47	3283.10	61.25	0.97	38.46	41.99	102.50	64.04	6.10	538.21	6mm-55V-120sec-H125
	74.82	65.00	88.47	4558.39	60.89	1.15	39.04	43.97	127.10	88.06	7.00	650.77	6mm-65V-120sec-H125
	99.81	75.00	88.47	6127.07	61.01	1.33	39.77	46.66	180.80	121.03	7.90	775.58	6mm-75V-120sec-H125
6mm Solid	0.44	5.00	88.47	26.77	60.48	0.09	37.81	38.15	38.13	0.32	0.00	N/A	6mm-05V-120sec-H002
	3.93	15.00	88.47	240.27	60.36	0.27	45.20	47.35	47.11	1.91	0.00	N/A	6mm-15V-120sec-H002
	11.07	25.00	88.47	680.80	61.52	0.44	59.80	65.63	64.79	4.99	2.45	277.92	6mm-25V-120sec-H002
	21.59	35.00	88.47	1309.11	60.35	0.62	81.58	93.38	90.78	9.20	4.25	308.03	6mm-35V-120sec-H002
Low Flow	35.85	45.00	88.47	2218.40	61.88	0.80	110.80	130.50	125.20	14.40	5.56	398.99	6mm-45V-120sec-H002
	53.57	55.00	88.47	3270.32	61.05	0.97	147.10	178.40	168.20	21.10	6.87	490.30	6mm-55V-120sec-H002
	74.82	65.00	88.47	4628.69	61.87	1.15	191.00	232.10	220.30	29.30	7.56	612.25	6mm-65V-120sec-H002
	99.81	75.00	88.47	6128.06	61.50	1.33	241.90	296.60	280.50	38.60	8.32	736.31	6mm-75V-120sec-H002
8mm Shell	0.44	5.00	87.04	26.50	60.46	0.09	37.42	37.74	37.83	0.40	0.00	N/A	8mmshell-05V-120sec-H004
	3.94	15.00	87.04	242.72	61.53	0.26	40.75	43.84	44.32	3.57	0.00	N/A	8mmshell-15V-120sec-H004
	10.96	25.00	87.04	667.38	60.91	0.44	47.40	55.44	57.05	9.65	1.75	381.36	8mmshell-25V-120sec-H004
	21.48	35.00	87.04	1326.62	61.77	0.61	57.93	73.28	75.62	17.69	3.90	340.16	8mmshell-35V-120sec-H004
	35.50	45.00	87.04	2134.00	60.11	0.79	70.68	90.61	93.73	23.05	5.30	402.64	8mmshell-45V-120sec-H004
	53.03	55.00	87.04	3229.42	60.90	0.96	87.24	120.50	122.40	42.16	6.40	504.60	8mmshell-55V-120sec-H004
	74.07	65.00	87.04	4471.64	60.37	1.14	107.10	161.60	165.20	58.10	7.30	612.55	8mmshell-65V-120sec-H004
	98.81	75.00	87.04	5939.19	60.23	1.31	130.30	202.90	207.30	77.00	8.01	741.47	8mmshell-75V-120sec-H004
8mm Shell	0.44	5.00	87.04	26.50	60.46	0.09	37.01	37.04	37.58	0.57	0.00	N/A	8mmshell-05V-120sec-H125
	3.94	15.00	87.04	242.72	61.53	0.26	37.10	37.30	42.23	5.13	0.00	N/A	8mmshell-15V-120sec-H125
	10.96	25.00	87.04	677.58	61.84	0.44	37.27	38.05	51.39	14.12	0.00	N/A	8mmshell-25V-120sec-H125
	21.48	35.00	87.03	1307.20	60.86	0.61	37.53	39.05	64.84	27.11	3.30	396.12	8mmshell-35V-120sec-H125
High Flow	35.50	45.00	87.04	2163.57	60.95	0.78	37.88	40.44	81.90	44.02	4.90	441.54	8mmshell-45V-120sec-H125
	53.03	55.00	87.04	3210.58	60.84	0.96	38.31	42.07	102.60	64.59	6.10	526.32	8mmshell-55V-120sec-H125
	74.11	65.00	87.01	4554.04	61.43	1.14	38.93	44.09	127.70	88.87	7.10	641.41	8mmshell-65V-120sec-H125
	98.81	75.00	87.04	6028.56	61.14	1.31	39.46	46.46	156.60	117.10	7.90	763.15	8mmshell-75V-120sec-H125
8mm Shell	0.44	5.00	87.04	26.50	60.46	0.09	37.81	38.27	38.07	0.26	0.00	N/A	8mmshell-05V-120sec-H002
	3.94	15.00	87.04	242.72	61.53	0.26	44.52	48.44	46.58	2.26	0.00	N/A	8mmshell-15V-120sec-H002
	10.96	25.00	87.04	663.08	60.52	0.44	57.28	68.72	63.19	5.91	2.35	282.16	8mmshell-25V-120sec-H002
	21.48	35.00	87.04	1298.84	60.47	0.61	75.89	98.19	87.73	11.84	4.20	309.20	8mmshell-35V-120sec-H002
Low Flow	35.50	45.00	87.04	2192.43	61.78	0.78	102.70	140.10	120.00	17.30	5.60	391.51	8mmshell-45V-120sec-H002
	53.03	55.00	87.04	3257.39	61.42	0.96	135.00	190.90	160.50	25.50	6.66	489.10	8mmshell-55V-120sec-H002
	74.07	65.00	87.04	4500.84	61.57	1.14	173.90	252.10	209.30	35.40	7.58	603.28	8mmshell-65V-120sec-H002
	98.81	75.00	87.04	5957.20	60.41	1.31	218.90	332.80	265.90	47.00	8.21	725.61	8mmshell-75V-120sec-H002

Table A1 - Analysis Data - 60 Second Ablation Runs

Electrode Type	Power	Voltage	Impedance	Energy	Time	Current	Min Temp (Electrode)	Max Temp (Electrode)	Max Temp (Tissue)	Temperature Difference Electrode/Tissue	Lesion Depth	Energy/mm	OOB File
8mm	0.44	5.00	58.46	28.71	60.48	0.09	37.45	37.69	37.83	0.38	0.00	N/A	8mm-MB-05V-H004
	5.99	15.00	58.21	245.17	61.53	0.27	41.00	43.48	44.44	3.34	0.00	N/A	8mm-MB-15V-H004
	11.07	25.00	58.42	674.57	60.85	0.44	48.28	54.34	57.38	8.04	3.60	374.78	8mm-MB-25V-H004
98% Mass Matched	21.69	35.00	58.47	1317.15	61.64	0.62	59.12	70.85	75.28	12.14	5.68	544.63	8mm-MB2-35V-H004
Against	35.88	45.00	58.42	2185.77	60.98	0.80	73.52	92.68	100.70	27.10	5.30	412.41	8mm-MB2-45V-H004
Radiator	53.67	55.00	58.47	3304.91	61.70	0.97	91.50	120.10	131.10	39.50	6.43	513.98	8mm-MB2-55V-H004
Electrode	74.82	65.00	58.47	4519.92	60.80	1.15	113.10	152.00	167.60	64.40	7.33	620.59	8mm-MB2-65V-H004
	93.60	75.00	58.47	5673.50	60.80	1.33	136.40	191.40	210.40	72.00	8.10	749.63	8mm-MB2-75V-H004
8mm	0.44	5.00	58.46	28.77	60.90	0.09	37.01	37.04	37.68	0.67	0.00	N/A	8mm-MB-05V-H125
	3.99	15.00	58.47	245.17	61.63	0.27	37.21	37.32	42.20	5.09	0.00	N/A	8mm-MB-15V-H125
	11.09	25.00	58.48	684.10	61.64	0.44	37.30	38.03	51.30	14.00	0.00	N/A	8mm-MB-25V-H125
100% Mass Matched	21.69	35.00	58.47	1325.23	61.09	0.62	37.56	39.02	64.48	26.00	3.30	401.38	8mm-MB2-35V-H125
Against	35.85	45.00	58.47	2183.99	60.91	0.80	37.90	40.36	87.63	43.67	4.87	448.40	8mm-MB2-45V-H125
Radiator	53.57	55.00	58.47	3283.17	61.29	0.97	38.43	41.99	102.50	64.07	6.13	535.59	8mm-MB2-55V-H125
Electrode	74.82	65.00	58.47	4550.12	60.63	1.15	38.80	43.98	122.10	88.10	7.03	646.38	8mm-MB2-65V-H125
High Flow	93.61	75.00	58.47	5727.50	61.52	1.33	39.67	46.20	150.00	116.33	7.80	775.83	8mm-MB2-75V-H125
8mm	0.44	5.00	58.48	28.77	60.48	0.09	37.68	38.10	38.13	0.25	0.00	N/A	8mm-MB-05V-H002
	3.96	15.00	58.47	245.17	61.53	0.27	44.94	47.81	47.14	0.20	0.00	N/A	8mm-MB-15V-H002
	10.89	25.00	57.40	674.57	61.86	0.44	59.03	65.42	64.73	6.69	2.42	278.75	8mm-MB-25V-H002
100% Mass Matched	21.69	35.00	58.47	1312.10	60.48	0.62	80.10	94.81	90.83	10.57	4.20	312.40	8mm-MB2-35V-H002
Against	35.80	45.00	58.47	2218.88	61.73	0.80	108.30	132.50	124.60	16.50	5.67	390.42	8mm-MB2-45V-H002
Radiator	53.37	55.00	58.47	3280.71	60.80	0.97	143.40	178.40	167.50	21.10	6.70	488.58	8mm-MB2-65V-H002
Electrode	74.82	65.00	58.47	4608.5	61.60	1.15	185.60	236.20	219.30	33.60	7.80	606.38	8mm-MB2-65V-H002
Low Flow	99.61	75.00	58.47	5965.09	61.09	1.33	234.60	302.10	279.40	34.60	8.30	733.14	8mm-MB2-75V-H002

60458856.032803

Table A1-4: Analysis Data - 60 Second Ablation Runs

Electrode Type	Power	Voltage	Impedance	Energy	Time	Current	Min Temp (Electrode)	Max Temp (Electrode)	Max Temp (Tissue)	Temperature Difference Electrode/Tissue	Lesion Depth	Energy/mm	ODB File
4mm Solid	0.27	5.00	93.28	18.49	61.83	0.05	37.61	37.17	37.89	0.38	0.00	N/A	4mm-05V-120sec-H004
	2.51	15.00	89.50	151.42	60.30	0.17	42.47	43.38	48.82	3.35	0.00	N/A	4mm-15V-120sec-H004
	8.84	25.00	91.44	414.82	60.69	0.27	52.19	54.68	61.09	6.90	2.15	192.94	4mm-25V-120sec-H004
	13.40	35.00	91.43	812.82	61.19	0.38	66.78	71.62	83.43	16.67	4.00	204.96	4mm-35V-120sec-H004
	22.15	45.00	91.43	1338.23	60.47	0.49	86.16	94.18	112.30	26.14	5.30	252.68	4mm-45V-120sec-H004
	33.08	55.00	91.43	2031.54	61.41	0.60	110.40	122.50	148.60	38.20	6.30	322.47	4mm-55V-120sec-H004
	46.21	65.00	91.43	2833.06	61.31	0.71	139.50	156.30	192.50	63.00	7.20	393.48	4mm-65V-120sec-H004
	61.52	75.00	91.43	3783.35	61.09	0.82	173.40	193.90	243.50	70.10	7.78	483.03	4mm-75V-120sec-H004
4mm Solid	0.27	5.00	91.44	18.53	60.40	0.05	37.02	37.04	37.64	0.62	0.00	N/A	4mm-05V-120sec-H125
	2.45	15.00	91.44	148.53	60.38	0.16	37.14	37.33	42.74	5.60	0.00	N/A	4mm-15V-120sec-H125
	8.84	25.00	91.43	423.77	61.99	0.27	37.39	37.90	52.81	15.42	0.00	N/A	4mm-25V-120sec-H125
	13.40	35.00	91.43	817.48	61.02	0.38	37.77	38.77	67.30	20.53	3.35	244.03	4mm-35V-120sec-H125
High Flow	22.15	45.00	91.43	1367.28	61.74	0.49	38.27	39.93	88.25	47.58	4.78	286.04	4mm-45V-120sec-H125
	33.08	55.00	91.43	1997.42	60.37	0.60	38.89	41.36	109.00	70.11	5.86	341.44	4mm-55V-120sec-H125
	46.21	65.00	91.43	2788.80	60.67	0.71	39.64	43.11	138.20	88.58	6.74	415.25	4mm-65V-120sec-H125
	61.52	75.00	91.43	3786.03	61.70	0.82	40.82	45.14	168.30	127.78	7.46	508.83	4mm-75V-120sec-H125
4mm Solid	0.27	5.00	91.44	18.53	60.46	0.05	38.14	38.25	38.36	0.11	0.00	N/A	4mm-05V-120sec-H002
	2.48	15.00	91.43	151.05	61.38	0.10	47.25	48.23	49.21	1.96	0.00	N/A	4mm-15V-120sec-H002
	6.64	25.00	91.44	420.56	61.53	0.27	65.45	68.19	70.46	5.01	2.70	155.77	4mm-25V-120sec-H002
	13.40	35.00	91.43	819.06	61.13	0.38	82.66	98.07	101.70	9.02	4.40	186.15	4mm-35V-120sec-H002
Low Flow	22.15	45.00	91.43	1332.04	60.14	0.49	128.30	137.80	143.10	14.20	5.61	237.44	4mm-45V-120sec-H002
	33.08	55.00	91.43	2025.65	61.23	0.60	174.30	187.70	195.30	21.00	6.58	307.88	4mm-55V-120sec-H002
	46.21	65.00	91.43	2847.53	61.62	0.71	228.60	247.50	258.00	29.70	7.42	383.78	4mm-65V-120sec-H002
	61.52	75.00	91.43	3794.60	61.68	0.82	292.40	317.30	292.40	0.00	8.08	469.65	4mm-75V-120sec-H002
4mm Shell	0.28	5.00	90.63	18.83	60.30	0.05	37.58	37.76	37.98	0.40	0.00	N/A	4mmshell-05V-120sec-H004
	2.48	15.00	90.63	152.76	61.63	0.17	42.02	43.83	45.60	3.58	0.00	N/A	4mmshell-15V-120sec-H004
	6.90	25.00	90.63	417.41	60.53	0.28	50.83	55.96	60.48	9.65	2.10	198.77	4mmshell-25V-120sec-H004
	13.52	35.00	90.63	818.63	60.66	0.39	64.29	74.15	82.20	17.91	3.95	207.22	4mmshell-35V-120sec-H004
	22.34	45.00	90.64	1363.63	61.12	0.50	82.09	98.44	110.40	28.31	5.23	260.10	4mmshell-45V-120sec-H004
	33.28	55.00	90.64	2020.19	60.63	0.61	104.30	128.70	145.50	41.20	6.23	324.27	4mmshell-55V-120sec-H004
	48.62	65.00	90.63	2875.35	61.08	0.72	131.00	165.20	188.20	67.20	7.11	404.41	4mmshell-65V-120sec-H004
	62.08	75.00	90.64	3737.32	60.22	0.83	162.00	207.60	237.60	75.60	7.73	483.48	4mmshell-75V-120sec-H004
4mm Shell	0.28	5.00	90.63	16.60	60.48	0.06	37.01	37.06	37.64	0.63	0.00	N/A	4mmshell-05V-120sec-H125
	2.48	15.00	90.63	149.84	60.36	0.17	37.13	37.49	42.75	5.62	0.00	N/A	4mmshell-15V-120sec-H125
	6.90	25.00	90.63	417.29	60.51	0.28	37.36	38.35	52.80	15.44	0.00	N/A	4mmshell-25V-120sec-H125
	13.52	35.00	90.63	838.69	61.90	0.39	37.71	39.65	67.37	29.58	3.35	249.76	4mmshell-35V-120sec-H125
High Flow	22.34	45.00	90.63	1371.67	61.39	0.50	38.17	41.38	89.30	48.13	4.78	286.96	4mmshell-45V-120sec-H125
	33.38	55.00	90.63	2046.01	61.20	0.61	38.74	43.54	109.20	70.46	5.84	350.34	4mmshell-55V-120sec-H125
	48.61	65.00	90.64	2809.00	60.28	0.72	39.43	48.14	138.30	96.67	6.80	413.09	4mmshell-65V-120sec-H125
	62.06	75.00	90.63	3780.82	61.02	0.83	40.25	49.15	168.40	128.15	7.50	504.91	4mmshell-75V-120sec-H125
4mm Shell	0.28	5.00	90.67	18.58	60.48	0.06	38.07	38.31	38.31	0.24	0.00	N/A	4mmshell-05V-120sec-H002
	2.48	15.00	90.63	152.38	61.38	0.17	48.60	48.83	48.78	2.18	0.00	N/A	4mmshell-15V-120sec-H002
	6.00	25.00	90.64	415.79	60.30	0.28	63.61	69.61	69.15	6.64	2.85	158.90	4mmshell-25V-120sec-H002
	13.52	35.00	90.84	821.46	60.78	0.39	89.09	101.30	99.23	10.14	4.40	186.70	4mmshell-35V-120sec-H002
Low Flow	22.34	45.00	90.63	1357.38	60.75	0.50	123.00	143.30	139.00	18.00	5.61	241.96	4mmshell-45V-120sec-H002
	33.37	55.00	90.64	2028.10	60.60	0.61	185.40	195.70	189.00	23.60	6.56	309.31	4mmshell-55V-120sec-H002
	48.62	65.00	90.63	2812.55	60.33	0.72	216.20	258.50	249.00	32.80	7.35	382.66	4mmshell-65V-120sec-H002
	62.07	75.00	90.63	3844.48	61.94	0.83	275.60	332.60	319.60	43.80	8.00	480.56	4mmshell-75V-120sec-H002

APPENDIX-2

Figure A2-1. Voltage vs. Maximum Tissue Temperature (H=.004)

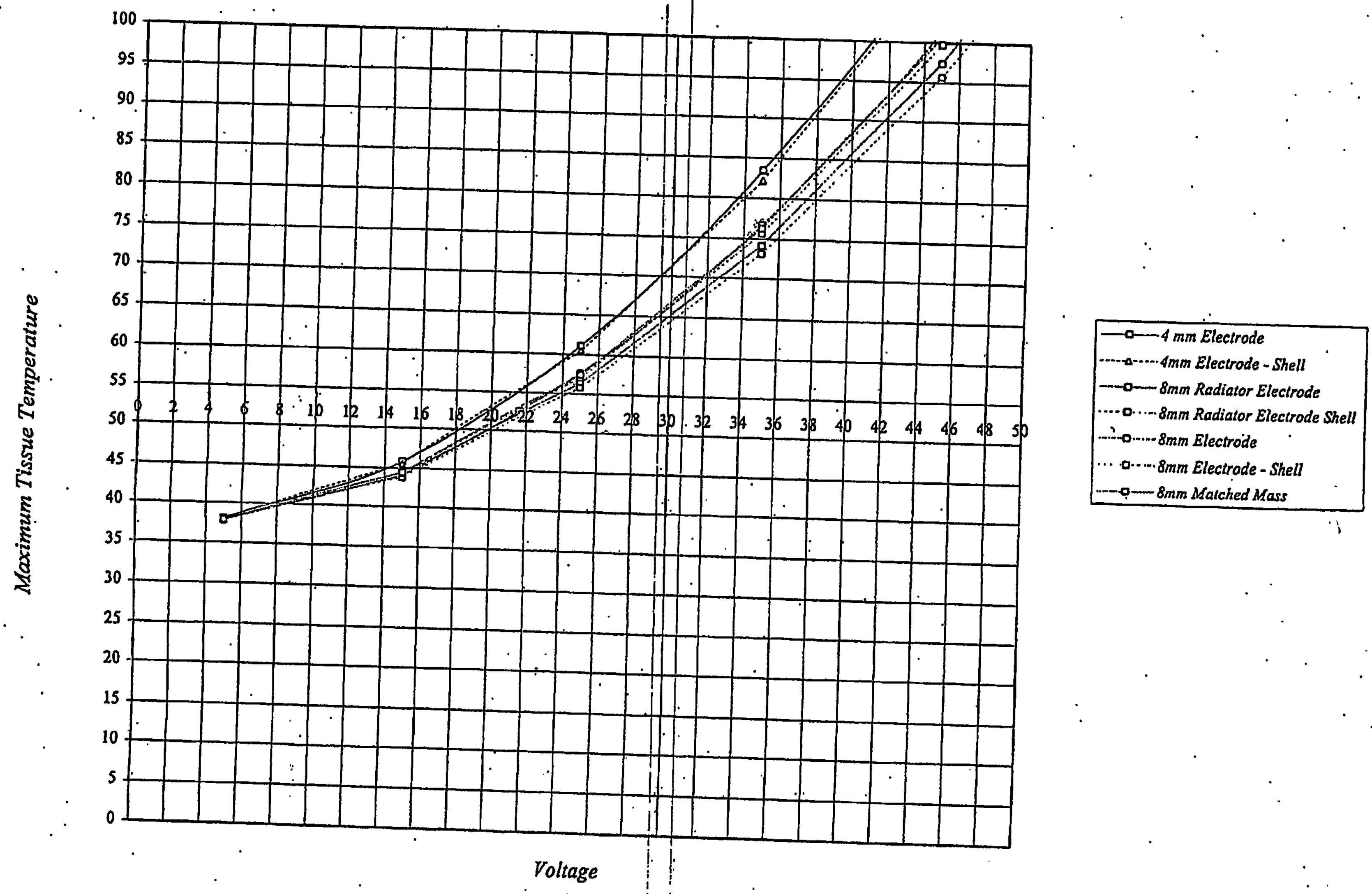

Figure A2-2. Voltage vs. Maximum Tissue Temperature (H=.125)

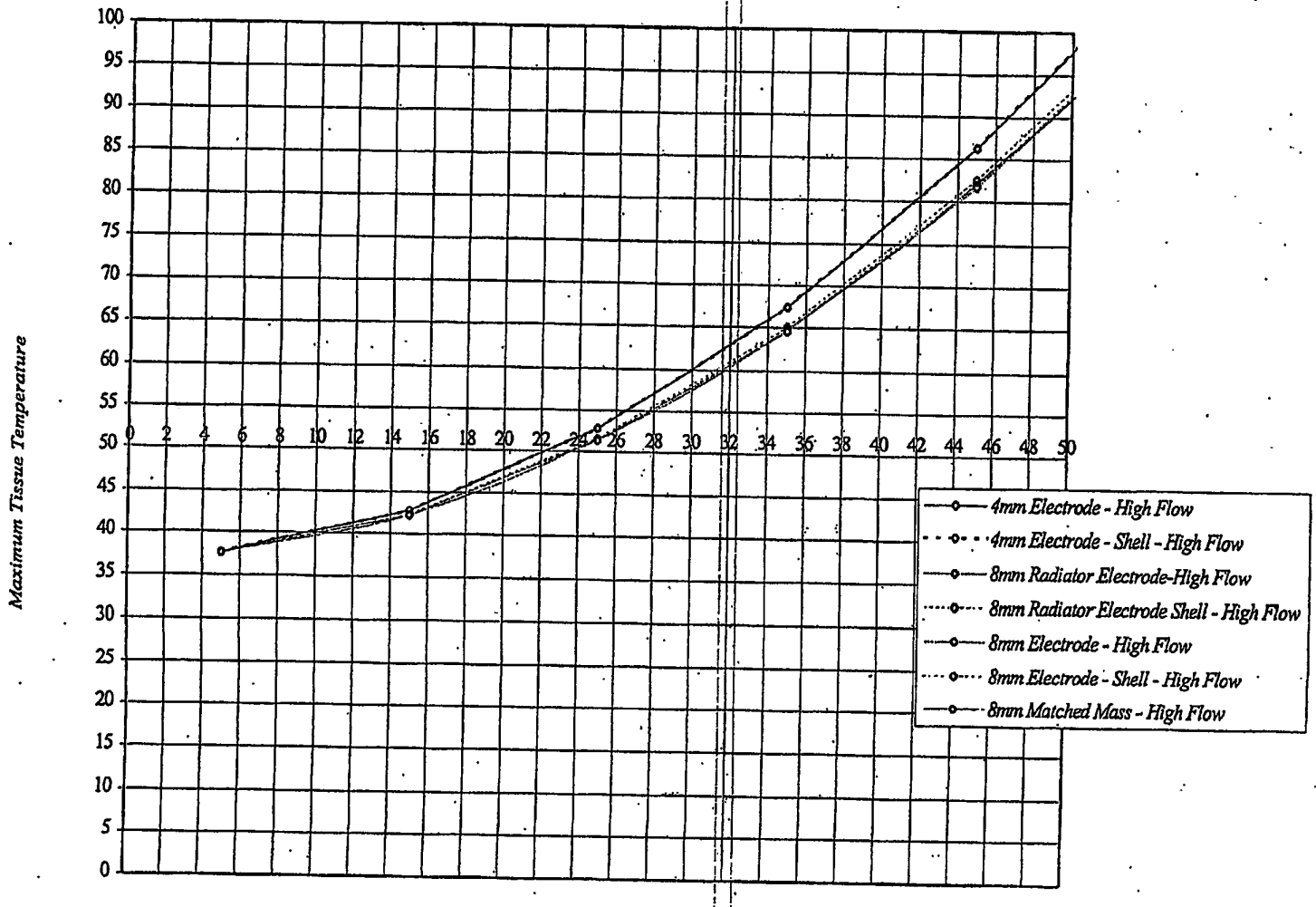

Figure A2-3. Voltage vs. Maximum Tissue Temperature (H=.002)

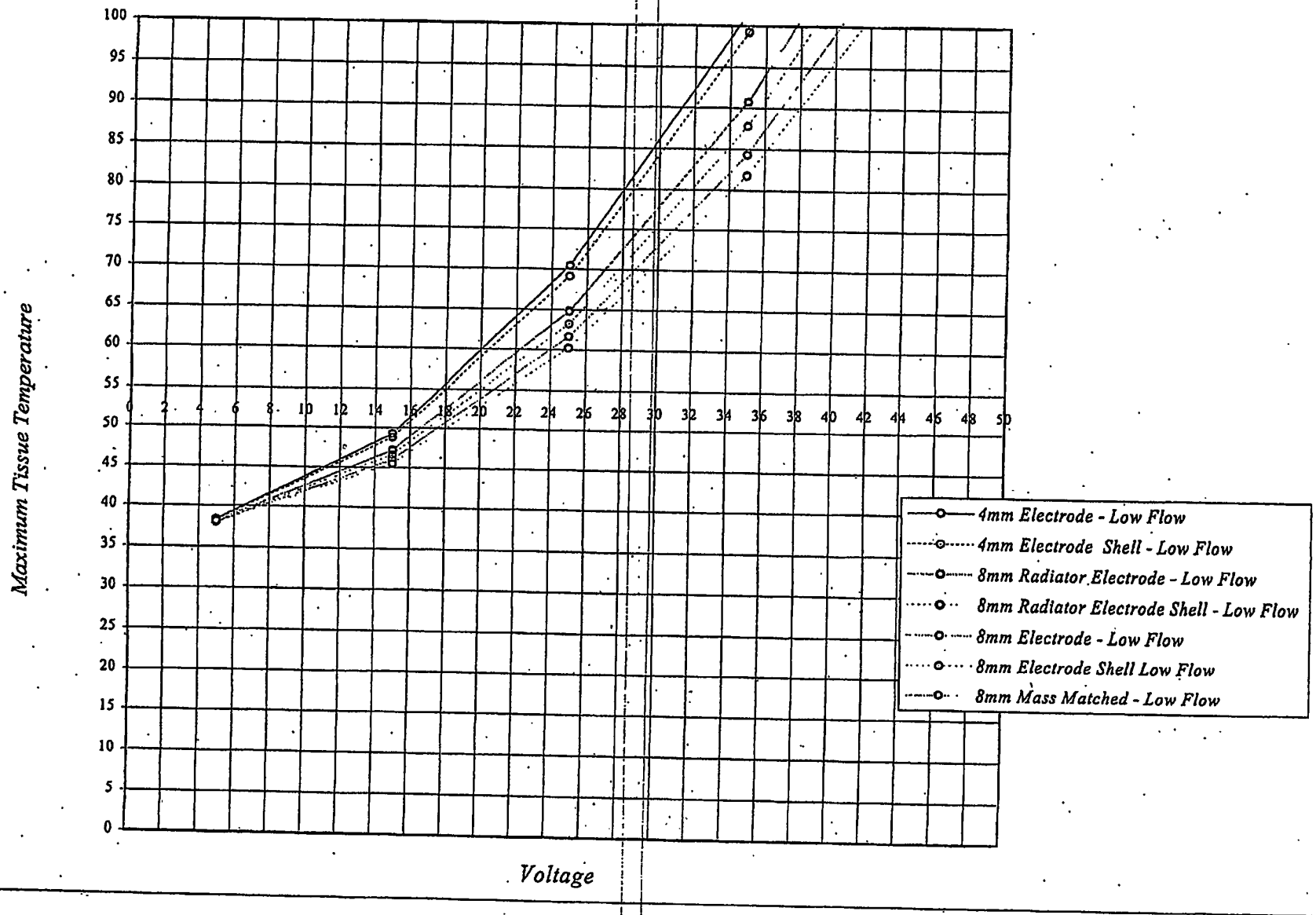

Figure A2-4. Voltage vs. Maximum Tissue Temperature

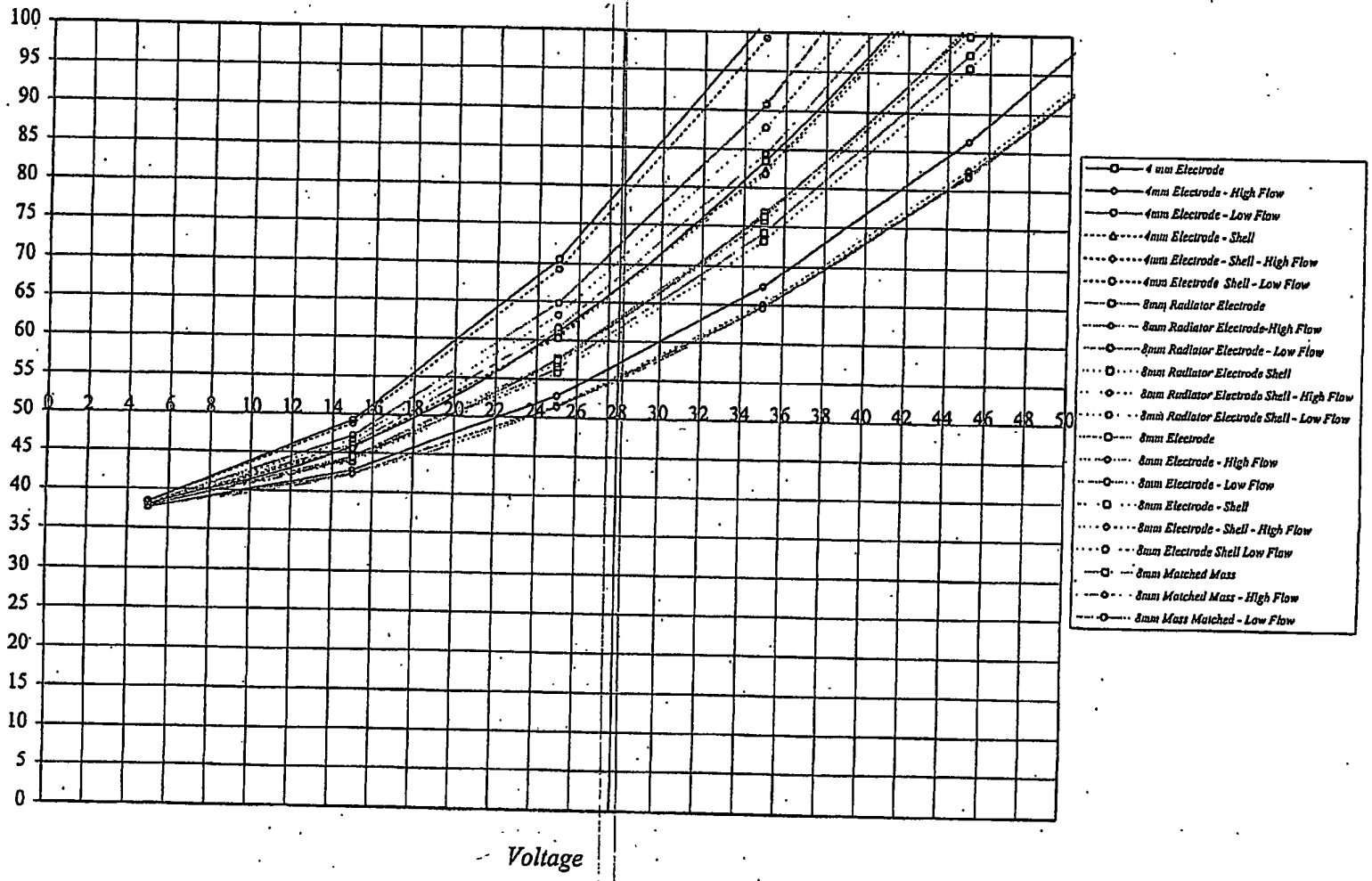

Figure A2-5. Power vs. Maximum Tissue Temperature (H=.004)

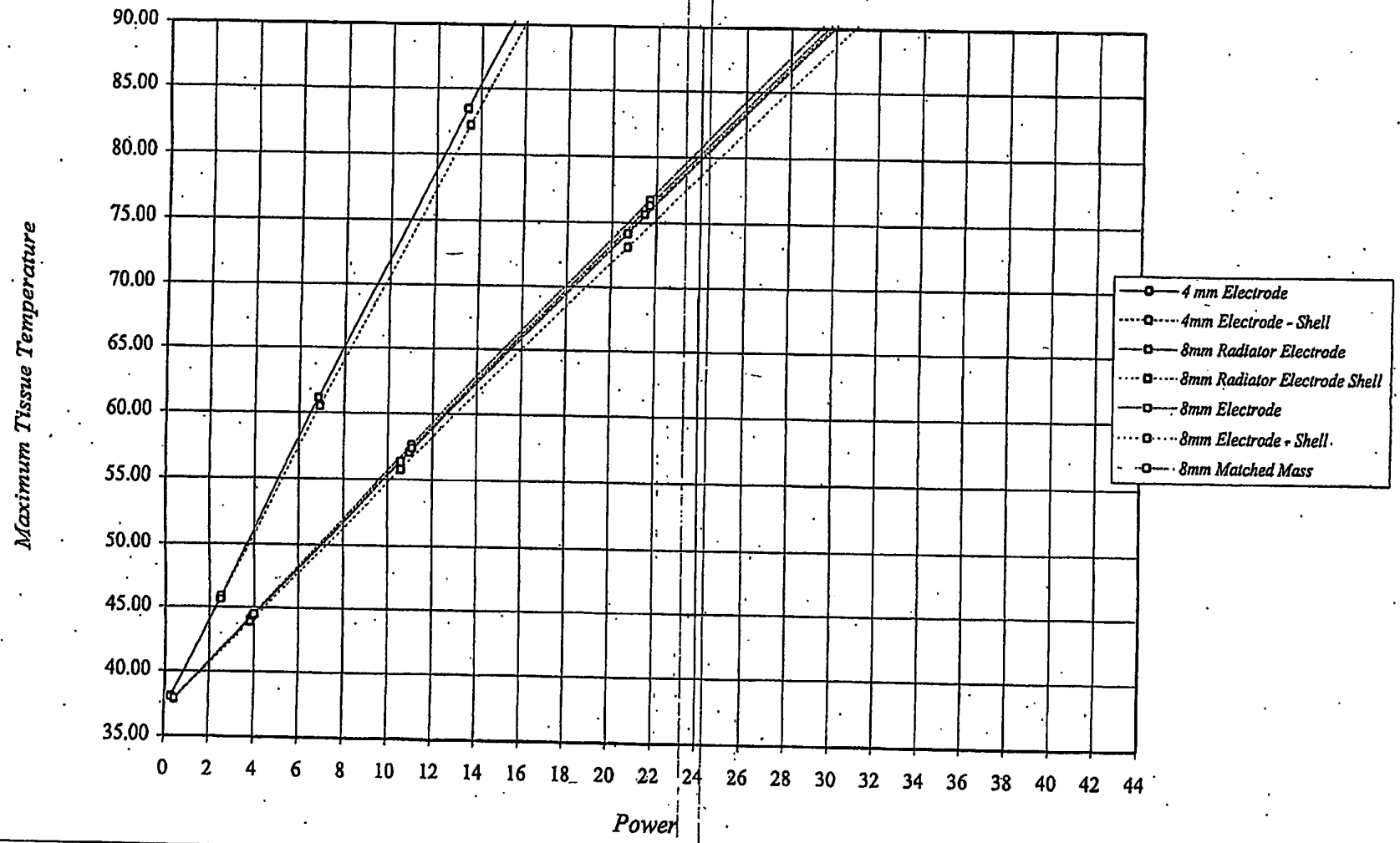

Figure A2-6. Power vs. Maximum Tissue Temperature (H=.125)

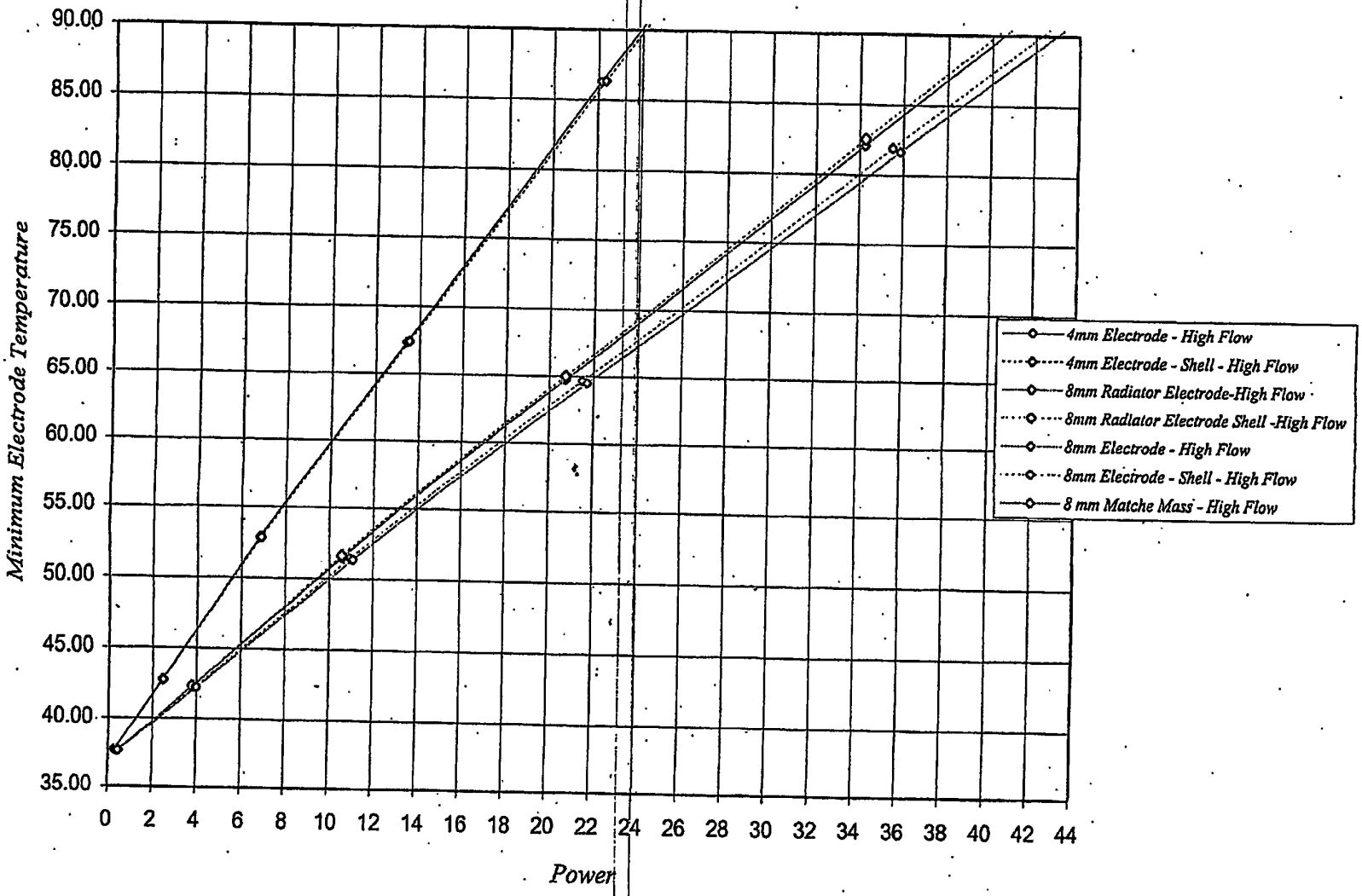

Figure A2-7. Power vs. Maximum Tissue Temperature (H=.002)

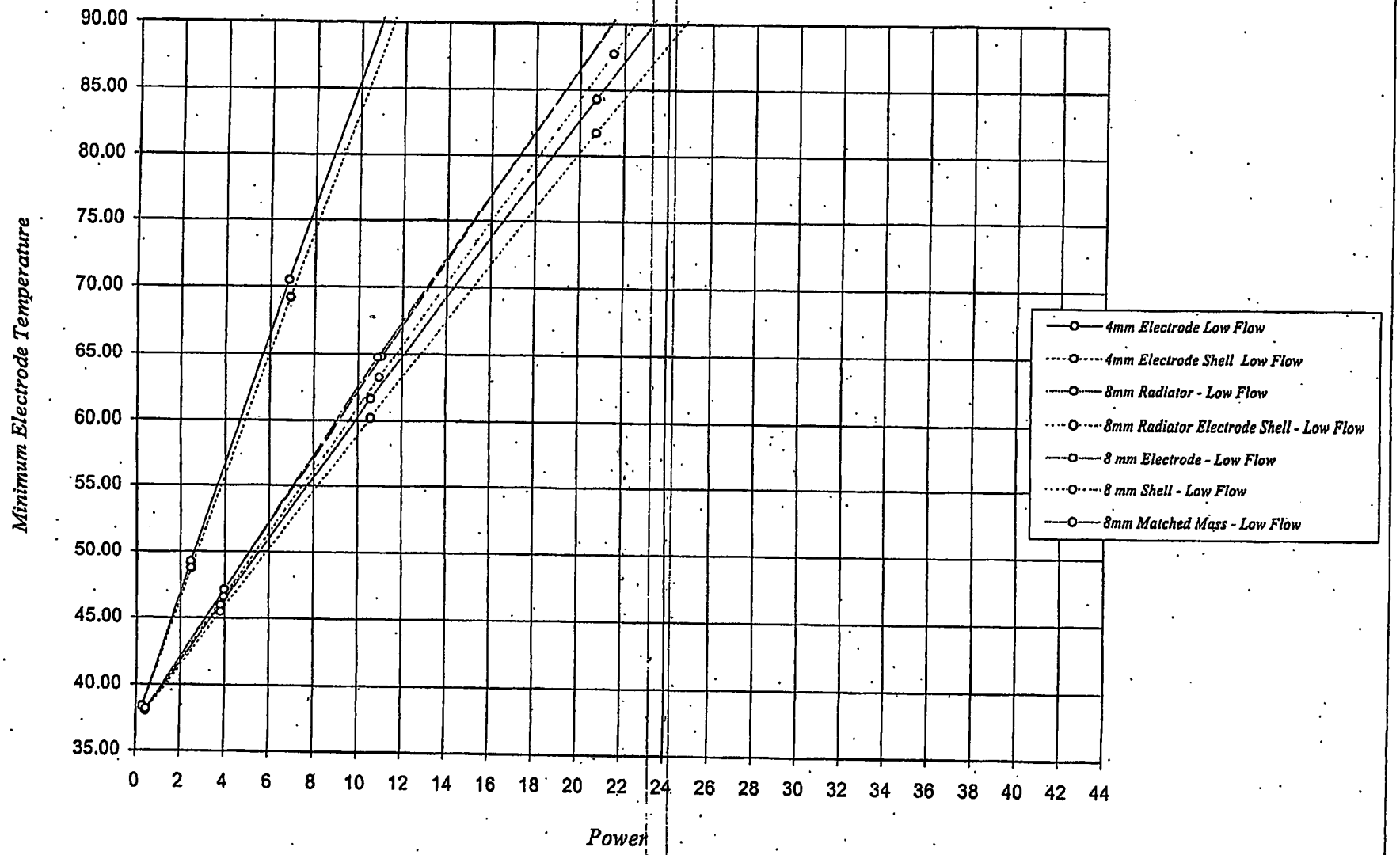

Figure A2-8. Power vs. Maximum Tissue Temperature

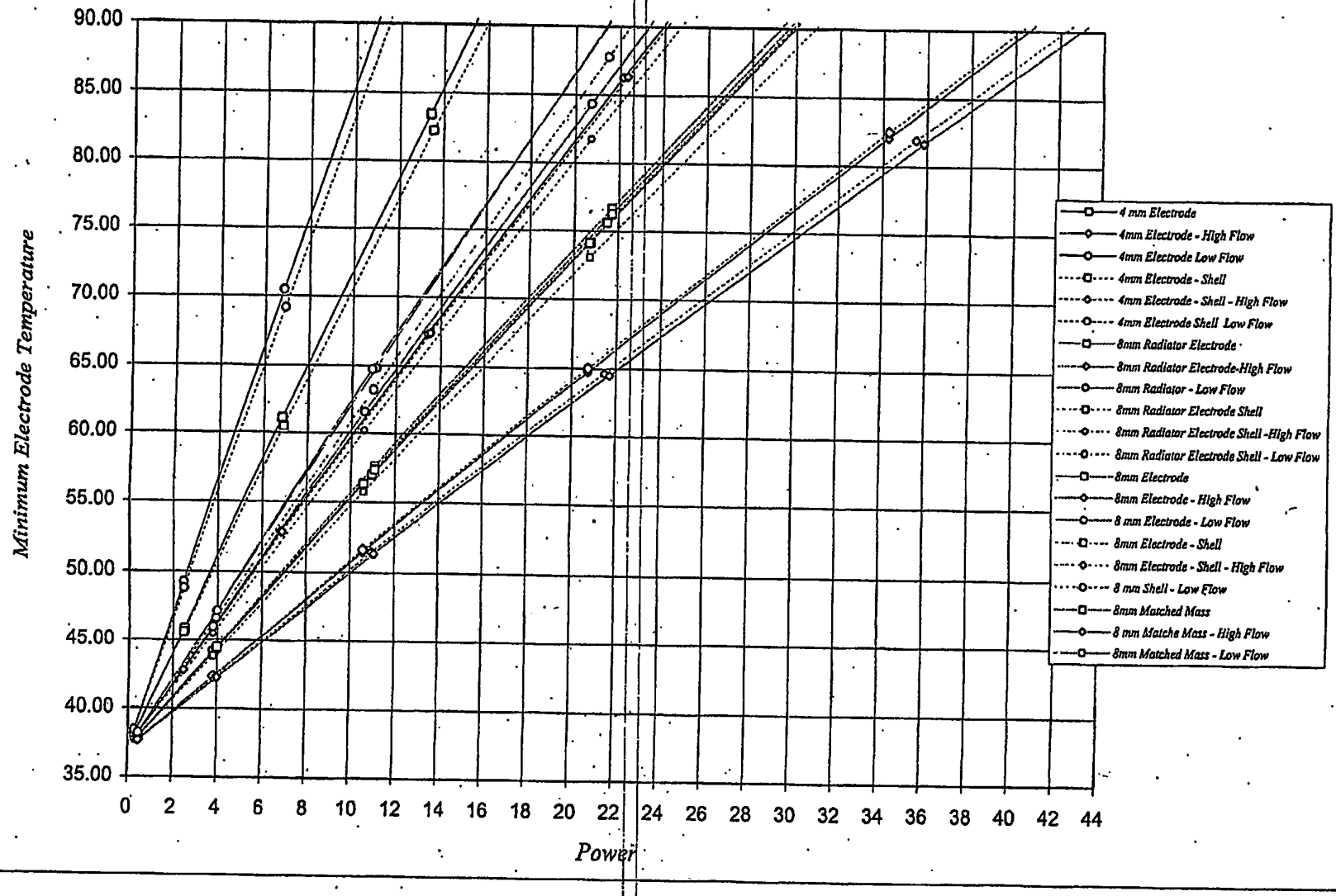

Figure A2-9. Maximum Electrode Temperature vs. Maximum Tissue Temperature (H=.004)

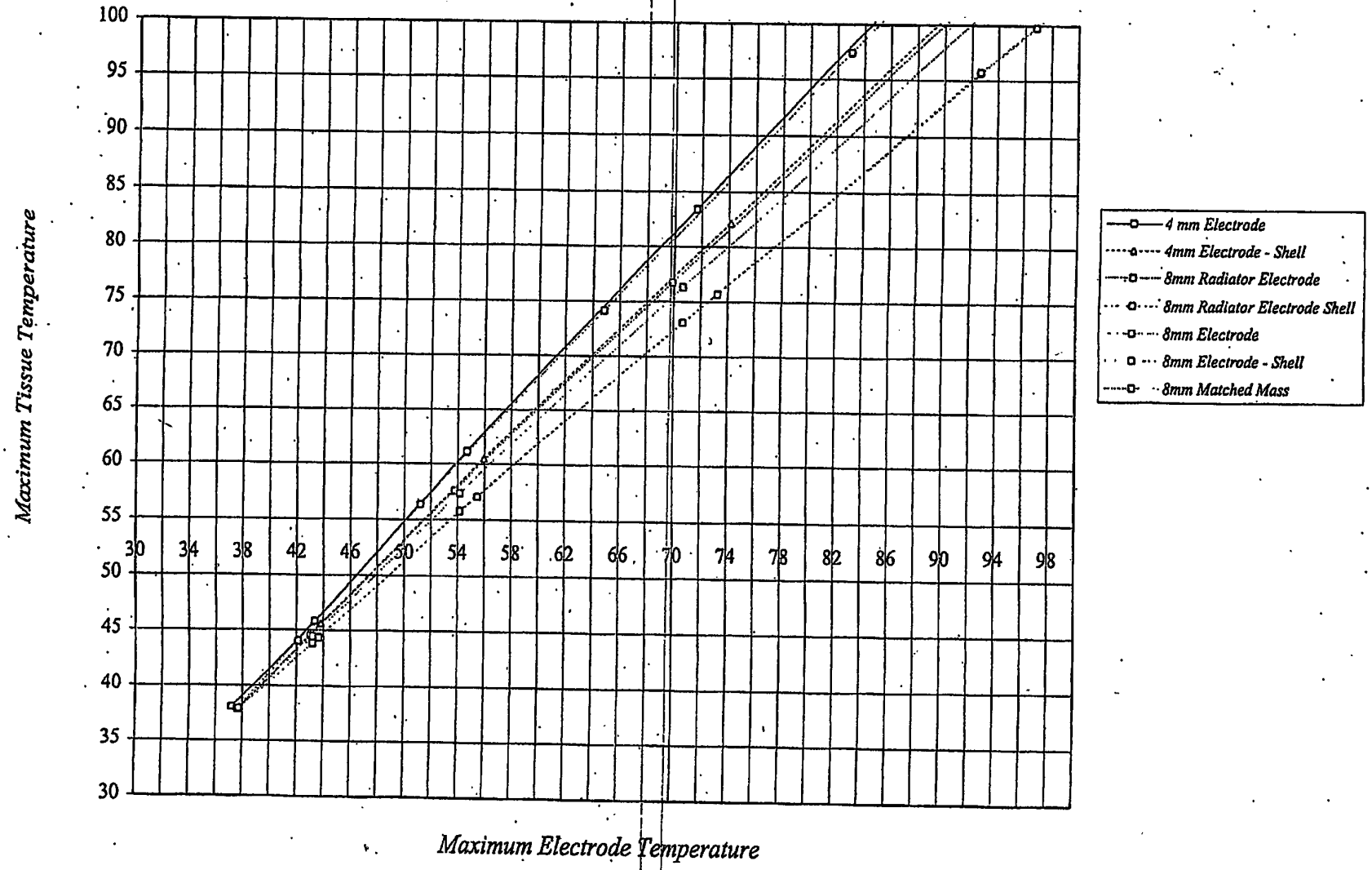

Figure A2-10. Maximum Electrode Temperature vs. Maximum Tissue Temperature (H=.125)

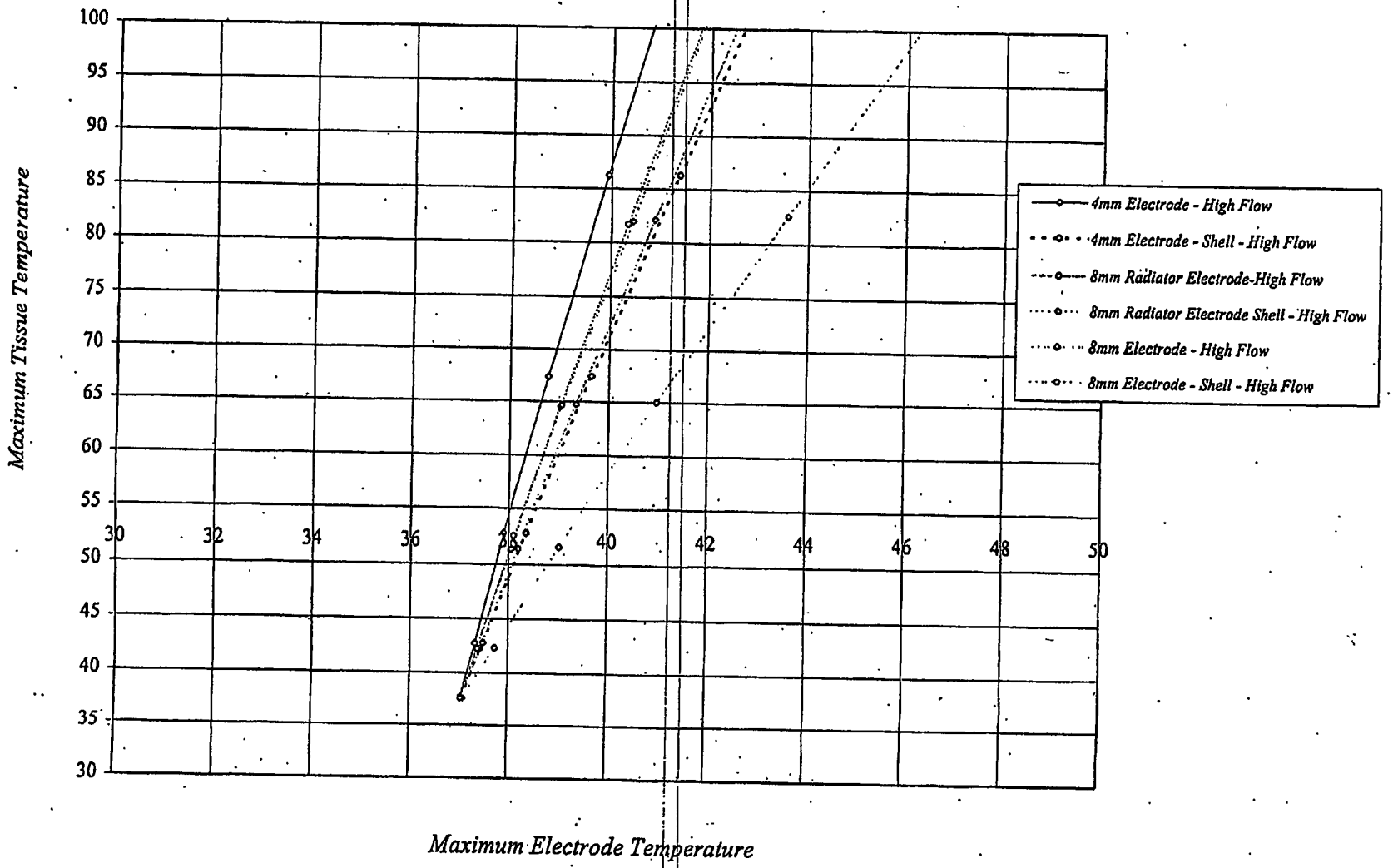

Figure A2-11. Maximum Electrode Temperature vs. Maximum Tissue Temperature (H=.002)

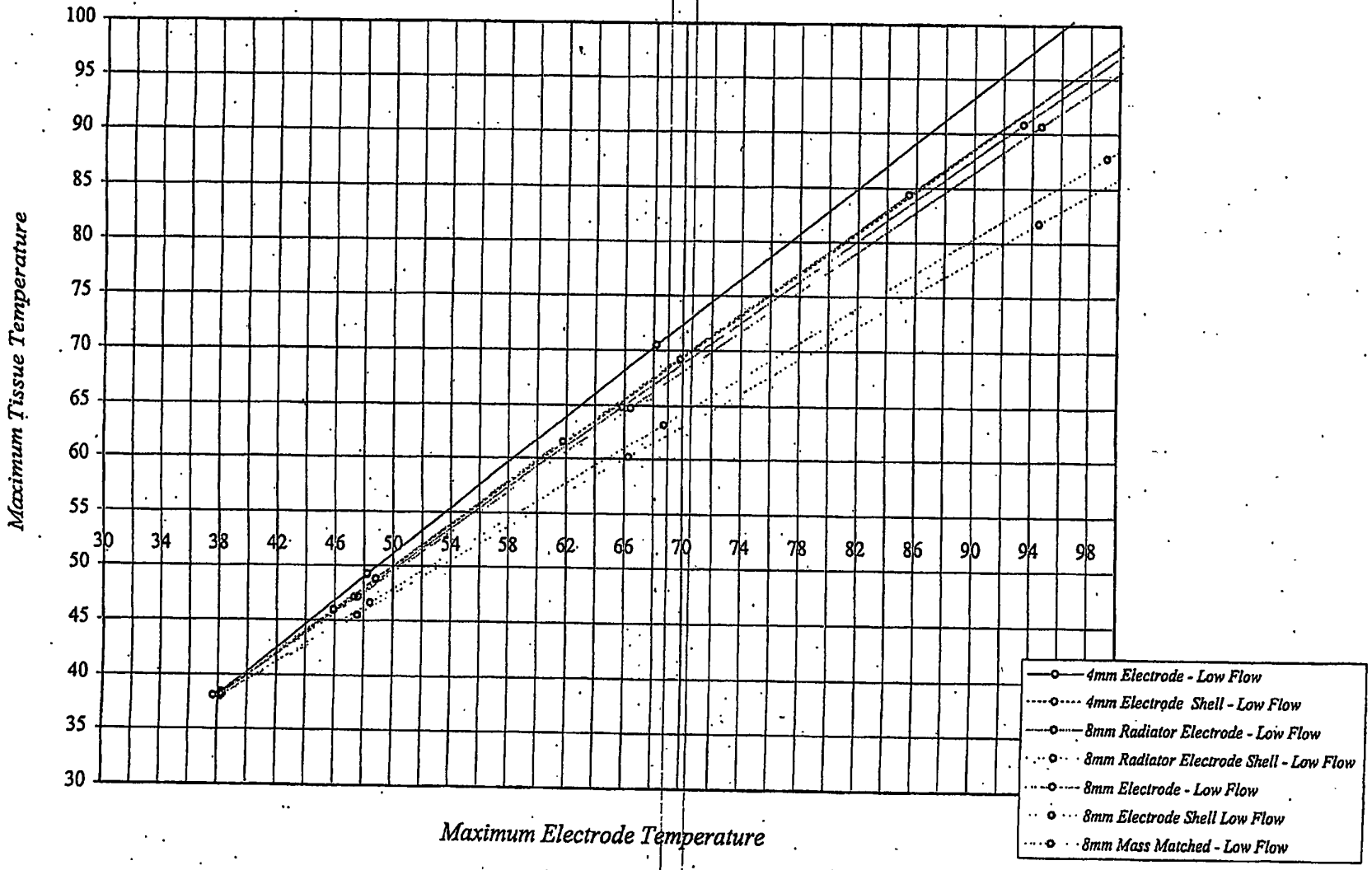

Figure A2-12. Maximum Electrode Temperature vs. Maximum Tissue Temperature

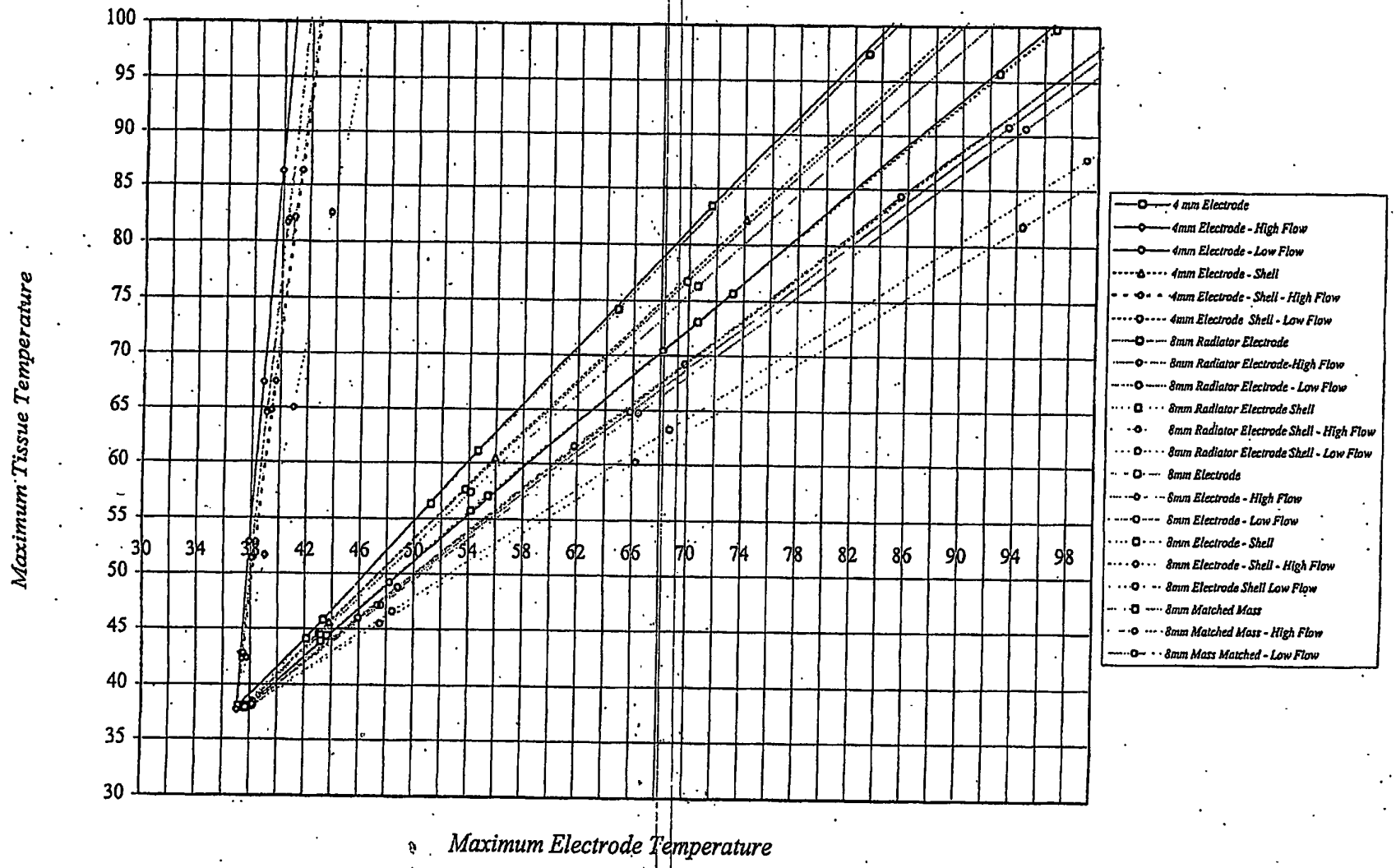

Figure A2-13. Minimum Electrode Temperature vs. Maximum Tissue Temperature(H=.004)

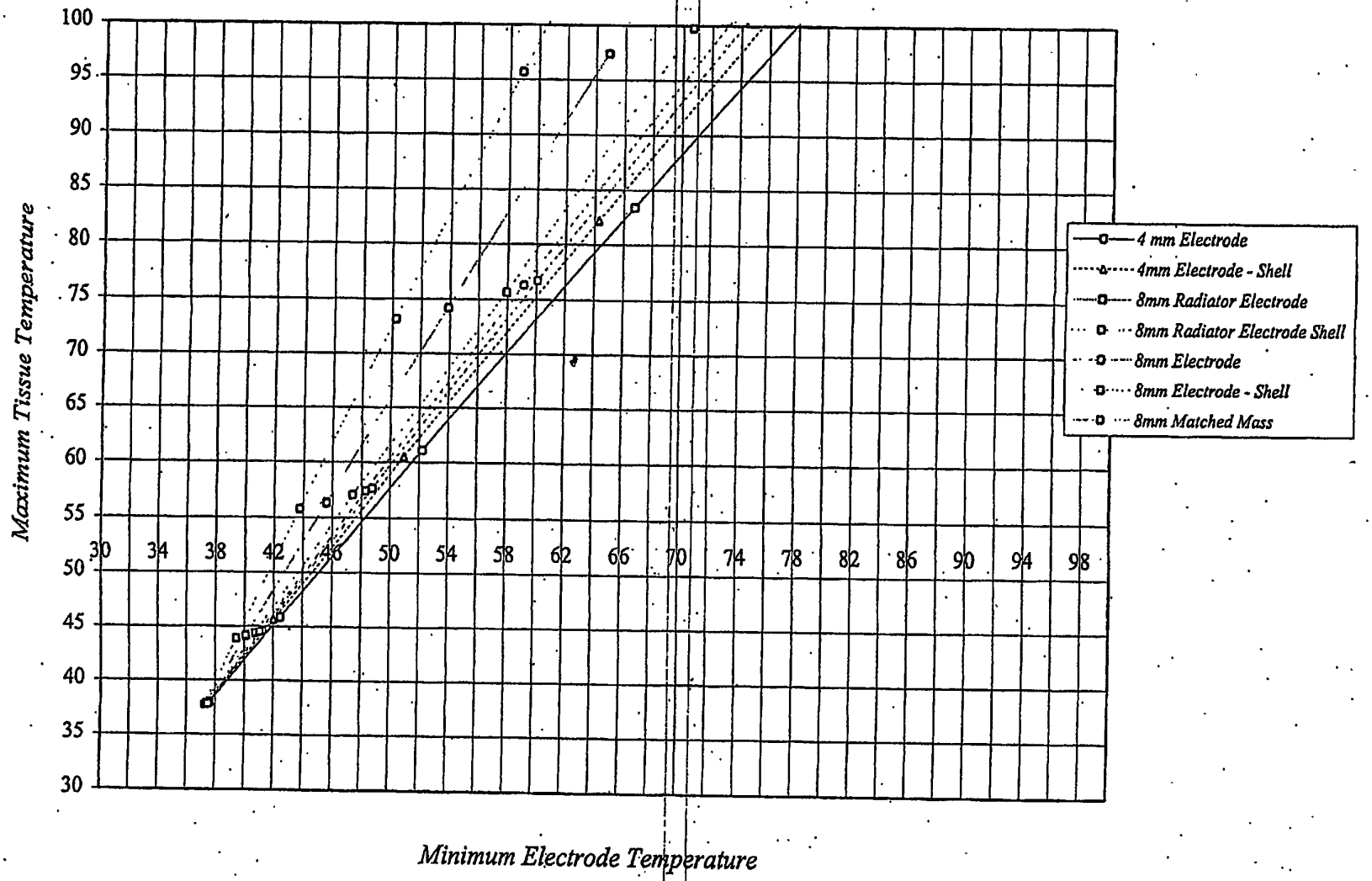

Figure A2-14. Minimum Electrode Temperature vs. Maximum Tissue Temperature (H=.125)

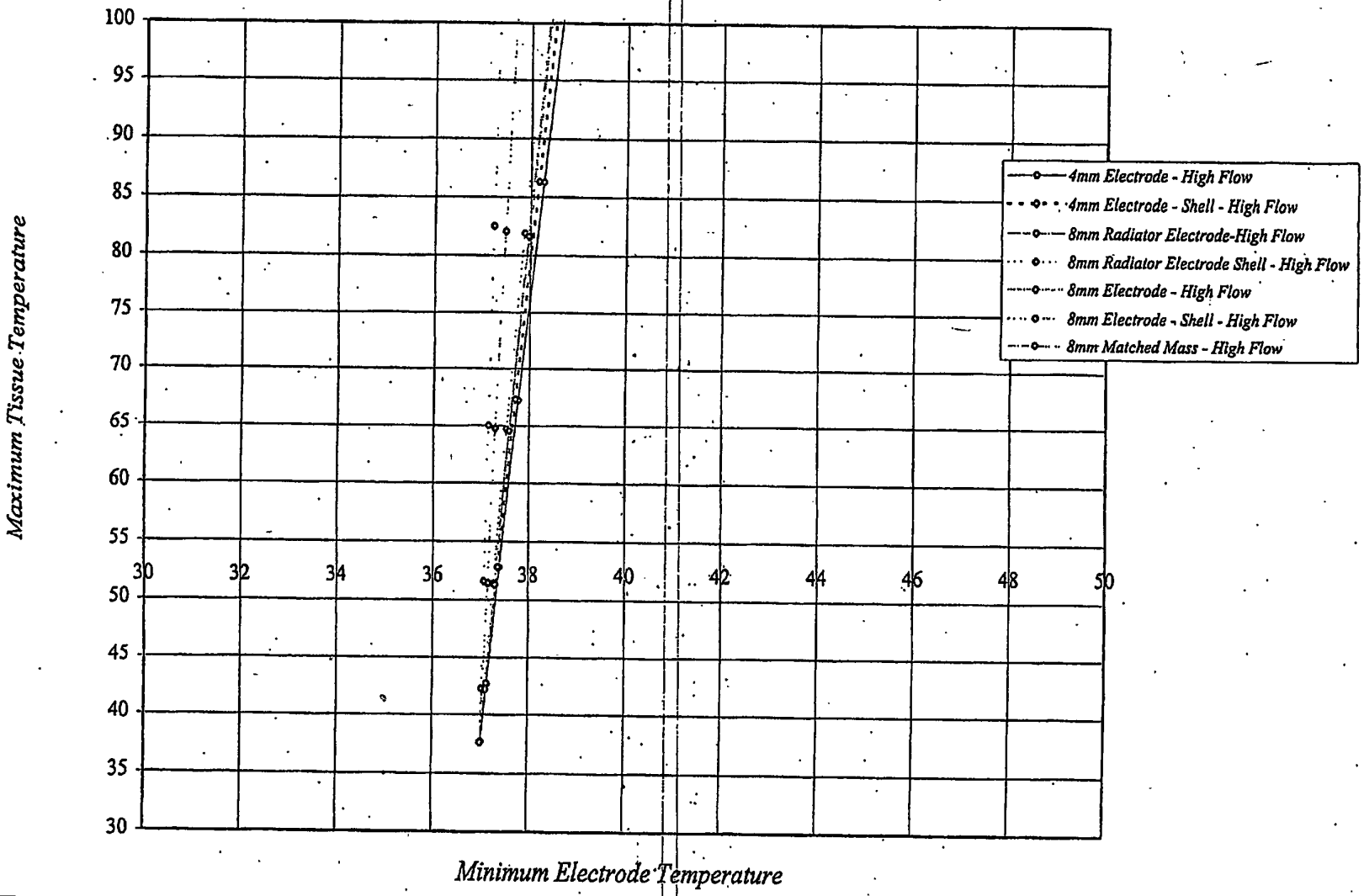

Figure A2-15. Minimum Electrode Temperature vs. Maximum Tissue Temperature (H=.002)

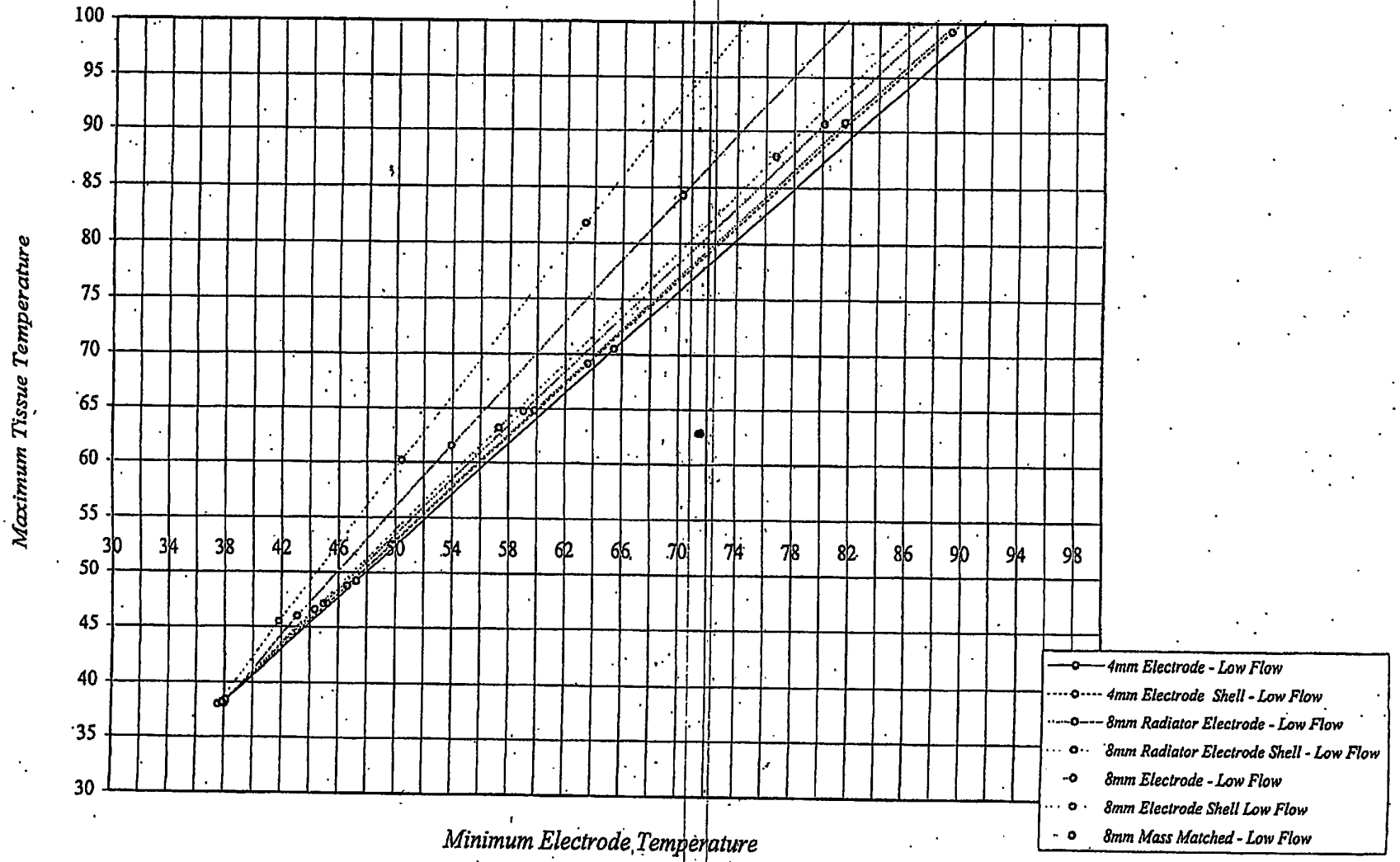

Figure A2-16. Minimum Electrode Temperature vs. Maximum Tissue Temperature

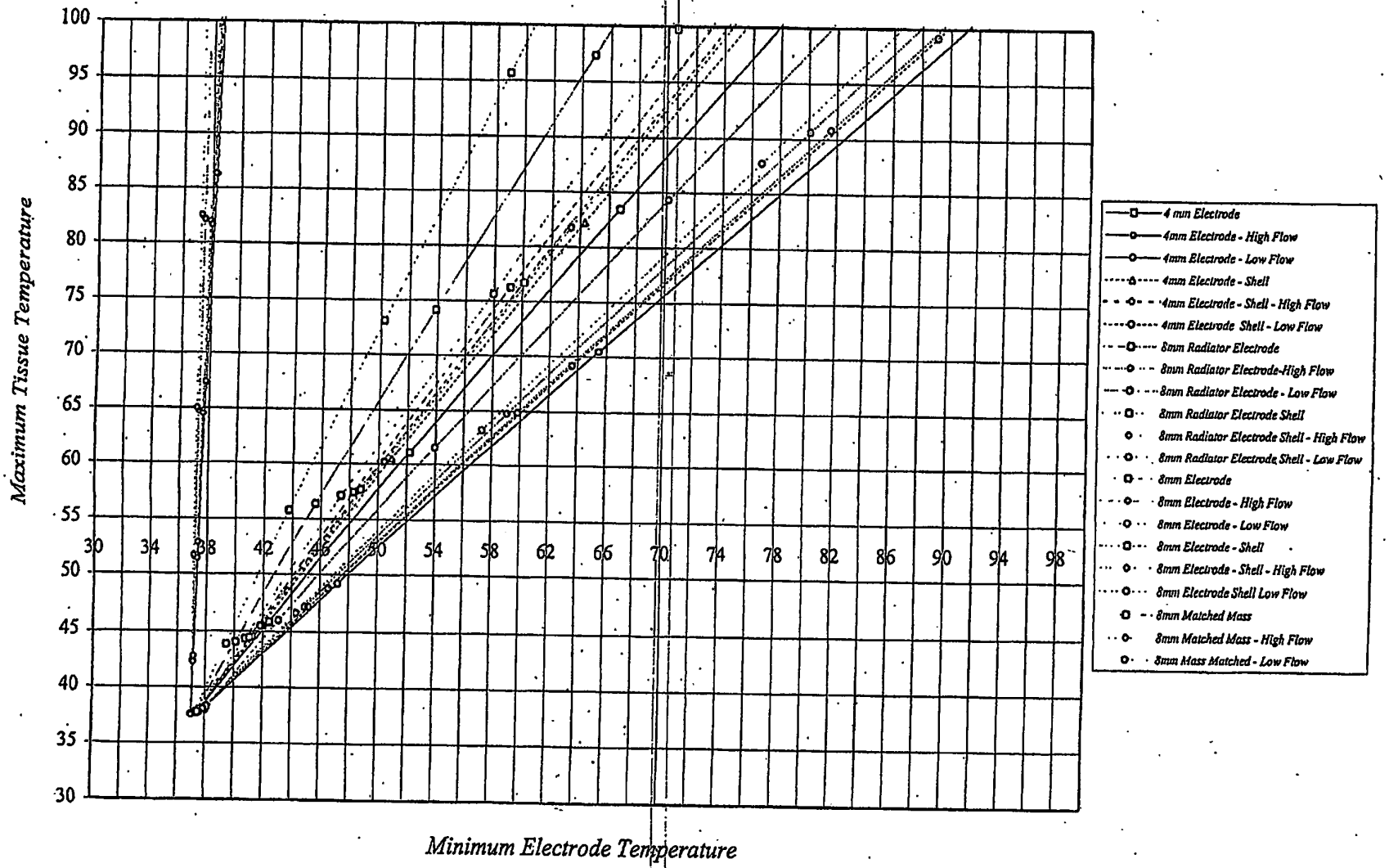

Figure A2-17. Power/Voltage Curves

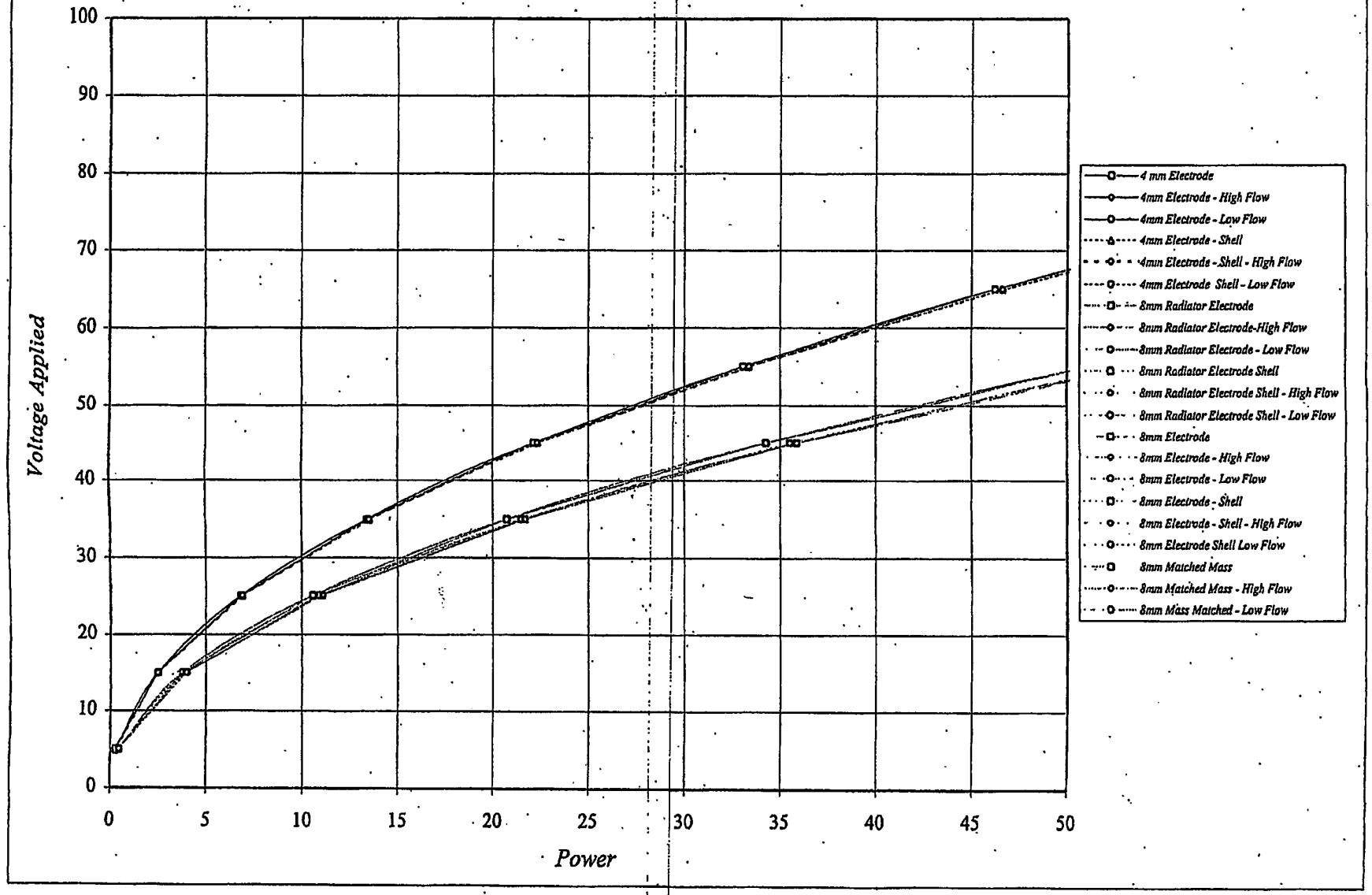

APPENDIX-3

60458856.032803

Figure A3-1. Cooling Effect of Radiator Type Electrode

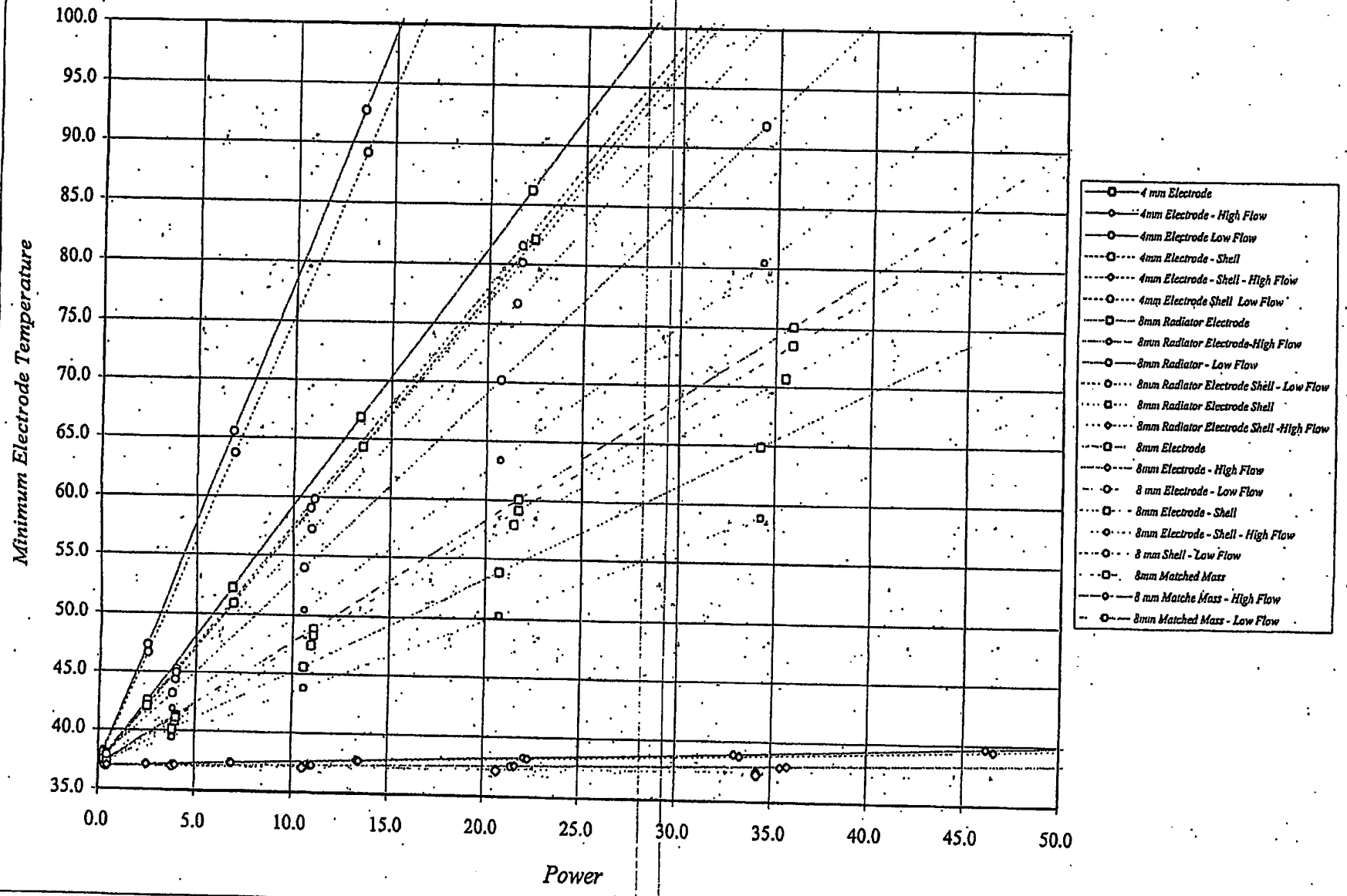

Figure A3-2. Cooling Effect of Radiator Type Electrode

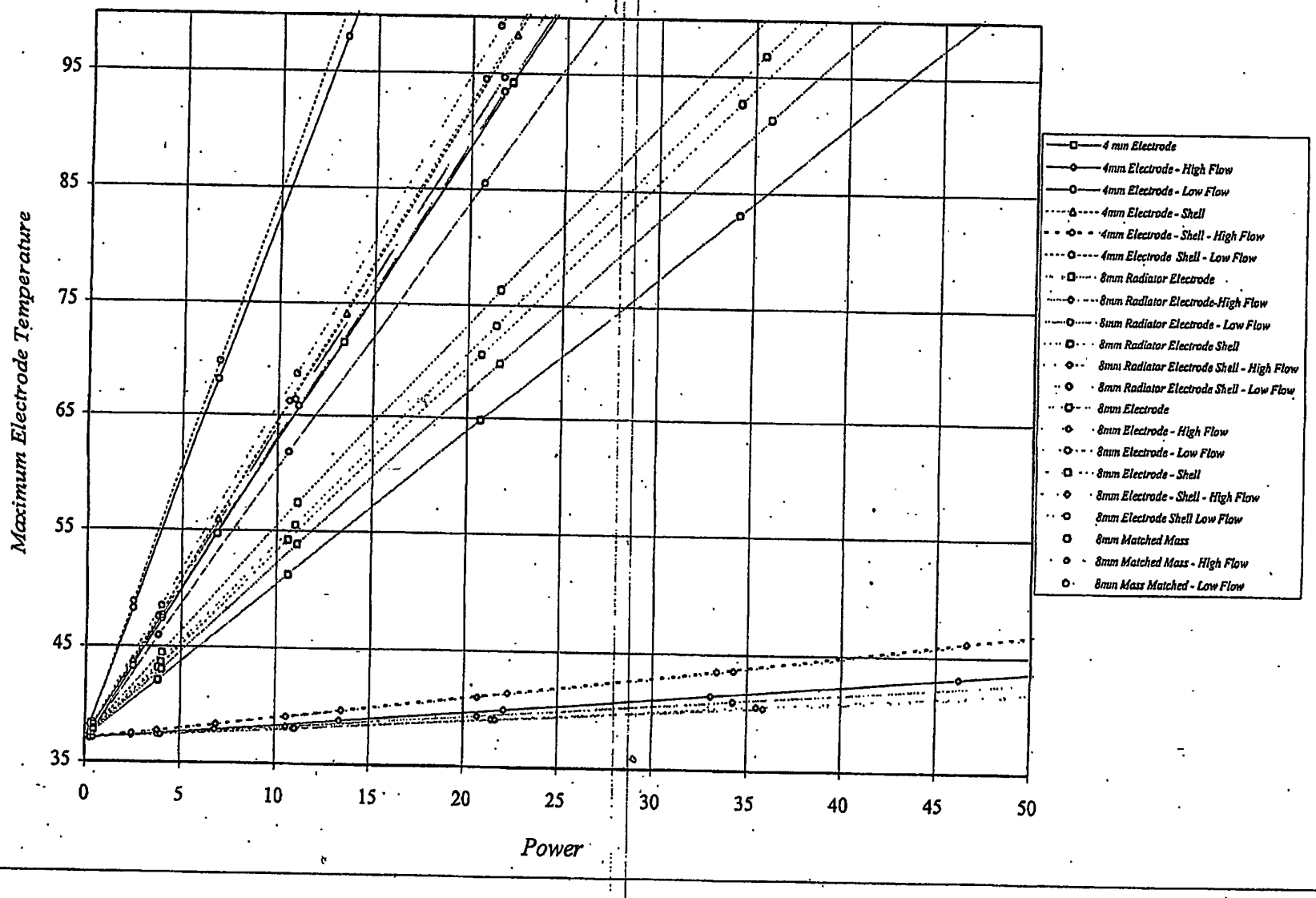

APPENDIX-4

Figure A4-1. Lesion Depth vs. Maximum Electrode Temperature

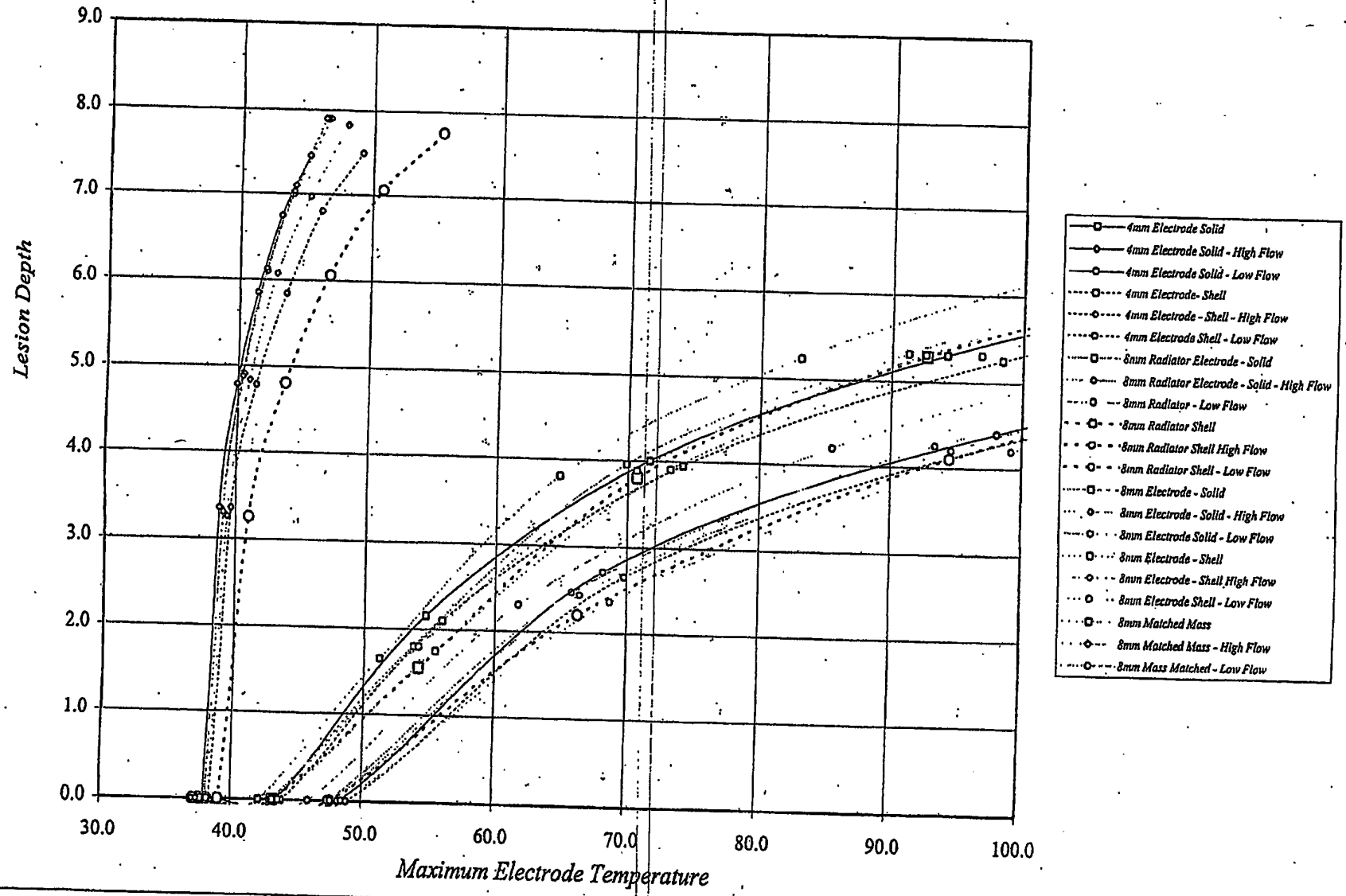

Figure A4-2. Lesion Depth vs. Minimum Electrode Temperature

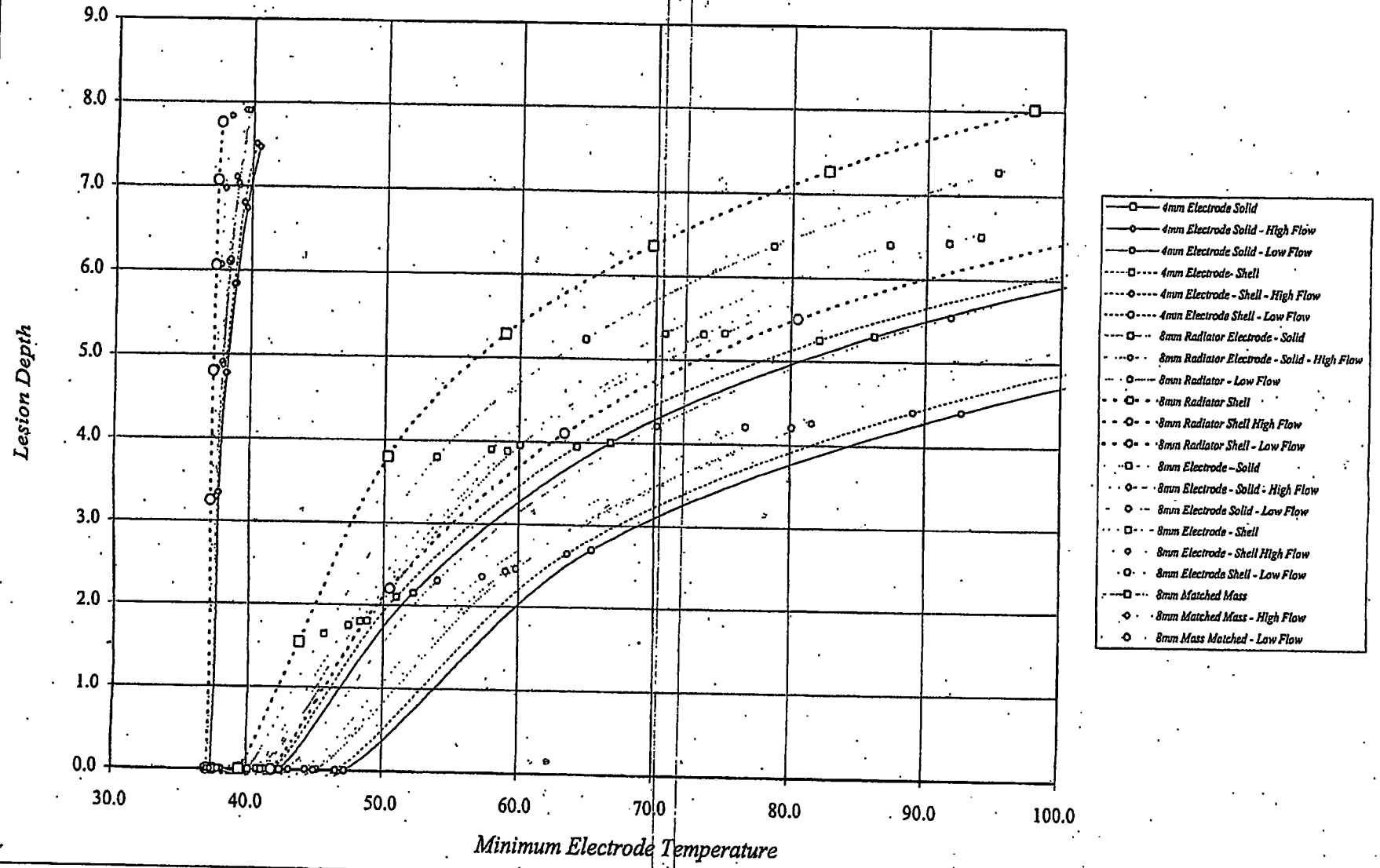

Figure A4-3. Lesion Depth vs. Maximum Tissue Temperature

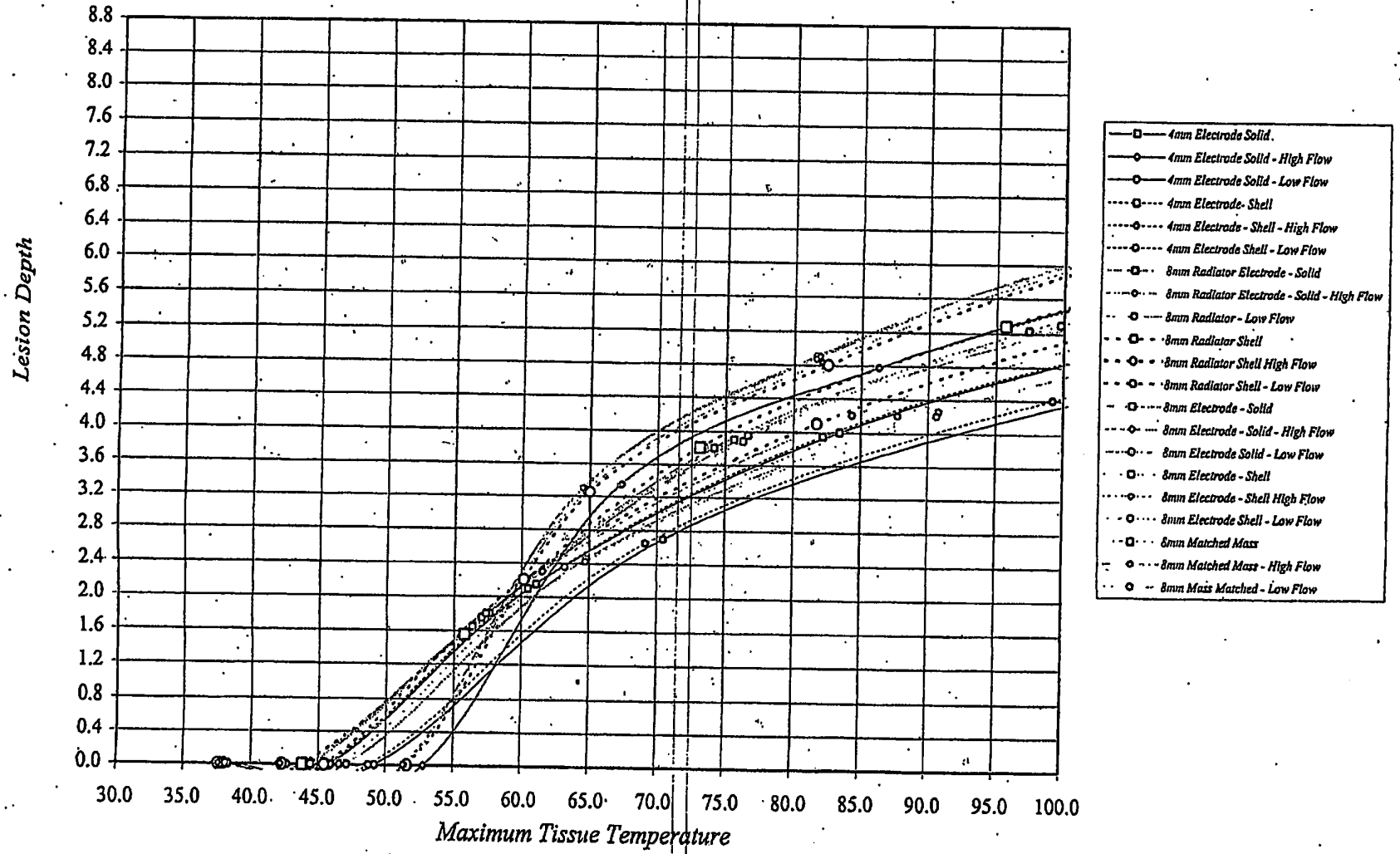

TITLE Catheter Electrode / Tip Junction Design

m Page No.

Morgan FEA analysis has shown that the previously described design could be extended to ring type electrode as shown below

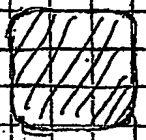

electrode edges are rounded and extended into fluid flow

By increasing the surface area at tip/electrode transition and pushing this area further into the flow, hot spots at the electrode edge are minimized or eliminated. This reduction in heating at the edges results in an electrode with fairly uniform heating and lower maximum electrode temperatures. The provision of the rounded extended edges competes with the cooling provided by radiator type electrodes. Increasing the convective cooling rate faster than the increased heating caused by high current densities at the junction seems to be the mechanism of cooling.

To Page No.